UNIVERSIDAD DE MÁLAGA

$RGS14_{414}$ - mediated prevention of an episodic memory loss: a study of molecular mechanism

· Ph.D Thesis ·

Irene Navarro Lobato

Lab. Neurobiología, CIMES, UMA

Programa de Doctorado:
Neurociencia y sus Aplicaciones Clínicas

Thesis supervisor:
Dr. Zafaruddin Khan

Málaga, 2015

UNIVERSIDAD DE MÁLAGA

FACULTAD DE MEDICINA

Ph.D. Thesis

Programa de Doctorado: *Neurociencia y sus Aplicaciones Clínicas*

$RGS14_{414}$-mediated prevention of an episodic memory loss: a study of molecular mechanism

Irene Navarro Lobato

Lab. Neurobiología, CIMES, UMA

Thesis supervisor: Dr. Zafaruddin Khan

Málaga, 2015

UNIVERSIDAD
DE MÁLAGA

Dr. Zafaruddin Khan, Director del laboratorio de Neurobiología del Centro de Investigaciones Médico Sanitarias y Profesor del departamento de Medicina y Dermatología en la facultad de Medicina de la Universidad de Málaga,

INFORMA

Que Doña Irene Navarro Lobato, Licenciada en Biología por la Universidad de Málaga, ha realizado bajo su dirección el trabajo experimental que ha llevado a la redacción de la presente memoria de Tesis Doctoral, titulada "$RGS14_{414}$-mediated prevention of an episodic memory loss: a study of molecular mechanism". Considerando que constituye trabajo de Tesis Doctoral, se autoriza su presentación para optar al Grado de Doctor.

Y para que así conste y surta los efectos oportunos, se firma el presente documento en Málaga, a 20 de octubre de 2015.

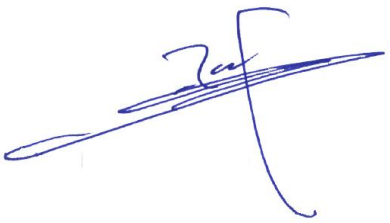

Fdo: Zafaruddin Khan

AGRADECIMIENTOS

Los años de formación que he vivido culminan con este manuscrito que sin quitarle importancia, tan sólo es una parte de todo el trabajo que encierran sus páginas, de muchos consejos y la magnífica y útil ayuda de muchas personas que han sido imprescindibles en todo su desarrollo y en el mío personal. En este pequeño espacio mi intención no es agradecer, sino dejar bien claro que son ellos también sus dueños. Todo lo que me habéis aportado a distintos niveles es mi más preciado tesoro que me ha ayudado a crecer y madurar como profesional y como persona, porque somos lo que somos por la gente que nos rodea. Yo he tenido la suerte de cruzarme con 'GRANDES'.

En primer lugar, quiero agradecer a mi director de tesis, el Dr. Zafaruddin Khan, por su confianza en mí a la hora de acogerme en su laboratorio y darme la oportunidad de sumergirme en este mundo sacrificado, y a veces no tan fructífero como desearíamos, que en el fondo nos aporta más de lo que seríamos capaces de percibir. Gracias por guiar mis pasos y permitir que llegase al destino. Espero haber estado a la altura.

En segundo lugar, mostrar mi más sincera gratitud a los grupos con los que realicé mis estancias predoctorales por haber hecho hecho muy fructífero el timpo que pasé con vosotros aportando resultados importantes en este trabajo de tesis:

-A la Dra. Diana Frechilla y al Dr. Alberto Mediavilla del CIMA (Pamplona) y sus miembros (Esther, María y Ana María) cuya colaboración en el trabajo de Alzheimer ha sido crucial. Quiero agradecer muy especialmente a Ana María, una gran amiga, el dedicarme su tiempo enseñándome las técnicas de ORT de ratón, las inmunos, el haberme hecho sentir como en casa, sus valiosos consejos sobre el mundo de la ciencia y de la vida en general y el haberme enseñado algunos rincones de Pamplona y San Sebastian.

-A la Dra. Antonia Vlahou y al Dr. Ieronymos-Jerome Zoidakis,"Makis", así como a todo su grupo Manoussos, Alexander, Vassiliki, Maria Frantzi, Anggeliki y al *Dr. Konstantinos Vougas del Biomedical Research Foundation of Athens; tuvieron mucha paciencia con aquella inexperta en proteómica que se presentó en su laboratorio. Gracias a vuestra magnífica experiencia y buen hacer aprendí muchísimo en tan sólo 5 meses y todo el trabajo salió a adelante. Quiero hacer una mención especial a Makis, que me dedicó tantas horas, gracias por tu optimismo y positivismo y por poseer esa "locura" particular que me amenizó todo el proceso de aprendizaje. También a Idili que sin ser parte de este grupo compartió laboratorio conmigo especialmente aquel agosto en Atenas. Eres una amiga muy especial a la que tengo que agradecer muchísimo, fuiste mi apoyo donde no tenía a nadie más y me abriste las puertas de tu casa y de tu maravillosa familia sin más. Eternamente te estaré agradecida.*

Mi agradecimiento también al departamento de Fisiología Humana y de la Educanción Físico Deportiva y en especial a su director, el Dr. Marc Stefan, tutor de mi DEA, que siempre se ha mostrado muy servicial y amable cuando lo he necesitado en toda la burocracia que supone la defensa de una tesis doctoral.

Mil gracias a los miembros de distintos grupos de investigación con los que hemos colaborado o nos han aportado su conocimiento, su ayuda, sus consejos, así como material necesario durante la realización de experimentos. Sois todos grandísimos profesionales y mejores personas con las que ha sido y es un lujo contar:

A la Dra. Antonia Gutiérrez y a su equipo, Eli, Raquel, Vanessa, Mercedes y en especial a mi casi paisana Laura, un grupo con el que compartimos muchos lazos y que siempre está dispuesto a hacerte un favor; gracias por lo que me habéis aportado en el mundo de la inmunohistoquímica y por vuestra amistad. A la Dra. Alicia Rivera y a su grupo, mi querida Alejandra y a Jose, siempre dispuestos a prestarnos su material de estereotaxia; gracias por vuestra valiosa amistad. Al Dr. Antonio González por cedernos el estereotáxico de ratón cada vez que lo hemos necesitado. Al Dr. Luis Santín y su grupo (Carmen Pedraza, Estela, Cristina, Jorge,...) por sus aportanciones en el campo de la conduta. A María José y José Rioja, "los del fondo", gracias por permitirnos amablemente usar vuestros

equipos y por vuestros consejos.También debo agradecer a esos grupos fuera de la Universidad de Málaga que me han acogido tan amablemente en su laboratorio para realizar proyectos de investigación en colaboración. Gracias al Dr. Juan José Canales y sus discípulos, Toni y Clara por acogerme en Valencia e introducirme en el estudio de la memoria de miedo, aportando siempre muy buenas ideas para continuar. Muchas gracias al Dr. Juan Carlos López y a Esperanza de la Universidad de Sevilla por enseñarnos la técnica de aversión condicionada al sabor.

Mi agradecimiento también a todos aquellos que a diario nos allanáis el camino, el personal del estabulario (nuestro preciado e imprescindible veterinario, Ricardo, a Ana, Eva, Isa, Conchi, Marivi, Vanessa, Sole, Loli y nuestra querida Soraya), los técnicos de cultivos celulares y de biología molecular del SCAI (Casimiro y Reme), los bedeles y miembros de seguridad del CIMES (Miguel, María Jesús, Antonio, Jaime, Cárdenas, Raquel, Guerra, Ricardo…). A Gema que siempre está pendiente de Mariam y de mí y se alegra mucho de vernos terminar por fin esta etapa.

Agradecer profundamente a aquellos con los que día a día a lo largo de esta etapa he compartido laboratorio, gracias por en mayor o en menor medida dejar una huella en mí:
A Manuel, por enseñarme entre risas al principio de los tiempos, por tu meticulosidad en la realización de los experimentos, por sentar las bases de este trabajo y enseñarme las técnicas de ORT y estereotaxia en rata, así como por tu participación en el proyecto de aging y Alzheimer.
A Eduardo, por tu humor irónico y por lo que me has aportado en el campo de la psicología y del estudio conductual con animales.
A Elisa por enseñarme la técnica de Morris aunque, por ser una buena profesional, que pesar de todo lo que lleva para adelante siempre sabe buscarte un hueco cuando lo necesitas. Además, agradecerte las horas que has dedicado a la corrección de este manuscrito y a la preparación de la presentación. Tu minuciosidad me ha sido de gran ayuda.
A Sinforiano, por compartir con nosotros su experiencia en qRT-PCR y ayudarme con los experimentos relacionados con ese tema, también por iniciarme en las técnicas de epigenética que retomaré seguro más adelante.
A mi queridísima Gloria, gracias por tu buen trabajo y ayuda con el estudio de arborización neuronal, tu paciencia y el cariño que le pones a todo incluyendo a las personas que te rodeamos es lo que te hace única y lo que hace que te adoremos. Gracias por tu amistad, tus consejos y tu preocupación, amiga.
A Juan, al que debo tanto, ese "hermano mayor" al que considero me ha enseñado la mayor parte de lo que soy profesionalmente, desde mis inicios en el labo como alumna interna hasta mis conocimientos en las distintas tecnologías que conozco, biología molecular, cultivos, inmunohistoquímica, Western blot... Con tu gran experiencia y sabiduría has sabido disminuir mi "petardismo" particular. Gracias por todo, por ser como eres y por preocuparte siempre. Sin ti las cosas hubiesen sido mucho más difíciles o imposibles.
A Mariam, mi mejor amiga, trabajar codo con codo contigo ha sido un verdadero placer; sin ti no sé si hubiese llegado a la meta. Gracias por no sólo por tu profesionalidad y tu minuciosidad, sino también por tu bondad y generosidad, siempre has estado cuando te he necesitado, ¿quién me iba a entender mejor que tú? Te admiro como amiga y como colega, y lo sabes. Sé que llegarás muy alto porque sabes pelear y no te conformas con un porque sí, al igual que cualquier GRANDE haría. Compañera de viaje, al final nuestro apoyo mutuo ha merecido la pena, y lo mejor de todo es que he ganado la mejor amiga que hubiese podido imaginar.Y contigo también a Zouhir, sois magníficos y seréis muy felices, amigos.
También a las chicas que llegaron al laboratorio en la fase final del trabajo, Inma, Lucía y María Elena, gracias por vuestro apoyo moral, por haceros cargo del labo mientras Mariam y yo escribíamos para evitar nuestra distracción; gracias por los momentos de risa y por escucharme. Así como a todos los demás, María, Marta, Carlos y José.

A Mª Jesús, una miembro no oficial del grupo, que se ha convertido en una gran y valiosa amiga. Lo mejor de tus largos días de estabulario y de los míos, fueron sin duda conocerte. Muchísimas gracias por escucharme y por ser como eres. Me alegro tanto de tu nuevo brillo de ojos…

La última parte de este apartado de agradecimientos lo reservo para aquellos que forman parte de mi vida por circunstancias ajenas a la realización de mi tesis, pero que también me acompañaron durante el viaje y han sido y son muy importantes para mí:
A mis amigas de toda la vida (Ana, Eli y Rosa) y a mis 'amigos políticos' (Óscar, Grajales, Burra, Ángel, Pepi, Beli, Patri, Sandra) que siempre se alegran de cada paso y con los que me lo paso muy bien celebrándolo; tenésis el don de estar siempre que se os necesita. También, a mis amigas de la "flacu": Carmen, María Victoria y en especial a Isa y Andrea.
Infinitas gracias a esa persona que sabe disimular muy muy bien la molestia que supone aguantar mi mal humor y mis quejas, mis tardanzas y mis ausencias. Pedro, muchas gracias por apoyarme en todo, y estar ahí siempre que te necesito sin esperar nada más que mi felicidad. Tu abrazo es la mejor terapia para los malos momentos y han sido imprescidibles para seguir día a día.
Y por supuesto agradecer a mi familia, mis padres, mi hermanita, con la que ni contigo ni sin ti, mis abuelos, tíos y primos, esa gran familia que te lo da todo sin esperar nada a cambio porque te quieren de corazón. Esos que por el simple hecho de saber que se sentirán orgullosos de tí merece la pena levantarse cada mañana. Gracias por vuestro cariño y vuestra confianza en mí ¡Qué haría sin vosotros! A Cristobal, ese cuñado tan apañado que tengo que siempre me ayuda con el photoshop y con toda su paciencia y profesionalidad me ha preparado la portada de este trabajo. No obstante, quiero agradecerle especialmente a mi madre, muchas gracias mamá por todo lo que haces no sólo por mí sino por todos, tu carácter lleno de amor nos conduce por el buen camino. Este trabajo va dedicado especialmente a ti, porque sé la ilusión que te hace.

Para terminar sólo me que me queda pedir disculpas si ha faltado alguien que debiese estar, dejar este apartado para el final y escribirlo bajo la presión del tiempo que se agota no fue una buena idea.

A mis padres

y a mi hermana

A Pedro

"[…], the new biology posits that consciousness is a biological process that will eventually be explained in terms of molecular signaling pathways used by interacting populations of nerve cells[…]."

Eric Kandel, 2007

.

ABBREVIATIONS

AD: Alzheimer´s disease
AKT: Protein kinase B
aMCI: Amnestic mild cognitive impairment
Amp^r: Ampicillin resistance gene
ANOVA: Analysis of variance
AP: Anteroposterior
hAPP: Human amyloid protein precursor
BDNF: Brain-derived neurotrophic factor
BSA: Bovine serum albumin
CA1: Cornu ammonis area 1
CamKII: Ca^{2+} / calmodulin - dependent protein kinase II
cDNA: Complementary DNA
CFU: Colony-forming unit
CRE: cAMP response element
CREB: cAMP response element-binding protein
Ct: Threshold cycle
DABCO: 1,4-Diazabicyclo [2.2.2] octane
DAB: 3,3'-diaminobenzidine
DI: Discrimination index
DNA: Deoxyribonucleic acid
DV: Dorsoventral
ERK: Extracellular signal-regulated kinase
FBS: Fetal bovine serum
FGF2: Fibroblast growth factor 2
FGFR: Fibroblast growth factor receptor
GAP: GTPase-activating protein
GDI: GDP dissociation inhibitory
GDP: Guanosine diphosphate
GPCR: G protein-coupled receptor
GPR domain: G protein regulatory domain
GTP: Guanosine triphosphate
LB: Lennox broth
LTD: Long-term depression
LTM: Long-term memory
LTP: Long-term potentiation
MALDI-TOF: Matrix-assisted laser desorption/ionization Time-of-Flight
MAPK: Mitogen-activated protein kinase
MAPKK (MKK): Mitogen-activated protein kinase kinase
MCS: Multiple-cloning site
MEM: Eagle's minimum essential medium
ML: Mediolateral
mRNA: Messenger ribonucleic acid
MTL: Medial temporal lobe
NGF: Nerve growth factor
O.D: Optical density
ORM: Object recognition memory
PBS: Phosphate buffered saline
PBST: PBS Tween-20
PCR: Polymerase chain reaction
PDGF: Platelet-derived growth factor B chain promoter
PFC: Prefrontal cortex
PI3K: Phospatidyl inositol-3 kinase
PKA: Protein kinase A or cAMP-dependent protein kinase
PLC-γ: Phospholipase C-gamma

PLP: Periodate-lysine-paraformaldehyde

PRh: Perirhinal cortex

Puro^{r}: Puromycin resistance gene

p-value: Error probability value

PVDF: Polyvinylidene difluoride

qRT-PCR: Quantitative reverse transcription PCR

r: Correlation coefficient

RACK1: Activated protein kinase 1

RBD domain: Raf-like Ras binding domains

RGS: Regulator of G protein signaling

RNA: Ribonucleic acid

Rpl19: Ribosomal protein L19

RT: Reverse transcription reaction

SDS-PAGE: Sodium dodecyl sulfate polyacrylamide gel electrophoresis

ssDNA: Single-stranded DNA

STM: Short-term memory

TGS: Tris-glycine-SDS buffer

TBE: Tris-boric acid-EDTA buffer

TrkA receptor: Tropomyosin receptor kinase A

TrkB receptor: Tropomyosin receptor kinase B

Tukey's HSD test: Tukey's honest significant difference test

V2: Secondary visual cortex

WB: Western blot

2-DE: Two-dimensional electrophoresis

TABLE OF CONTENTS

I. INTRODUCTION

1 Regulator of G protein signaling 14 (RGS14)

RGS14 is a protein that belongs to a family of more than 30 members (Ishii & Kurachi 2003; Koelle 1997). All RGS proteins share a 120-130 amino acids long RGS domain at N-terminal. RGS domain binds GTP-bound Gα subunit of activated heterotrimeric G proteins and acts as a GTPase-activating protein (GAP) to catalyze GTP hydrolysis and disrupt G-protein-coupled receptor (GPCR) signaling (De Vries et al 2000; Hollinger & Hepler 2002; Ross & Wilkie 2000; Woodard et al 2015) (figure 1). A selective attenuation in GPCR signaling is accomplished through binding with distinct isoforms of Gα subunits (Arshavsky & Pugh 1998; Berman & Gilman 1998; Berman et al 1996; De Vries & Farquhar 2002; Hepler 1999; Hollinger & Hepler 2002; Neubig & Siderovski 2002; Ross & Wilkie 2000; Tesmer et al 1997). In contrast to other RGS, RGS14 engages with Gαi/o subfamily to promote GTP hydrolysis (Cho et al 2000; Hollinger et al 2001; Traver et al 2000; Traver et al 2004).

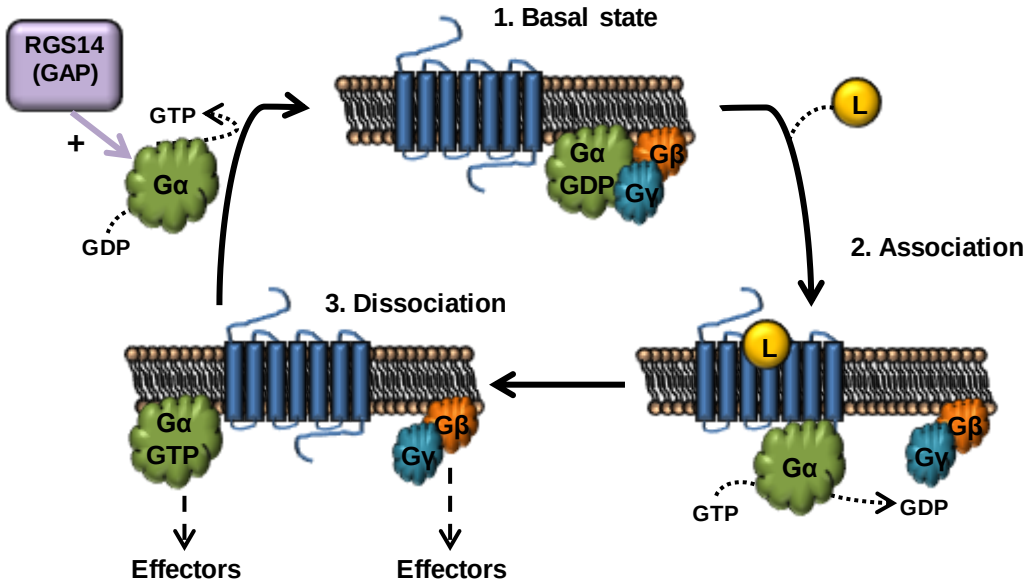

Figure 1. Heterotrimeric G-protein signaling. Classically defined G protein signaling begins with a heterotrimeric G protein (Gαβγ) bound to a G protein-coupled receptor (GPCR). GPCR activation promotes GDP release and subsequent GTP binding to activated Gα. Activation of Gα leads to dissociation of the heterotrimeric complex and allows Gα and Gβγ to interact with downstream effectors. As a GTPase, the α-subunit then rapidly initiates its own inactivation through GTP-hydrolysis and returns to its basal state (Gα-GDP), which leads the reassociation of the three subunits with a GPCR. RGS proteins with GAP activity accelerates GTP hydrolysis of Gα subunit regulating the G protein signaling (Oldham & Hamm 2008).

RGS14 is a multidomain protein, which apart from RGS domain contains a C-terminal G protein regulatory (GPR; also known as GoLoco) motif of ≈ 20 amino acids, and two central tandem Raf-like Ras binding domains (RBD), RBD1 and RBD2. (Kimple et al 2001; Siderovski et al 1999) (figure 2). Through GPR motif, RGS14 selectively binds inactive isoforms of $G_{\alpha i1}$-GDP or $G_{\alpha i3}$-GDP to inhibit GDP dissociation (GDI). This activity leads to

avertion of its activation and targeting to the plasma membrane (Kimple et al 2001; Kimple et al 2002; Mittal & Linder 2004; Shu et al 2007; Willard et al 2004). Phosphorylation of RGS14 at threonine 497 by protein kinase A (PKA) enhances its GDI activity (Hollinger et al 2003). In addition, through its RBD1 domain, RGS14 binds activated forms of H-Ras and Rap2 allowing RGS14 to engage H-Ras signaling pathways such as Ras/Raf/MAP kinase (Formstecher et al 2005; Kiel et al 2005; Mittal & Linder 2006; Shu et al 2010; Traver et al 2000; Willard et al 2009; Wohlgemuth et al 2005). At present, binding partners of RBD2 are unknown. Due to the presence of several binding domains, RGS14 has been considered as a scaffold protein with multiple functions. This idea is further strengthened by a dynamic spatial and temporal distribution pattern of RGS14 across the whole brain and even in different cellular compartments (Evans et al 2014; Lopez-Aranda et al 2006; Shu et al 2007). Northern blot experiments (Snow et al 1997), *in situ* hybridization studies (Grafstein-Dunn et al 2001), and quantitative polymerase chain reaction (qPCR) (Larminie et al 2004) have independently reported that RGS14 mRNA is present in rat and human brain tissue. Similarly, immunohistochemical studies (Lopez-Aranda et al 2006) and immunoblot experiments (Hollinger et al 2001) have shown that RGS14 protein is enriched in rat and monkey brain.

1.1 $RGS14_{414}$, a spliced variant of RGS14

A human RGS14 gene spliced variant of 1245 base pairs (GenBank, AY987041) that encodes a RGS14 protein of 414 amino acids ($RGS14_{414}$) (Uniprot, O43566-5) was cloned in our laboratory from cortical brain cDNA library (see figure 2). In the current thesis work, we will focus on this gene because of its demonstrated role in recognition memory (Lopez-Aranda et al 2009). In contrast to complete human (GenBank, NP_006471.2) and rat (GenBank, NC_005116.4) genes, $RGS14_{414}$ represents a deletion of 153 amino acids at N-terminal within RGS domain. This deletion causes removal of GTPase activity, a process that is mediated through RGS domain. Apart from human, rodent RGS14 gene, which encodes a protein of 544 amino acids ($RGS14_{544}$), has often been used in studies (Lee et al 2010). However, considering not only the absence of crucial RGS domain for GTPase activity but also the presence of significant differences throughout the whole sequence (figure 3), we believe that mature protein of human $RGS14_{414}$ is very distinct from rat $RGS14_{544}$, and human $RGS14_{414}$ might be exclusively involved in brain functions that are not associated with GTP hydrolysis.

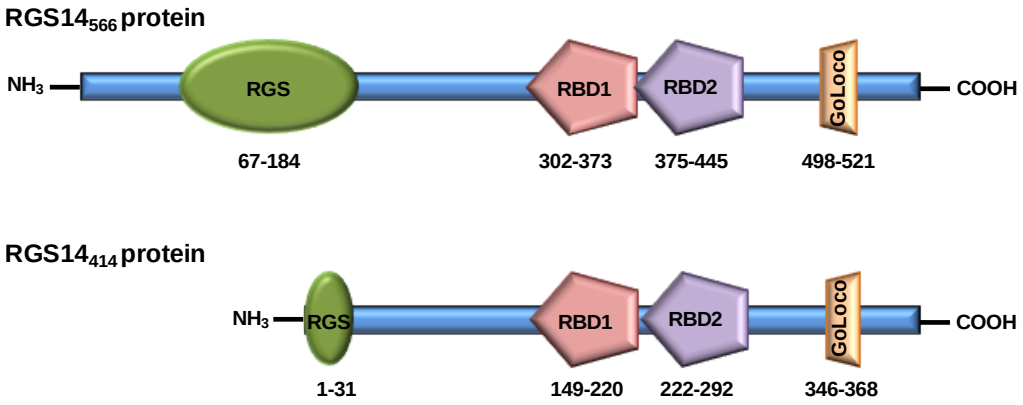

Figure 2. A graphic representation of human RGS14 protein.

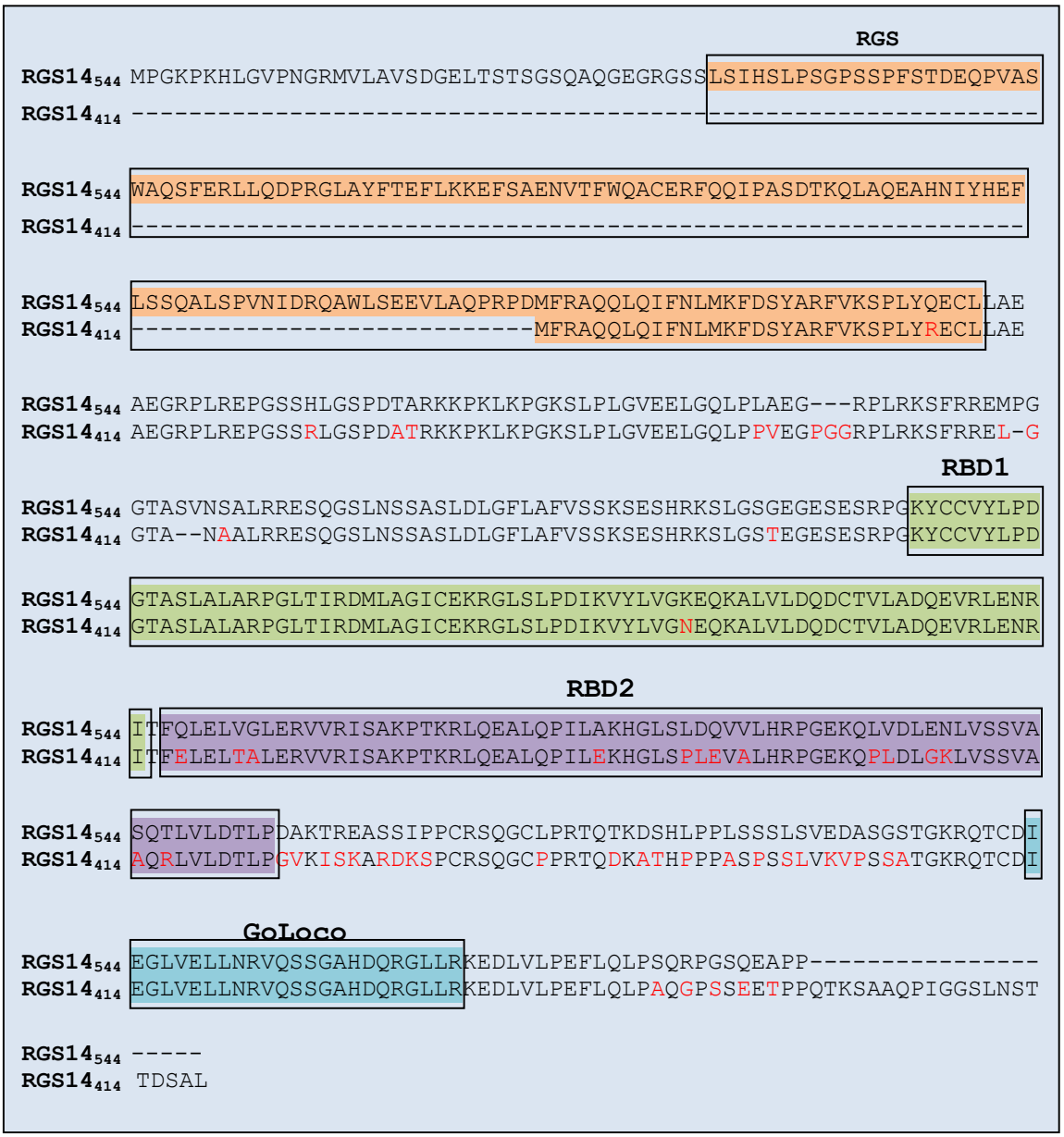

Figure 3. Comparison of human RGS14$_{414}$ with rat RGS14$_{544}$ protein.

2 Object recognition memory and $RGS14_{414}$

2.1 Object recognition memory (ORM)

Recognition memory is one of the most studied examples of episodic memory. Recognition memory is a process of identifying an object, a person, a place or an event that has been encountered previously. Recognition memory is widely viewed as consisting of two components: recollection and familiarity (Diana et al 2007; Yonelinas 2001; Yonelinas et al 2010). Interest in this distinction greatly increased when Brown and Aggleton (Brown & Aggleton 2001) proposed a neuroanatomical basis for these two processes. Their proposal was that recollection depends on the hippocampus, whereas familiarity relies on the adjacent perirhinal cortex. However, other researchers argue that recognition memory is a single process dependent on both the hippocampus and adjacent cortex (Donaldson 1996; Haist et al 1992; Squire et al 2004; Squire et al 2007).

Over the years, it has been shown that medial temporal lobe (MTL) is central to ORM processing. However, different subregions of the MTL make distinct contributions (Aggleton & Brown 2006; Eichenbaum et al 2007; Yonelinas et al 2002). Novel objects recognition on basis of simple features, such as size, shape or color relies on perirhinal cortex (Aggleton et al 1997; Barker et al 2007; Bussey et al 1999; Meunier et al 1993; Mumby & Pinel 1994), whereas hippocampus contributes to object recognition within familiar environment, such as location or context (Bachevalier et al 2015; Barbosa et al 2012; Barker & Warburton 2011; Bussey et al 2000; Hunsaker et al 2008; Lee et al 2005). In addition to MTL, other brain structures, such as medial prefrontal cortex (PFC) (Morici et al 2015) and area V2 of visual cortex (Lopez-Aranda et al 2009), have also been implicated in ORM processing.

2.2 $RGS14_{414}$ in ORM enhancement

A previous study from our laboratory showed that area V2, an area localized outside the MTL, plays a critical role in ORM. Stimulation of area V2 by overexpression of $RGS14_{414}$ led to robust memory enhancement. This effect on ORM was of such extent that converted an ORM normally lasting for 45 min into long-term memory that could be traced even after many months (Lopez-Aranda et al 2009). Furthermore, a selective elimination of area V2 neurons by an immunotoxin resulted in complete loss of normal as well as RGS14-mediated enhanced ORM. In addition to enhancement in memory, capacity to retain information on multiple objects was more than 3 fold higher in these animals. Normal rats could only retain

information of two objects, while RGS-rats were able to keep up to six objects. These findings suggest that $RGS14_{414}$ is a robust memory enhancer and this might be useful in treatment against memory loss.

3 Memory loss in aging and Alzheimer´s disease

Deficits in memory function has been observed not only in aging but also in many neurological and neurodegenerative diseases. However, here, we will describe two most studied conditions of memory loss: aging and Alzheimer´s disease (AD), because they will be part of this thesis work.

3.1 Aging

It has consistently been shown that in aging, there is substantial loss in episodic memories, such as ORM (Nilsson 2003), however in contrast, semantic memory, implicit or procedural memory (unconscious automated actions and movements) are relatively unaffected (Churchill et al 2003). Nevertheless, there is a disagreement on what kind of recognition memory is impaired in aging (Koen & Yonelinas 2014). Some studies have reported that aging and amnestic mild cognitive impairment (aMCI) are associated with specific recollection impairment but not familiarity-based episodic memory (Anderson et al 2008; Luo et al 2007; Westerberg et al 2013; Westerberg et al 2006; Yonelinas & Levy 2002). Whereas others have found that aging and aMCI are associated with declines in both recollection- and familiarity-based episodic memory (Friedman et al 2010; Peters & Daum 2008; Wang et al 2012; Wolk et al 2011). It is widely believed that this episodic memory loss in aging is not due to neurodegeneration in areas related to learning and memory (Burke & Barnes 2006; Morrison & Hof 1997; Rapp & Gallagher 1996; Rasmussen et al 1996; Wickelgren 1996), but it is caused by decrease in soma size (de Brabander et al 1998; Wong et al 2000), loss of dendrites and dendritic spines (Duan et al 2003; Jacobs et al 1997; Page et al 2002; Peters et al 1998), loss of synapses (Chen et al 1995; Wong et al 1998), aberration in neuronal networks and diminished synaptic activity (Khan et al 2014; Rizzo et al 2014; Wilson et al 2006).

3.2 Alzheimer's disease

Similar to normal aging, a loss in episodic memory in AD has also been reported (Ally et al 2009; Wolk et al 2011). The loss in episodic memory observed in AD is believed to be

due to a disruption in the communications between neurons caused by a neuronal synaptic loss and pruning of dendrites in temporal lobe and diencephalon. This neurodegeneration, specially in cholinergic neurons (Mufson et al 2008), has been related to different causes: high concentration of amyloid-β peptide (Kamenetz et al 2003; Puzzo et al 2008; Puzzo et al 2012; Shankar et al 2008) promoting formation of amyloid-β plaques; hyperphosphorylation of tau protein causing aggregation of neurofibrillary tangles (Alonso et al 2001) and disruption in microtubule assembly (Lindwall & Cole 1984). Microtubule assembly is necessary for the intracellular trafficking of neurotrophins and other functional proteins and a disruption in this process causes decrease in synaptic availability of molecular components crucial for memory processing (Salehi et al 2003).

4 Memory processing in brain

There are generally two kind of memories: short-term memory (STM), which lasts for minutes or longer (Castellucci et al 1989; Xia et al 1998); long-term memory (LTM), which can persist for days, months, even a lifetime (Bailey et al 1996; Castellucci et al 1989; Reissner et al 2006; Sangha et al 2003). Unlike STM that is usually mediated by posttranslational modifications, LTM requires protein synthesis and long-lasting changes in synaptic transmission, including long-term potentiation (LTP) and depression (LTD). It has been argued that these underlying processes of LTM produces structural changes for the formation of neural circuits that encode representations of memory (Bailey & Kandel 2008; Bosch et al 2014; Caroni et al 2012; Lamprecht & LeDoux 2004). There are large number of molecules and pathways that have been implicated in memory; however, we will focus here on some that are pertaining to this thesis work.

4.1 Neuronal structural remodeling

A tremendous level of structural plasticity which characterizes mammalian brain, is believed to underline the ability to extract and store information about past experiences and is crucial for animals and human to form long-lasting memories (Bailey et al 2015; Bosch et al 2014; Fu & Zuo 2011). In fact, impairments in the active remodeling have been related with memory loss observed in aging and AD (Badhwar et al 2013; Bloss et al 2011; Selkoe 2002; Spires-Jones & Knafo 2012). Dendrites of a neuron are the sites of most synaptic contacts in different cortical and subcortical brain areas (Hofer et al 2009; Restivo et al 2009; Roberts et al 2010; Xu et al 2009; Yang et al 2009) and synaptic strengthening of these contacts is

thought to be a critical substrate for the acquisition and consolidation of long-term memories (Bailey & Kandel 1993; Yang et al 2009). In fact, changes in the length of neck of spine, in dendritic spine volume, in dendritic turnover through the loss and/or addition of dendrites have been related with learning and memory (Lamprecht & LeDoux 2004; Segal 2005). In recent years, neurotrophic factors and its signaling cascades have been shown to be linked to remodeling of neuronal dendrites via dendritic branching (Kopec & Carew 2013; McAllister et al 1999).

4.2 Neurotrophic factors

Neurotrophic factors are secreted molecules which bind membrane-associated extracellular receptors and activate intracellular signaling cascades that ultimately promotes cellular survival, neurogenesis, synaptogenesis and activity-dependent pruning, including axon outgrowth, dendritic growth and dendrite maturation (Dijkhuizen & Ghosh 2005; Horch & Katz 2002; Ji et al 2005; Park & Poo 2013). Neurotrophic factors have been shown to be involved in induction of long-lasting synaptic plasticity (Conner et al 2009; Chao 2003; Egan et al 2003; McAllister et al 1999; Poo 2001) and protein synthesis (Tanaka et al 2008), activities fundamental for the formation of LTM. Considering that there is a large list of neurotrophic factors (Kopec & Carew 2013), we have restricted to some of them which are found abundant in brain and have been shown to be related to structural plasticity and memory, and are pertaining to this thesis work.

4.2.1 Fibroblast growth factor 2 (FGF2)

In the central nervous system, FGF2 is the most abundant member of FGF family. It has been shown that FGF2 is localized in several brain areas (Bean et al 1991; Gonzalez et al 1995; Grothe & Janet 1995) and is present in both types of brain cells: neurons and glial cells (Eckenstein et al 1991). Like other members of FGF family, it acts through specific fibroblast growth factor receptor (FGFR). However, FGF2 has highest affinity for FGFR1 (Ornitz et al 1995). Functions of FGF2 have been mainly studied in hippocampus, where it plays an important role in neurogenesis (Cheng et al 2002; Gomez-Pinilla et al 1994; Raballo et al 2000), in induction of LTP form of synaptic plasticity (Zhao et al 2007) and in spatial learning (Gomez-Pinilla et al 1998). FGF2 has also been related to axonal and dendritic branching in cortical structures (Comeau et al 2007; Szebenyi et al 2001).

4.2.2 Nerve growth factor (NGF)

NGF has been found in hippocampus, cerebral cortex, olfactory regions and forebrain (Korsching et al 1985; Large et al 1986; Levi-Montalcini & Angeletti 1968). It binds to tropomyosin receptor kinase A (TrkA) and induces neuronal survival, neurite outgrowth and synaptic plasticity (Barrett 2000; Chao & Bothwell 2002; Dechant & Barde 2002; Miller & Kaplan 2001). NGF contributes to changes in neuronal networks by promoting formation of newer dendritic spines in mature brain (Alleva & Aloe 1989). In fact, NGF not only is indispensable for the survival of basal forebrain cholinergic neurons (Allard et al 2012; Chen et al 1997; Niewiadomska et al 2011; Van der Zee et al 1995), but also is crucial for cholinergic connections in insular cortex and subsequent acquisition of new memories associated to conditioned taste aversion and contextual fear conditioning (Gutierrez et al 1997). Also, septal NGF and its receptor TrkA in CA1 are required for hippocampal LTP (Conner et al 2009), spatial memory (Conner et al 2009) and fear memory consolidation (Woolf et al 2001).

4.2.3 Brain-derived neurotrophic factor (BDNF)

BDNF and its receptor tropomyosin receptor kinase B (TrkB) are widely expressed in brains of rodent and human, with higher expression in hippocampus and cerebral cortex (Aid et al 2007; Maisonpierre et al 1990; Timmusk et al 1994). BDNF is secreted from neurons and glial cells, and binding of this neurotrophic factor with its receptor TrKB activates several signaling pathways, including Ras/mitogen-activated protein kinase (Ras/MAPK), phospholipase C-gamma (PLC-γ) and phospatidyl inositol-3 kinase/protein kinase B (PI3K/AKT) (Andero et al 2014; Chao 2003). Many works have demonstrated the function of BDNF in dendritic remodeling of cortical neurons; in regulation of dendritic outgrowth and branching; in increment of proximal dendrite growth and spine density; in rise in number of pyramidal and non-pyramidal neurons during development and in adult brain (Horch 2004; Horch et al 1999; Jin et al 2003; Wirth et al 2003). Also, BDNF expression has been revealed to be essential for the maintenance of dendritic structure and the size of cortical neurons in adult brain (Gorski et al 2003).

Apart from participation in neuronal structural events, BDNF has also been found to be implicated in activity-dependent LTP formation and maintenance (Lu 2003; Poo 2001; Tongiorgi 2008; Tongiorgi & Baj 2008). Enhanced BDNF signaling leads to local synaptic protein synthesis and that in fact, is thought to cause facilitation of activity-dependent

plasticity in a synapse-specific manner (Bramham & Messaoudi 2005). BDNF is required for both STM and LTM formation of inhibitory avoidance learning (Alonso et al 2002). In addition, this neurotrophic factor contributes to acquisition and storage of long-lasting memories (Andero et al 2014; Bekinschtein et al 2008a; Bekinschtein et al 2014) and to spatial and contextual fear memory (Alonso et al 2002; Koponen et al 2004; Linnarsson et al 1997; Mizuno et al 2000; Tyler et al 2002). BDNF is required at early time points during formation of inhibitory avoidance LTM, for regulation of phosphorylated state of synaptic proteins and their persistence through new protein synthesis (Bekinschtein et al 2007; Bekinschtein et al 2008b). Furthermore, an increase in BDNF was observed within 2 h of the acquisition of object information (Romero-Granados et al 2010). A BDNF V(66)M polymorphism, which significantly hampers memory performance in human, has been shown to be linked to an impairment in episodic memory (Kauppi et al 2013). In contrary, exercise boosts spatial memory through an increase in BDNF transcripts I and IV in hippocampus (Intlekofer et al 2013).

4.3 14-3-3ζ protein

This scaffolding protein is a member of 14-3-3 protein family of seven and is widely expressed in mammal brain (Aitken 2006). This protein family is one of the major constituents in brain, with almost 1 % of total cytosolic proteins. 14-3-3ζ is considered as a 'hub protein' because it interacts with many proteins and intercedes in several signaling pathways. Therefore, this protein participates in broad range of cellular functions, including learning and memory (Broadie et al 1997; Cheah et al 2012; Qiao et al 2014; Skoulakis & Davis 1996). In addition, 14-3-3ζ has been implicated in aging and several neurological diseases, including AD and schizophrenia (Shimada et al 2013; Umahara et al 2012). Dimeric as either heterodimeric or homodimeric, and monomeric forms of 14-3-3ζ protein interact with other proteins and modulate cellular functions (Aitken 2006; Sluchanko et al 2012; Sluchanko & Gusev 2012). This interaction usually involves phosphorylation of the interacting protein and in some cases the phosphorylation of 14-3-3 isoform itself (Aitken 2006). An *in-vitro* study demonstrated that phosphorylation of tau protein at Ser 214 by protein kinase A or protein kinase B augments its affinity for 14-3-3ζ binding up to 14 folds and this interaction ultimately inhibits the formation of tau aggregates seen in AD (Sadik et al 2009a; Sadik et al 2009b).

First evidence that related 14-3-3ζ with memory was done in Drosophila melanogaster where leonardo gene, a homologous of vertebrate 14-3-3ζ, is abundantly expressed in mushroom body neurons. Mutant Drosophila that lacked leonardo gene, showed significant decrease in capacity for olfactory memory but not for olfactory sensory (Philip et al 2001; Skoulakis & Davis 1996; 1998). Similarly, a study using mutant mice with deletion of 14-3-3ζ, displayed remarkably reduced capacity of spatial memory and ORM compared to their wild-type siblings (Cheah et al 2012). Furthermore, functional knockout mice of 14-3-3 in hippocampus presented impairments in associative memory and a deficit in LTP (Qiao et al 2014).

II. OBJECTIVES

Previously, we have shown that $RGS14_{414}$ is a robust memory enhancer and it produces an enduring effect on memory. We found that $RGS14_{414}$ gene treatment in area V2 of visual cortex led to a memory enhancement of such extent that it converted an object recognition memory normally lasting for 45 min into long-term memory that could be traced even after many months (Lopez-Aranda et al 2009). Therefore, considering this long-lasting effect of $RGS14_{414}$ on memory, we planted to study whether memory loss observed in rodent models of aging and Alzheimer´s disease can be prevented by $RGS14_{414}$ gene treatment or not. Next, we explored through various biological processes in brain to provide explanation of RGS-mediated memory enhancement in rodents. Following objectives were considered:

Objective 1: Examine the effect of $RGS14_{414}$ gene treatment on prevention of an episodic memory loss in aging and Alzheimer's disease.

A number of psychiatric and neurological disorders are associated with memory impairments; however Alzheimer's disease and aging related cognitive decline are the most studied examples of it. With the use of normal aging rats and transgenic mice of Alzheimer´s disease, we have evaluated whether RGS14 gene treatment into area V2 could serve as a therapeutic tool in prevention of episodic memory loss seen in aging and in many neurological and neurodegenerative diseases.

Objective 2: Determination of relationship between neuronal arborization and RGS14-mediated enhancement in ORM.

Considering the enduring effect of $RGS14_{414}$ protein on memory enhancement, we believe that this long-lasting effect are due to permanent structural change caused by surge in neuronal connections and enhanced neuronal remodeling. Therefore, in this objective, brains of RGS-animals were subjected to analysis of cell body neurites outgrowth in both pyramidal and non-pyramidal neurons and of proliferation in dendritic branching in pyramidal neurons.

Objective 3: Study of neurotrophic factors in RGS14-mediated memory enhancement.

Permanent structural plasticity that causes a long-term change in memory functions, such as seen in $RGS14_{414}$-treated animals, has often been associated with neurotrophic

factors. Thus, in this objective, we have studied the effect of RGS14 treatment on FGF2, NGF and BDNF, neurotrophic factors that are abundant in brain and are related with structural plasticity and memory.

Objective 4: Explore the implication of 14-3-3ζ in facilitation of RGS-mediated memory enhancement.

This objective was designed to explore into the regulation of neurotrophic factors and their relationship with structural plasticity and memory enhancement in RGS-animals. 14-3-3ζ was identified in proteomics analysis and in this objective we have focused on the role of this protein in RGS-mediated memory enhancement.

III. MATERIALS & METHODS

1 First block of experiments. Effect of $RGS14_{414}$ gene treatment on prevention of an episodic memory loss in aging and Alzheimer's disease

In this block, we have explored whether $RGS14_{414}$ gene treatment can prevent memory loss in aging and Alzheimer´s disease, because they are two most studied conditions where memory loss has consistently been observed (Drag & Bieliauskas 2010).

1.1 Experimental design

To achieve the objective, we have used rodent models of aging rats and transgenic mice of Alzheimer´s disease. A summary of methodological approach for this block of experiments is described in figure 4:

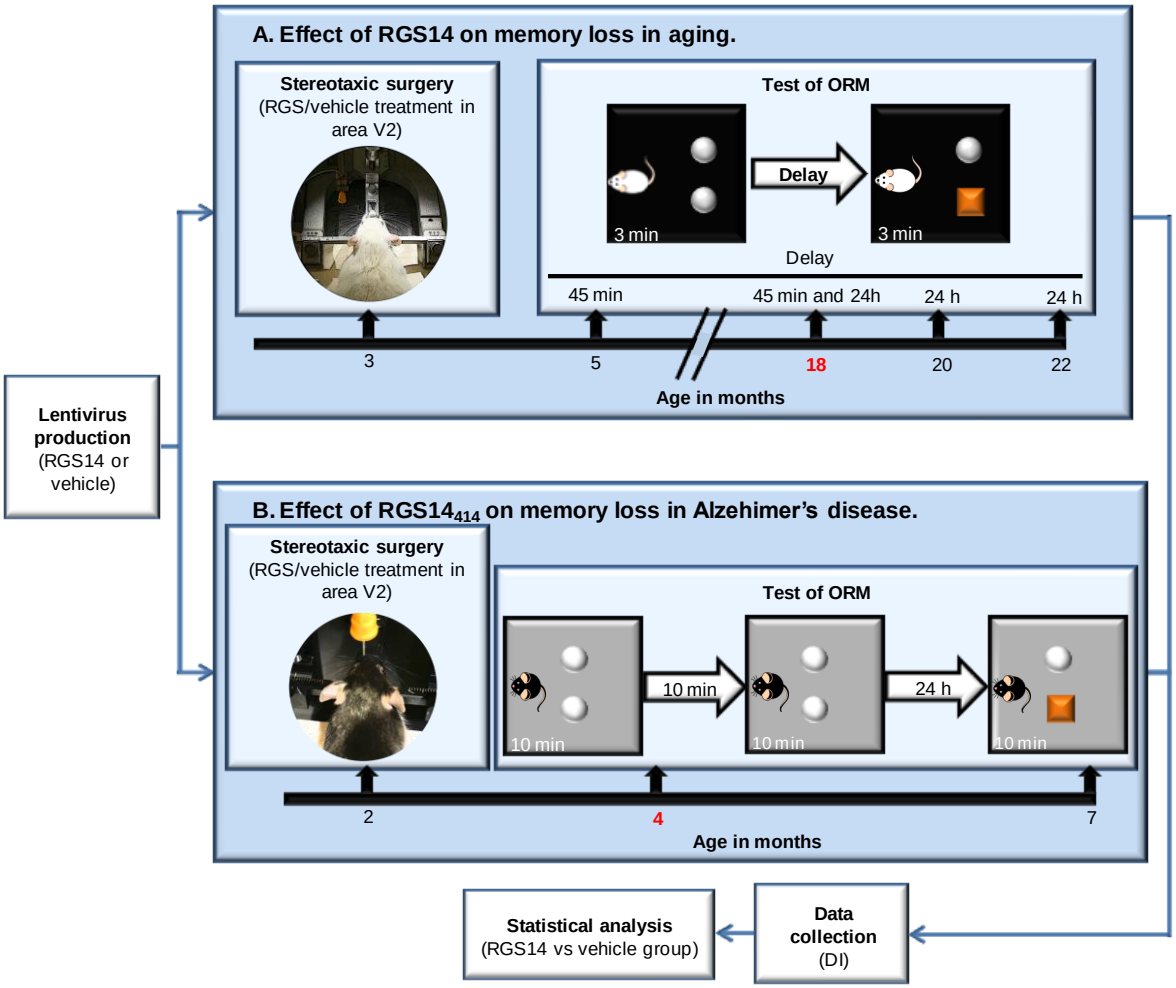

Figure 4. Scheme of experimental design (age of appearance of memory loss shown in red).

1.1.1 Effect of $RGS14_{414}$ on memory loss in aging

Male Wistar Han rats of 3 months and older were obtained from Charles River to be used in this study.

(i) One group of 12 rats was monitored for their ORM statuses from the age of 3 to 18 months to evaluate the age when memory loss emerges.

(ii) For the study of prevention of memory loss, 15 rats of 3 months old were treated with RGS14-lentivirus and 7 rats with vehicle-lentivirus and were further tested for ORM at ages of 5, 18, 20 and 22 months (figure 4.A).

1.1.2 Effect of $RGS14_{414}$ on memory loss in Alzheimer's disease

Transgenic mice with Alzheimer's disease of J20 line (AD-mice) were obtained from Jackson Laboratory. These mice overexpress human β-amyloid precursor protein (hAPP) with Swedish (K670N/M671L) and Indiana (V717F) familial AD mutations under control of platelet-derived growth factor B chain promoter (PDGF) (Mucke et al 2000). The mice were on an inbred C57BL/6J genetic background. For current study, in addition to AD-mice, we have used wild-type mice of C57BL/6J strain as control.

(i) 12 wild-type mice (C57BL/6J strain) and 8 AD-mice were tested for ORM status at ages of 2 and 4 months to monitor the age of appearnace of ORM loss.

(ii) For prevention study, twelve 2-month old AD-mice treated with RGS-lentivirus, 8 AD-mice treated with vehicle-lentivirus and 10 wild-type mice with no treatment were tested for ORM at ages of 4 and 7 months (figure 4.B).

1.2 Methods

1.2.1 Preparation of RGS14-lentivirus

A flow chart for the preparation of lentivirus is shown below:

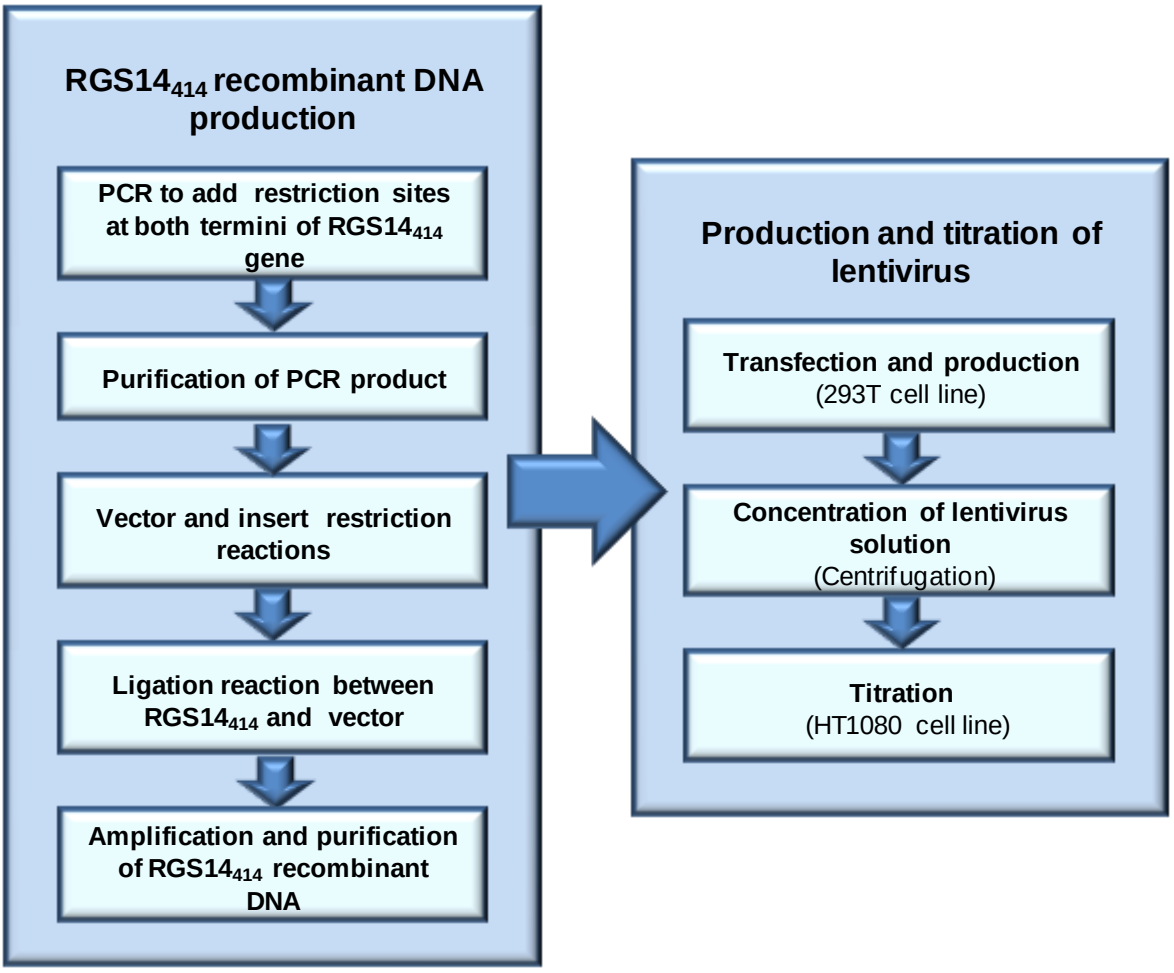

Figure 5. Scheme for the production of lentivirus containing $RGS14_{414}$ recombinant DNA.

1.2.1.1 Construction of recombinant $RGS14_{414}$

1.2.1.1.1 $RGS14_{414}$ gene

A 1245 base pair (bp) $RGS14_{414}$ gene was originally cloned from human brain (GenBank, AY987041) (Lopez-Aranda et al 2006), which translates to a protein of 414 amino acids (Uniprot, O43566-5).

1.2.1.1.2 Lentiviral plasmid

The plasmid *pLVX-DsRed-Monomer-C1* was obtained from Clontech (Cat. No., 632153) for insertion of $RGS14_{414}$ gene (figure 6.A). This vector is based on lentivirus HIV-1

and is 8800 bp long. $RGS14_{414}$ gene was cloned into multiple-cloning site (MCS) placed in the carboxyl terminus of DsRed-Monomer sequence. This vector allowed the expression of $RGS14_{414}$ gene fused to DsRed-Monomer, a monomeric mutant of the *Discosoma* specie red fluorescent protein, and therefore, facilitated the identification of RGS14-protein expression in brain cells.

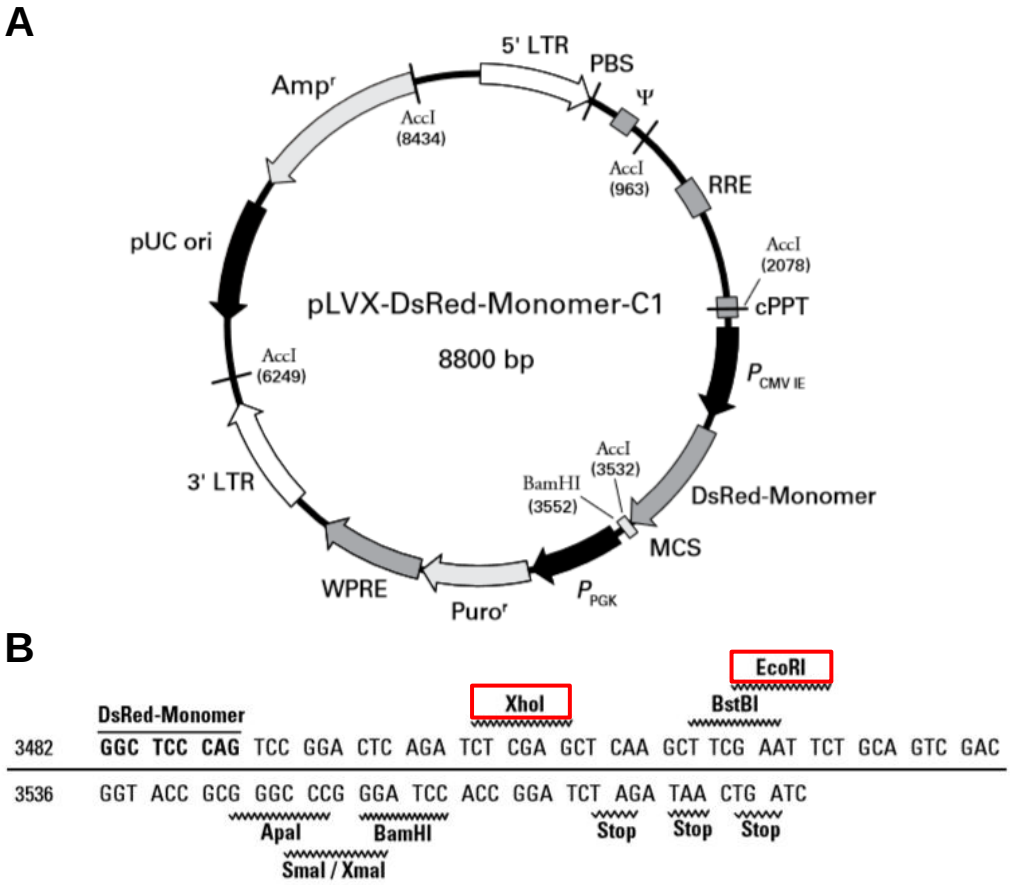

Figure 6. pLVX-DsRed-Monomer-C1. (A) pLVX-DsRed-Monomer-C1 vector map. The vector contains pUC sequence, the Escherichia coli replication origin and E. coli ampicillin resistance gene **(Amp^r),** for its amplification and selection in bacteria. Also, it includes puromycin resistance gene **(Puro^r)** under the control of the murine phosphoglycerate kinase **(PGK)** promoter **(PPGK)** for the selection of stable transductants eukaryotes cells. Moreover, this plasmid encompassed all of the viral processing elements necessary for the production of replication-incompetent lentivirus, as well as elements to improve viral titer, transgene expression, and overall vector function: the woodchuck hepatitis virus posttranscriptional regulatory element **(WPRE);** Rev-response element **(RRE);** central polypurine tract element **(cPPT);** primer binding site **(PBS)**; **LTRs** 3' and 5', long terminal repeats, which mediate integration of the retroviral DNA into any eukaryotic chromosome; and Psi packaging signal **(ψ)**. RGS14 gene is cloned in the multiple cloning site **(MCS)** placed in the carboxyl terminus of Ds-Red Monomer, a monomeric mutant of the Discosoma specie red fluorescent protein. The co-expression of both is controlled by the constitutively active human cytomegalovirus immediate early promoter **(PCMV IE). (B)** Multiple cloning site of pLVX-DsRed-Monomer-C1. XhoI and EcoRI endonucleases (both in red) were selected to clone $RGS14_{414}$**.** Image taken from Clontech datasheep.

1.2.1.2 **Amplification of RGS14$_{414}$ gene**

Prior to PCR, a restriction sites analysis of RGS14$_{414}$ gene was carried out by NEBcutter version 2.0 (New England Biolabs). Considering that both XhoI and EcoRI restriction sites of MCS of pLVX-DsRed-Monomer-C1 (figure 6.B) were absent in RGS gene, both were selected for cohesive end gene insertion.

A PCR was performed to include XhoI and EcoRI restriction sequences at 5' and 3' ends, respectively. Both forward (M103-XhoI), and reverse (M104-EcoRI) primers used in this reaction are shown in table 1 and were synthesized by Sigma Aldrich company. In addition to restriction sequence in forward primer, Shine-Dalgarne sequence (a ribosomal binding site in prokaryotic mRNA to initiate protein synthesis in prokaryotes) and Kozak sequence (a consensus sequence of eukaryotic mRNA necessary to initiate the translation process) were added to promote efficient protein synthesis of RGS gene.

Table 1. Primers to add XhoI and EcoRI restriction sites in RGS14$_{414}$.

PRIMER	SEQUENCE
[1]**M103-XhoI (forward)**	**5'-TACTC*TCGAGGAAGGAGATAGAACCATGGGATTTCGGGCA CAGCAGCTTCAGATC-3'**
[2]**M104-EcoRI (reverse)**	**5'-ACACG*AATTCGAGGGCTGAGTCGGTGGTGGA-3'**

[1]Xho target sequence in red; Shine Dalgarne sequence in purple and Kozak sequence in blue. Two underlined nucleotides were added to keep the open reading frame.
[2] *EcoRI target sequence in red.*
** shows the cleavage points of both endonucleases.*

The PCR was carried out using reagents from Promega (table 2) in *Sprint* thermocycler (Thermo Electro Corporation) as shown in table 3.

Table 2. PCR reaction.

REAGENT	VOLUME	FINAL CONCENTRATION
5X Go Taq® Flexi Buffer Mg free (Promega, Cat. No. M890A)	10 µl	1 X
$MgCl_2$ solution (25 mM) (Promega, Cat. No. A351B)	2 µl	1 mM
[1]**PCR Nucleotide Mix** (2 mM) (Promega, Cat No. C1141)	5 µl	0.2 mM
M103-XhoI (primer forward) (Sigma-Aldrich)	2 µl	0.4 µM
M104-EcoRI (primer reverse) (Sigma-Aldrich)	2 µl	0.4 µM
$RGS14_{414}$ cDNA (560 ng/µl)	0.5 µl	280 ng
GoTaq® g2 Flexi DNA polymerase (5 U/µl) (Promega, Cat. No. M78OA)	0.5 µl	2.5 U
Nuclease-Free water (Gibco, Cat. No. 10977)	28 µl	n/a
TOTAL VOLUME	**50 µl**	

[1] *2 mM of triphosphate deoxynucleotides (dNTPs) stock solutions means a final concentration of each dNTPs (dATP, dGTP, dCTP and dTTP).*

Table 3. Amplification cycles and temperatures.

STEP		TEMPERATURE	TIME
Initial denaturation		95 ºC	3 min
30 cycles	**Denaturation**	95 ºC	1 min
	Primer annealing	57 ºC	1 min
	Extension	72 ºC	3 min
Hold		4 ºC	--

1.2.1.2.1 Gel purification of PCR product

The PCR product from above was purified by 1 % agarose gel electrophoresis (see appendix 1.A.2). Samples mixed with 30 % glycerol in proportion 4:1 were loaded on gel, and separated with Tris-borate-EDTA (TBE) buffer (appendix 1.A.1) by applying 100 V power (Power-Pac 300, Bio-Rad). The DNA band was visualized under a long-wavelength UV light (Bio-Rad equipment *Gel Doc 2000*) (figure 7) and was excised using a sterile

scalpel and transferred to a previously weighted 1.5 ml tube. The weight of the excised band was 350 mg.

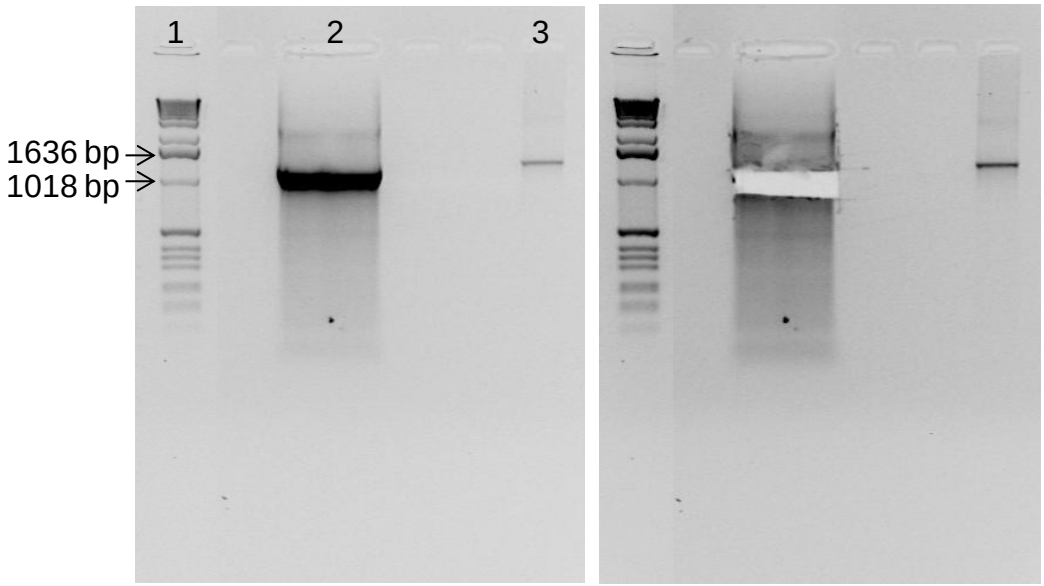

Figure 7. Electrophoresis of RGS14 DNA with restriction sites for XhoI and EcoRI to purify. (1) Molecular weight ladder, (2) $RGS14_{414}$ cDNA with endonuclease target sequence resulting from PCR (1283 bp) and (3) $RGS14_{414}$ cDNA used as PCR template (1245bp).

RGS DNA purification from excised gel was carried out following manufacture's protocol of *Wizard® SV Gel and PCR Clean-Up System kit* (Promega, Cat. No. A9281) with some modifications (see appendix 1.C.1). Recovered DNA solution (about 40 µl) with a final concentration of 55.63 ng/µl was stored at -20 ºC.

1.2.1.2.2 Restriction and ligation reactions

Compatible cohesive ends between $RGS14_{414}$ gene and pLVX-DsRed-Monomer-C1 were generated by XhoI and EcoRI endonuclease enzymes reaction as is shown in table 4. The reaction was carried out at 37 ºC in a thermostatic bath (SW22, Julabo) for 16 h in case of $RGS14_{414}$ gene and 4 h in case of vector. The endonucleases were inactivated by heating at 65 ºC in a dry block thermostat (Bio TDB-100, Boeco) for 20 min.

The DNAs resulting from restriction reactions were purified using agarose gel (figure 8) as explained in previous section (III.1.2.1.2.1) and their concentrations were determined by absorbance at 260/280 nm. The final concentration was 6.06 ng/µl in both cases.

Table 4. Restriction reaction of $RGS14_{414}$ and pLVX lentiviral vector.

REAGENT	VOLUME	
	$RGS14_{414}$ (55,63 ng/µl)	**pLVX (0,5µg/µl)**
DNA	1 µg (18 µl)	0.5 µg (1 µl)
XhoI (20000 U/ml) (New England Biolabs, Cat. No. R0146S)	1.5 µl (30U/µg DNA)	0.25 µl (10U/µg DNA)
EcoRI (20000 U/ml) (New England Biolabs, Cat. No. R0101S)	1.5 µl (30U/µg DNA)	0.25 µl (10U/µg DNA)
NEBuffer 2.1 (10X) (New England Biolabs, Cat. No. B7202S)	5 µl	2.5 µl
Nuclease-Free water (Gibco, Cat. No. 10977)	24 µl	25 µl
TOTAL VOLUME	**50 µl**	**25 µl**

To insert gene into the vector, a ligation reaction using the T4 DNA ligase (Life Technologies, Cat. No. 15224) was performed as it is detailed in table 5. All reagents, excluding the T4 ligase enzyme, were mixed previously and incubated at 45 ºC in the dry block thermostat (Bio TDB-100, Boeco) for 5 minutes to prevent non-specific binding between cohesive ends. After addition of ligase enzyme, the reaction was performed at 24 ºC for 1 hour. At the end of reaction, ligase enzyme was inactivated by incubation at 70 ºC for 10 min.

Table 5. Ligation reaction.

REAGENT	VOLUME
5X reaction buffer (Life technologies Cat. No. 46300-18)	4 µl
Gen $RGS14_{414}$ (6.06 ng/µl)	9.9 µl (60 ng)
pLVX vector (6.06 ng/µl)	3.3 µl (20 ng)
T4-Ligase enzyme (1 U/µl) (Life technologies, Cat. No. 15224)	1 µl
Nuclease-Free water (Gibco, Cat. No. 10977)	1.8 µl
TOTAL VOLUME	**20 µl**

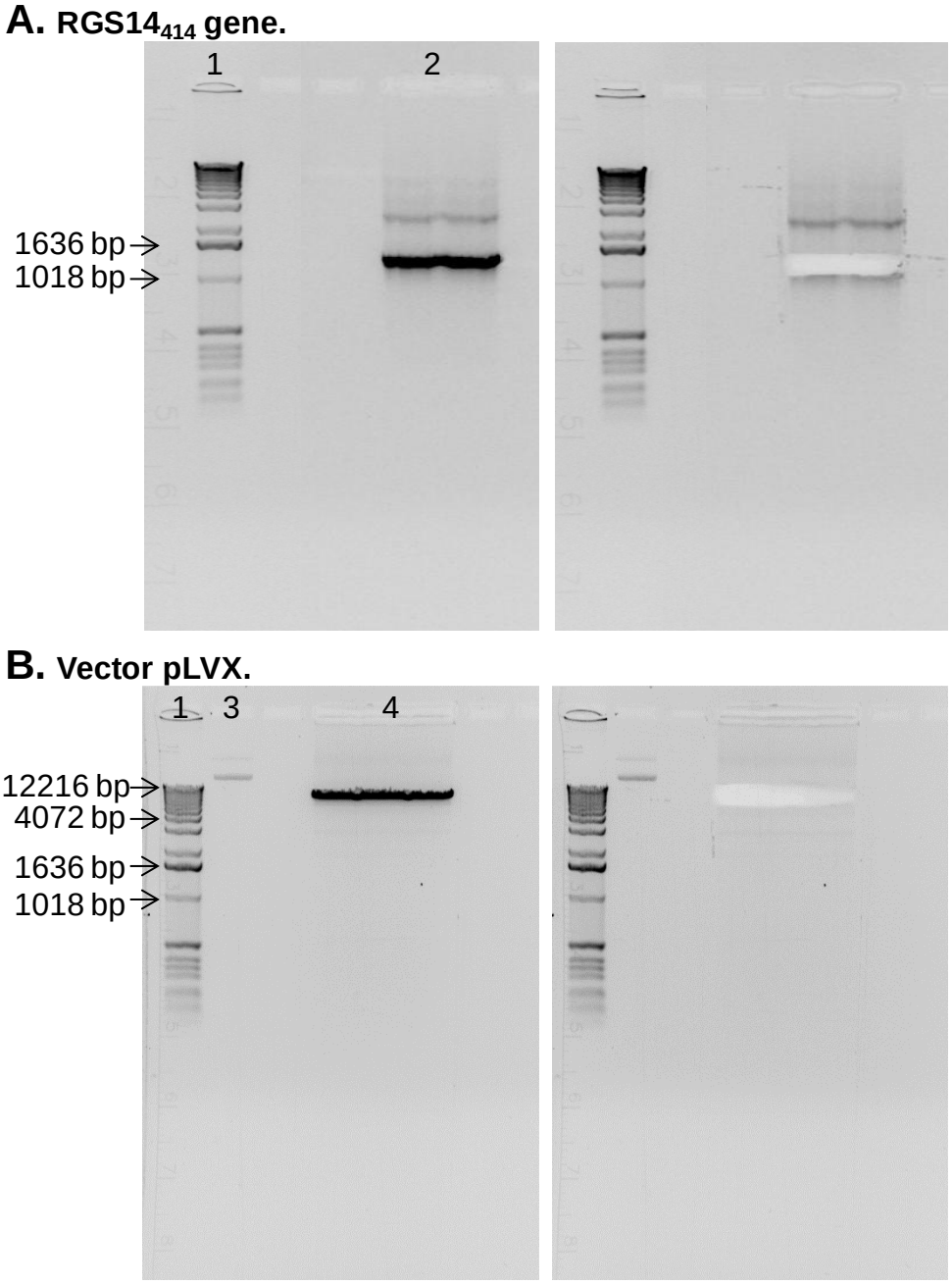

Figure 8. Electrophoresis of the RGS14 (A) and plasmid pLVX (B) cDNAs cut with XhoI and EcoRI. The gels on the right show the bands cut. (1) Molecular weight ladder, (2) $RGS14_{414}$ cDNA (1283 bp) restriction reaction, (3) pLVX cDNA without endonuclease cutting and (4) pLVX vector resulting from restriction reaction.

1.2.1.2.3 Transformation into *E.coli* and test of RGS gene insert

1.2.1.2.3.1 Transformation

With the goal to amplify, samples after ligation containing $RGS14_{414}$ recombinant DNA were transformed into One Shot® Omni Max™ 2 T1® Chemically Competent *E.coli*

(Life Technologies, Cat. No. C8540-03) by heat shock according to the manufacturer's protocol. In summary, 4 µl of the ligation product diluted 1:20, were added to a vial containing 50 µl of competent cells and gently mixed. The mixture was incubate on ice for 30 min and cells were heat-shocked for 30 s at 42 °C without shaking at the thermostatic bath SW22 (Julabo) to facilitate the entrance of DNA into *E. coli*. The vial was immediately returned to ice for 2 min and 250 µl of pre-warmed SOC medium was added to the transformed bacteria. This vial was incubated for 90 min at 37 ºC with shaking at 225 rpm in an orbital shaker incubator (Optic Ivymen System).

Aliquots of transformed bacteria (20, 50 and 200 µl) were spread on LB-Agar plates prepared with 100 µg/ml ampicillin (appendix 1.B.1) and were incubated for 18 h at 37 °C at an incubator (Incudigit, J.P Selecta). The ampicillin resistant colonies were then processed for miniprep to identify colonies expressing correct size of gene insert.

1.2.1.2.3.2 Miniprep

Among the grown colonies, four (Col. 1-4) were selected for the test of gene insert. Each colony was inoculated in 2 ml of LB liquid medium with 100 µg/ml ampicillin for 16 h at 37 ºC while shaking at 225 rpm in an orbital shaker incubator (Optic Ivymen System). An aliquot of each bacterial culture was spread on 90 mm diameter Petri plate of LB-agar with ampicillin. The plates were incubated for 24 h at 37 ºC and stored at 4 ºC as stock for further maxiprep preparations.

The rest of bacterial culture was processed to extract and purify recombinant DNA by using *StrataPrep plasmid miniprep kit* (Agilent technologies, Cat. No. 400761), following manufacturer's protocol with some modifications (appendix 1.C.2).

To test gene insert size in all 4 colonies, restriction reactions with XhoI and EcoRI enzymes were performed in each eluted recombinant DNA (see table 6). The restriction reactions took place for 16 h at 37 ºC. Then, 15 U of each enzyme was added and incubated at 37 ºC for additional 2 hours. Finally, the reaction was stopped by heating at 65 ºC for 20 min.

Table 6. Restriction reaction with XhoI and EcoRI endonucleases of DNA from miniprep.

REAGENT	VOLUME (for each colony)
DNA purified from Miniprep	5 µl
XhoI (20000 U/ml) (New England Biolabs, Cat. No. R0146S)	1.5 µl (30U/µg DNA)
EcoRI (20000 U/ml) (New England Biolabs, Cat. No. R0101S)	1.5 µl (30U/µg DNA)
NEBuffer 2.1 (10X) (New England Biolabs, Cat. No. B7202S)	2 µl
Nuclease-Free water (Gibco, Cat. No. 10977)	10 µl
TOTAL VOLUME	**20 µl**

The restriction products were loaded in a 1 % agarose gel (appendix 1.A.2) to visualize the result (figure 9.A), similar to as described in previous section (see III.1.2.1.2.1). As shown in figure 9.A, colonies 2 and 3 presented two main bands of 8.8 and 1.28 kbp, which corresponds to the vector pLVX and the $RGS14_{414}$ gene respectively. These results indicate that at least, colonies 2 and 3 retain the characteristics of vector as well as of RGS gene insert. For our future experiments, colony 2 was selected to proceed with the maxiprep and obtain a bigger amount of $RGS14_{414}$ recombinant DNA.

1.2.1.2.3.3 Maxiprep

Stored stock of bacteria of colony 2 was inoculated in 5 ml of LB liquid medium with 100 µg/ml ampicillin (appendix 1.B.1) for 8 h at 37 ºC with shaking at 225 rpm and then, this culture was added into a flask containing 300 ml of LB medium with ampicillin and further incubated at 37 ºC for 15 h, shaking at 225 rpm. A stock of bacteria with $RGS14_{414}$ recombinant DNA was prepared at this stage and stored at -80 ºC (appendix 1.B.2) for long-term use.

Maxiprep was done by using *Wizard ® Plus Maxiprep DNA Purification System kit* (Promega, Cat. No. A7270), following the manufacturer's protocol (appendix 1.C.3). After maxiprep, resultant $RGS14_{414}$ recombinant DNA concentration was 635 ng/µl. Aliquots of 20 µl of DNA solution were done in 20 in DNAase free tubes and stored at -80 ºC until their use. The integrity of RGS gene insert into vector was further examined by XhoI and EcoRI

restriction reaction as described previously (section III.1.2.1.2.3.2, table 6) (figure 9.B) and additionally by 5´and 3´ sequencing. The recombinant DNA obtained from colony 2 showed correct size and orientation of RGS gene insert. In addition, whole sequence was intact and showed no mutation (DNA sequencing was done by STAB VIDA; http://www.stabvida.net).

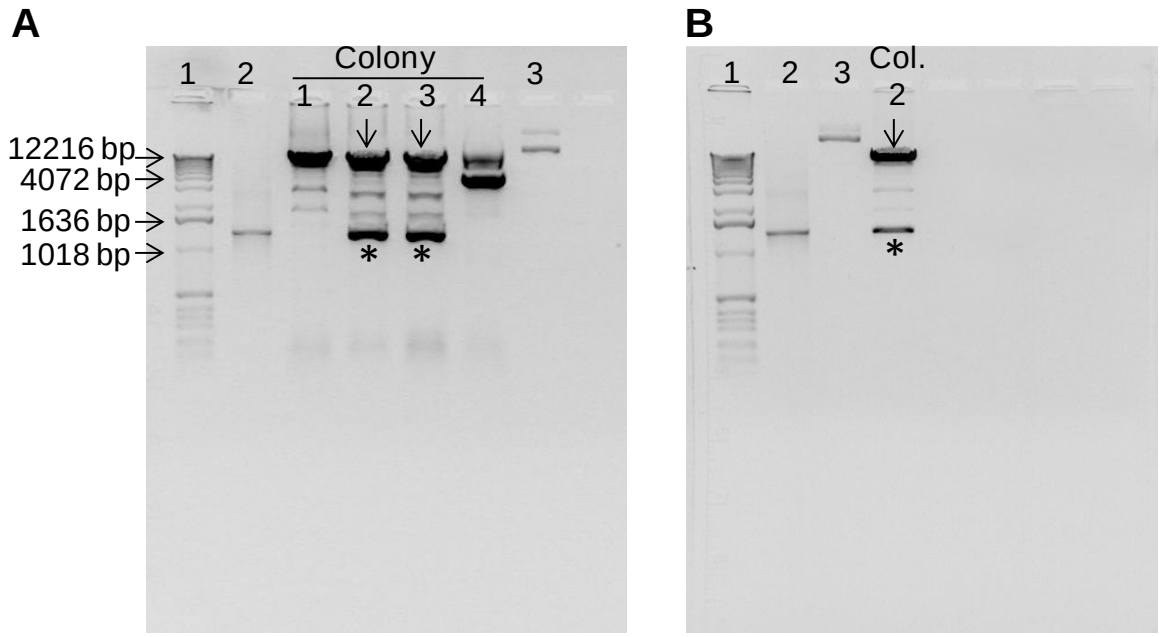

Figure 9. XhoI and EcoRI restriction reaction of DNA resulting of miniprep and maxiprep to prove the presence of $RGS14_{414}$ recombinant DNA. (A) Restriction reaction of miniprep from colonies 1-4, demonstrated that only, colonies 2 and 3 had included $RGS14_{414}$ recombinant. Thus, the restriction reaction generated two main bands of 8.8 and 1.280 kbp which correspond to the vector pLVX and the $RGS14_{414}$ gene respectively. Colonies 1 and 4 only had included the vector without the insert**. (B)** Restriction reaction of maxiprep from colony 2. Arrows indicate the vector pLVX and asterisks the $RGS14_{414}$ gene. Numbers 1, 2 and 3 indicate the molecular weight ladder, $RGS14_{414}$ as positive control and pLVX vector without endonucleases cutting respectively.

1.2.2 Production of lentivirus

1.2.2.1 Transfection of 293T cells and lentivirus collection

The lentivirus stock was produced in the 293T cell line (Clontech, Cat. No. 632180), a subclone of the transformed human embryonic kidney cell line, HEK 293, with type-5 human adenovirus. These eukaryotic cells are highly transfectable and support high levels of lentiviral protein expression (Pear et al 1993). A cryogenic tube (Nunc, Cat. No. 375418) containing 2.0 x 10^6 293T cells was thawed (appendix 2.C) and seeded in a 75-cm^2 culture flask (Nunc, Cat. No. 156499) with 10 ml of complete culture medium composed of: (i) 90 % Dulbecco's Modified Eagle's Medium (DMEM) with high glucose (4.5 g/L), 4 mM L-glutamine, 0.1 mM non-essential amino acids, 3.7 g/L sodium bicarbonate (Sigma-Aldrich,

Cat. No. D5796) and 1 mM sodium pyruvate (Sigma-Aldrich, Cat. No. S8636); (ii) 10 % Fetal Bovine Serum (Tet System Approved FBS); (iii) 1 % penicillin-streptomycin antibiotic (appendix 2.A.1). To facilitate cell attachment, flasks were pre-treated with a 0.3 % (w/v) gelatin solution (appendix 2.B). Cells were maintained in a 37 °C humidity incubator (5 % CO_2 and 21 % O_2). Complete culture medium was exchanged every 2 days and subcultures were performed when cells reached 80 %-90 % confluence (about 3-4 days; see appendix 2.E). A stock of 293T cell was prepared after first subculture and stored in liquid nitrogen for future use (appendix 2.D).

At the sixth subculture, 293T cells were seeded in two T175-cm^2 culture flasks (Nunc, Cat. No. 159910) with 25 ml of complete medium, with goal to obtain enough amounts of cells required for transfection with recombinant DNA. Both RGS-lentivirus and vehicle-lentivirus of empty vector were prepared by using *Lenti-X™ Packaging System* (Clontech, Cat. No. 631247) according to manufacturer's protocol. All steps were carried out according to biosafety level 2 instructions. In brief, 4.5 x 10^6 cells per plate were seeded in twelve 100-mm Petri plates (Corning, 734-1815) containing 10 ml of complete medium but without antibiotic. Here 6 plates were for control and other 6 were for RGS14. Cells were incubated in 5 % CO_2 incubator at 37 ºC for 24 h. Transfection solutions were prepared as shown in table 7. The polymer solution (tube 2) was mixed with the DNA solution (tube 1) and incubated for 10 min at room temperature to allow complex formation. Mixed solution of 1200 µl was added dropwise to cell culture plate and then, was gently rocked before incubating at 37 ºC in 5 % CO_2.

Table 7. Preparation of transfection solutions (volume per plate).

Tube 1 (DNA solution)	Tube 2 (polymer solution)
557µl **Xfect Reaction Buffer** (Clontech, 631317) 36 µl **Lenti-X HTX Packaging Mix** (Clontech, 631260) 11 µl **$RGS14_{414}$-pLVX (0.635 µg/µl)** **or** 14 µl **vector pLVX DsRed Monomer C1 0.5 µg/µl** (Clontech, 632153)	592.5µl **Xfect Reaction Buffer** (Clontech, 631317) 7.5µl **Xfect Polymer** (Clontech, 631317) ----------
TOTAL VOLUME 600 µl	**TOTAL VOLUME 600 µl**

Note: It is crucial that the Xfect Polymer does not remain in aqueous solution for longer than 30 min at room temperature.

After 24 h, transfection medium was replaced with 10 ml fresh complete cell culture medium and cell culture plates were incubated at 37 °C for an additional 48 h. During this period, transfected cells produce and release non-replicant lentivirus to medium. Therefore, lentiviral supernatants were harvested and pooled. Cellular debris was removed by centrifugation at 500 x g for 15 min at 4 ºC in CS15R Beckman centrifuge, followed by filtration of supernatants through 0.45 µm polysulfonic filter (Sarstedt, 831826). The lentiviral supernatants were maintained on ice during all the procedure.

Finally, to concentrate, lentiviral solutions were ultracentrifuged (Ichim & Wells 2011; Reiser 2000) at 25,000 rpm for 90 min at 4 ºC in *Ultra-Clear* tubes (Beckman Coulter, 344058) using Beckman XL-90 ultracentrifuge and SW29 rotor. Supernatants were discarded and 150 µl of sterile saline serum was added to pellet and placed at 4 ºC for overnight to facilitate the resuspension of lentivirus. Aliquots of 3.5 µl were prepared and stored at -80 ºC.

1.2.2.2 **Determination of lentivirus titer in HT1080 cell line**

The lentivirus titer was determined using HT1080 cells (ATCC, CCL-121), a cell line derived from human fibrosarcoma cell line. A cryogenic tube containing 1.1 x 10^6 HT1080 cells was thawed (appendix 2.C) and seeded in a 75-cm^2 culture flask (Nunc, Cat. No. 156499) with 10 ml of complete culture medium composed of: (i) 90 % (v/v) Eagle's Minimum Essential Medium supplemented with 1.5 g/L sodium bicarbonate (Sigma-Aldrich, Cat. No. D5796) and 1 mM sodium pyruvate (Sigma-Aldrich, Cat. No. S8636); (ii) 10 % (v/v) Fetal Bovine Serum; and 1 % (v/v) penicillin-streptomycin antibiotic (appendix 2.A.2). Cells were maintained in a CO_2 incubator at 37 °C. Complete medium was exchanged every 2 days and subcultures were performed when cells were 80 %-90 % of confluence (usually every 3 days) (appendix 2.E). At the second subculture, a stock of HT1080 cells was prepared and stored in liquid nitrogen for future use (appendix 2.D).

At fourth subculture, 2 x 10^5 cells were seeded in 2 ml per well of a 6-well plate (Nunc, Cat. No. 140675) and were incubated in CO_2 incubator for 24 h. For infection of HT1080 cells with concentrated lentivirus, 10x serial dilutions ranging from 10^{-3} to 10^{-7} were prepared in 1 ml complete medium and they were added in each well of 6-well plate together with one well as mock control, where lentivirus was replaced by complete medium. Cells were incubated in CO_2 incubator for 48 h. For the selection of transfected cells, culture medium

from 6-well plate was removed and replaced by 2 ml of complete HT1080 growth medium containing 1 µg/µl puromycin (Clontech, Cat. No. 631306). Since vector pLVX contains $Puro^r$ gene, transfected cells expressing this gene are expected to show resistance against this drug. In continuation, cells were incubated in this drug for 10 days with change of culture medium every two days. Survived cell colonies were stained in 1 % (w/v) crystal violet (Sigma Aldrich, Cat. No. C3886), 10 % (v/v) ethanol (JT Baker, Cat. No. 8025) solution. Cells were rinsed twice for 1 min in 1 ml of phosphate buffered saline (PBS) pH 7.4 (Gibco, Cat. No. 10010) to eliminate cellular debris, and then incubated in the stain solution for 10 min at room temperature. To remove staining solution, 3 washes of 1 min in PBS were done.

The titer in terms of colony-forming units (CFU) of lentivirus stock was estimated by calculating mean of the number of colonies generated by two least concentrated dilutions, multiplied by the dilution factor. As shown in figure 10, RGS-lentivirus titer was 1.75 x 10^7 CFU/ml, because 15 colonies were observed in well of 10^{-6} dilution and 2 colonies in 10^{-7} dilution. In contrast to RGS-lentivirus, vehicle-lentivirus titer was 2.75 x 10^6 CFU/ml.

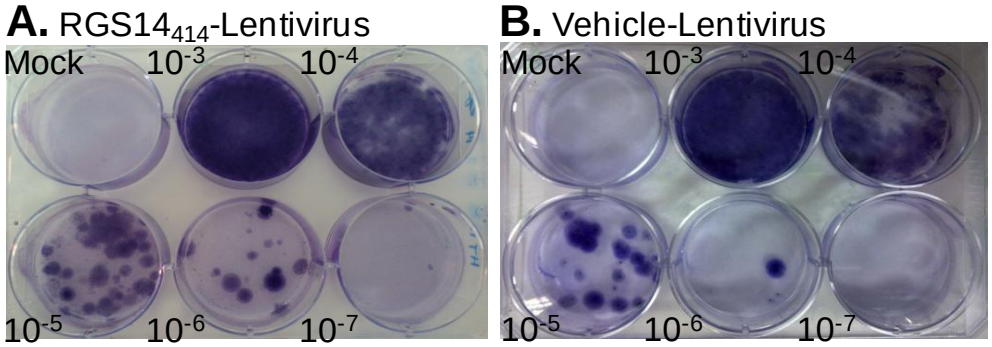

Figure 10. Titration of lentivirus stocks. (A) $RGS14_{414}$-lentivirus shows a titer of 1.75 x 10^7 CFU/ml and **(B)** vehicle-lentivirus presents a titer of 2.75 x 10^6 CFU/ml.

1.2.3 Animals

Rodents used in this study (see experimental design subsection for details, III.1.1) were housed individually in eurostandard cage with free access to food and water. Animals were housed in a temperature-controlled (20 ± 2 ºC) room on a 12 h light/dark cycle. All experimental procedures in animals were carried out in accordance with European and Spanish regulations (2010/63/EU, and RD53/2013). Research study performed in this thesis was approved by Committee of Ethics on Animals Use of University of Malaga (for rats) and University of Navarra (for transgenic mice).

1.2.4 Stereotaxic surgery

Approximately 4000 CFU in 2 µl (for rats) or 2000 CFU in 1 µl (for mice) of RGS-lentivirus or vehicle-lentivirus were delivered into area V2 of visual cortex by stereotaxic surgery (Cetin et al 2006; Cooley & Vanderwolf 2005; Fornari et al 2012), Before proceeding, animals were deeply anesthetized by administering intraperitoneally 75 mg/kg ketamine (Imalgene 1000; Merial Laboratorios) and 1 mg/kg (rats) or 0.5 mg/Kg (mice) of medetomidine (Domtor, Pfizer).

During surgery, animal body temperature was maintained with an electric blanket. Animals head was placed on the stereotaxic apparatus (Stoelting) as indicated in figure 11. For the surgery of mice, an adaptor (Cunningham mouse, Harvard Apparatus) was coupled.

The coordinates for injection in area V2 (see table 8) were taken from *The Mouse Brain in Stereotaxic Coordinates* (Paxinos & Franklin 2001) and *The Rat Brain in Stereotaxic Coordinates* (Paxinos & Watson 1998). In our experiments, anteroposterior (AP) and mediolateral (ML) coordinates are from bregma and dorsoventral (DV) from dura mater. To access the dura mater, the skull was perforated using a drill (Dremel), and the dura mater was punctured to prevent the carpule deviation.

Table 8. Rodent injection coordinates for area V2.

Rodent	Anteroposterior (AP)	Mediolateral (ML)	Dorsoventral (DV)
RAT	+ 4.3	- 2.1	- 1.9
MOUSE	- 2.3	-1.3	-0.7

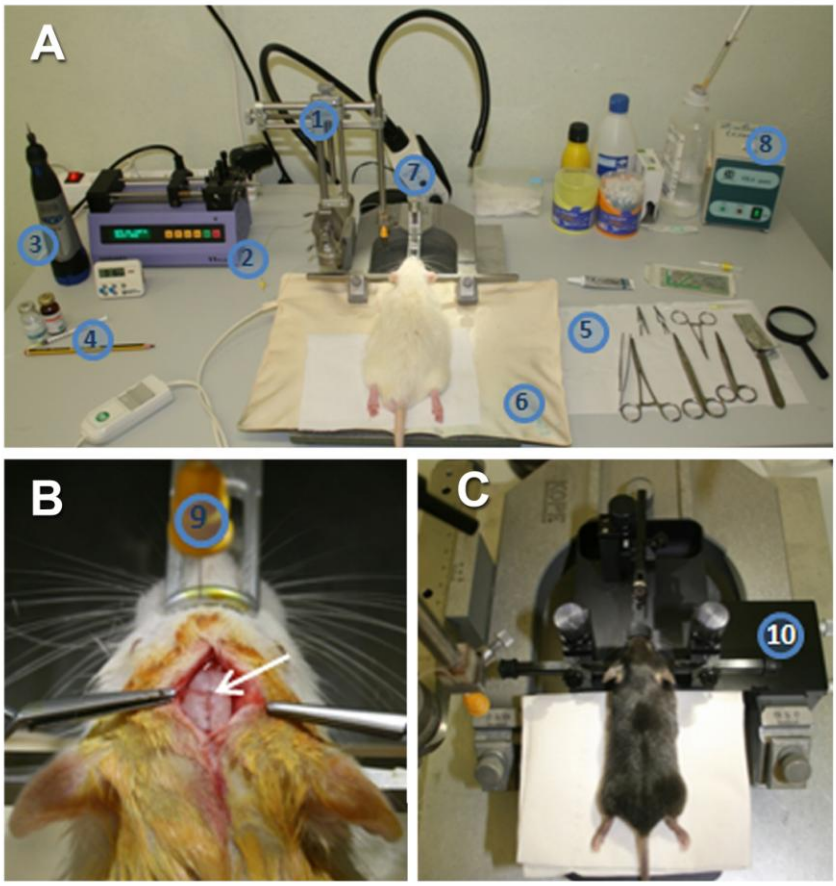

Figure 11. Illustration of the experimental setup for intracraneal lentivirus microinjection in rodents. (A) A picture representing a rat placed in the stereotactic frame. (**B)** A picture showing the bregma position (indicated by an arrow) in the rat skull. (**C)** A picture representing a mouse placed in the stereotactic frame. 1: stereotaxic apparatus; 2: infusion system; 3: drill; 4: anesthesia; 5: surgical instruments; 6: electric blanket; 7: cold light; 8: dry heat sterilizer; 9: dental carpule; 10: mouse stereotaxic adaptor.

The injection was carried out by a 30 G dental carpule (Heraeus Kulzer Iberia) connected to a 10 µl Hamilton syringe (Microliter^{TM} 701, Harvard Apparatus) through a plastic tube connector (Plastic One). Lentivirus was infused into area V2 at the rate of 10 µl/h using an infusion pump (11 Plus, Harvard Apparatus). Once the lentivirus injection was finished the carpule was maintained into the brain area for five more minutes to facilitate complete diffusion.

After stereotaxic surgery, animals were treated daily for 5 days with local antibiotic (Dermocan, Fatro) application on the incision and 150 µl intraperitoneal injection of Meloxicam analgesic (Metacam 5 mg/ml, Boehringer Ingelheim). After 21 days of injection and total recovery from the surgery, behavioral tests were performed in these animals.

1.2.5 Test of ORM

ORM test was used in our experiments to evaluate status of object memory in both rodent models. This test is based on spontaneous exploration and discrimination between novel and familiar objects (Ennaceur & Delacour 1988).

1.2.5.1 In rats

The protocol used for this study has been described previously (Lopez-Aranda et al 2009). In brief, prior to the task, rats were handled for 8 min during 5 consecutive days. This process included placing animals on arm, gently caressing on head and body with fingers, and moving up and down every 2 or 3 min by holding the whole body. Following this, rats were habituated with open field box, a black home-made square of 100 x 100 x 50 cm, where ORM test was going to take place. They were allowed to freely explore the open field for 12 min daily for 3 consecutive days. The day of ORM test, animals were left first to accommodate with test room for 1 h and then, test was performed in two steps as described below (figure 12):

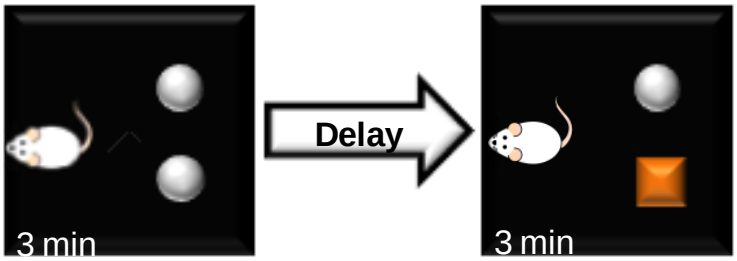

Figure 12. ORM test in rats.

(i) *Exposure to objects*. Two identical objects were placed at 30 cm distance from walls of open field box and animals were released into the box facing their nose towards the wall and opposite to the objects. They were allowed to explore the objects for 3 min.

(ii) *Discrimination of objects*. After a delay of 45 min or 24 h, animals were exposed to one familiar object (from above) and a novel object for 3 min. Novel and familiar objects were randomly placed on both sides to eliminate possible place preference.

Both steps were recorded with video camera and later were analyzed for exploration time. Open field box and objects were cleaned with 70 % (v/v) ethanol between each animal to eliminate interfering odor trails. Objects included in this study (appendix 3.A) showed no difference in previous object preference test.

1.2.5.2 **In mice**

We have followed the protocol for this work that has been done previously (Escribano et al 2009; Schiapparelli et al 2006). The handling and habituation of mice are similar to described before for rats except that the open field box was smaller (50 x 35 x 50 cm; Harvad Apparatus). Similar to rats, ORM test was done in two steps, but time of exploration for both steps was different (figure 13):

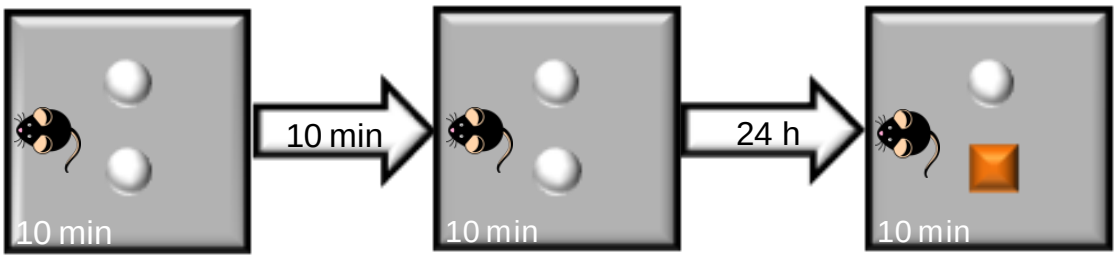

Figure 13. ORM test in AD-mice model.

(i) *Exposure to objects*. Two acquisition sessions of 10 min were done with 10 min apart. During each session, animals were allowed to explore two identical objects.

(ii) *Discrimination of objects.* After a delay of 24 h, animals were exposed for 10 min to one familiar object and a novel object.

The objects included in mice studies are shown in appendix 3.B.

1.2.6 Data analysis

Recorded videos were analyzed by investigators without any knowledge of which animal belongs to which group. Exploration time was computed by using the criteria of duration when animal touches the object with nose. Considering the data on time spent in exploration of each object, discrimination index (DI) was calculated as following, where N is exploration time of novel object and F is exploration time of familiar object:

$$\mathbf{DI = N / (N + F)}$$

DI value of 0.5 reflects equal exploration time of both familiar and novel objects and further suggests that animals were unable to keep the object information in memory. However a DI value above to 0.66 was considered that animals could retain the information in memory after a delay period.

DI values were presented as mean ± SEM and statistical analysis were performed using the software SigmaStat 3.5 (Jandel Scientific) with the purpose of detecting significant differences inter or intra-group accepting a 5 % error probability ($p \leq 0.05$). S*tudent's t-test* statistical analysis were run to compare DIs in aging study and ANOVA with the subsequent post-hoc pairwise comparisons using Tukey's HSD in case of AD study.

1.2.7 Immunohistochemistry

The expression of $RGS14_{414}$ protein into area V2 of rodent brains was confirmed by immunohistochemistry using a specific antibody (figure 14). This was performed similar to as described previously (Lopez-Aranda et al 2009). Details of the procedure are in appendix 4.

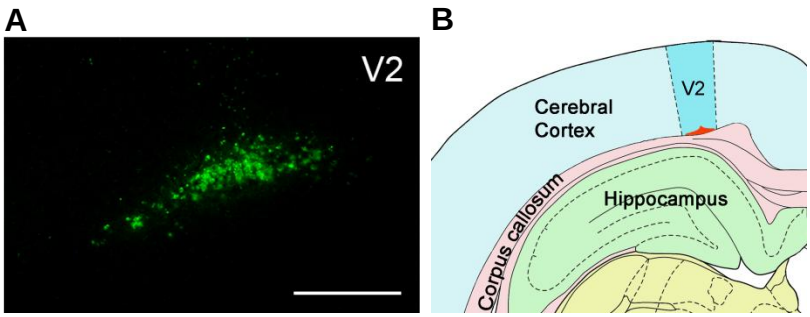

Figure 14. Confirmation of RGS14 protein expression in RGS14-treated rats. (A) Representative image illustrating expression of RGS14 by fluorescent immunohistochemistry in coronal brain sections of area V2 (V2). Bar represents 200 µm. **(B)** Schematic drawing representation of coronal section indicating the localization of RGS14 protein (in red) at the injection site.

2 Second block of experiments. Determination of a correlation between RGS-mediated enhanced object recognition memory and neuronal arborization

We posit that the enduring effect of $RGS14_{414}$ gene treatment is due to a permanent structural change rather than any short-lived activity in brain. Therefore, considering that this change in brain might be a key step to memory enhancement, we have intended to investigate RGS-mediated neuronal arborization of both pyramidal and non-pyramidal neurons.

2.1 Experimental design

Brains of young rats treated with RGS-lentivirus were subjected to Golgi-Cox staining with the goal to analyze neuronal arborization. A summary of methodological approach is shown in figure 15.

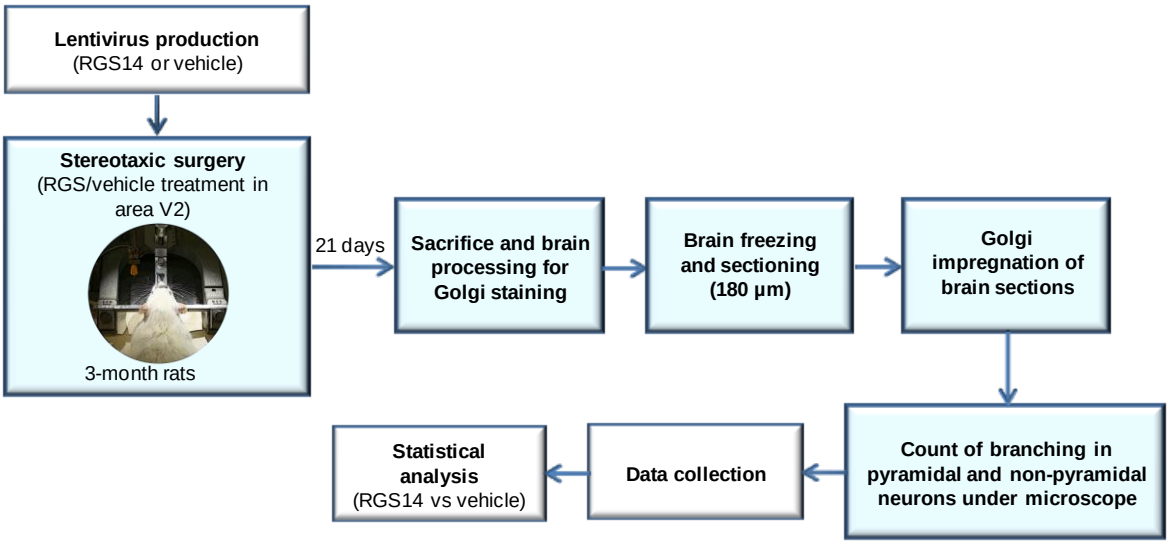

Figure 15. Scheme of experimental design.

2.2 Methods

2.2.1 $RGS14_{414}$ treatment and brain dissection

Eight 280-320 g male Wistar Han rats at age of 3-4 months were used in this study. Rats were housed and treated similar to as in Section I (see III.1.2.3). Four rats were injected with 2 µl of RGS-lentivirus and other four with vehicle-lentivirus (see subsection III.1.2.4 for details). Twenty-one days after treatment, animal were deeply anesthetized with 130 mg/ml sodium pentobarbital solution (Eutanax, Fatro; dosage: 0.5 g/Kg i.p) and decapitated. The brains were rapidly and carefully removed from skull and rinsed twice with saline serum to eliminate blood rests from the surface. Area V2 of these animals were dissected out in cubes of 1 cm and processed for Golgi staining.

2.2.2 Golgi-Cox staining

Golgi-Cox staining was performed using a Rapid GolgiStain kit (FD Neurotechnologies, Inc, PK401) following the manufacturer's protocol. All procedures were

done in light protection. Each dissected brain cubes were immersed in 20 ml of impregnation solution, which was prepared by mixing equal volumes of solutions A and B of the kit in a plastic container at room temperature, and the solution was replaced 24 h later and stored in dark for another 2 weeks. Then, brain cubes were transferred into solution C of the kit and stored at 4 ºC. After 24 h, solution C was replaced with fresh once and incubated for two additional days in the same conditions. Tissues were dipped for 1 min into iso-pentane (Sigma Aldrich, M32631) pre-cooled to -70 ºC and rapidly frozen in dry ice and stored at -80 ºC. For staining, 180 μm thick brain sections were cut on a cryostats (Leica, CM-1325), which were mounted on gelatin-coated slides (appendix 4.B) and dried at room temperature in darkness. Sections were rinsed twice in Milli-Q water for 2 min and incubated in freshly prepared staining solution for 10 min with frequent stirring. The staining solution was prepared by mixing solutions D and E of kit and Milli-Q water (1:1:2). Stained sections were rinsed twice in Milli-Q water and dehydrated by immersion for 4 min each in graded alcohols (50 %, 75 %, 95 % (v/v) and absolute ethanol (JT Baker, 8025) and finally in xylene solution (Sigma Aldrich, 33817). After the dehydration, the coverslips were placed on sections using a few drops of undiluted Permount mounting medium (Fisher Scientific, SP15-100).

2.2.3 Counting of neurites, neurites branching and dendritic branching

Golgi-Cox stained sections containing the treated area were analyzed under microscope *DM IRE2* (Leica Microsystems). For counting neurites and neuritic branching of both pyramidal and non-pyramidal neurons and dendritic branching of pyramidal neuron (figure 16), a *Leica MM AF version 1.6.0* (Leica Microsystems) software was used. A total of 55-56 of pyramidal and non-pyramidal neurons were studied in case of vehicle-lentivirus treated group and 56-79 neurons in RGS-lentivirus treated group.

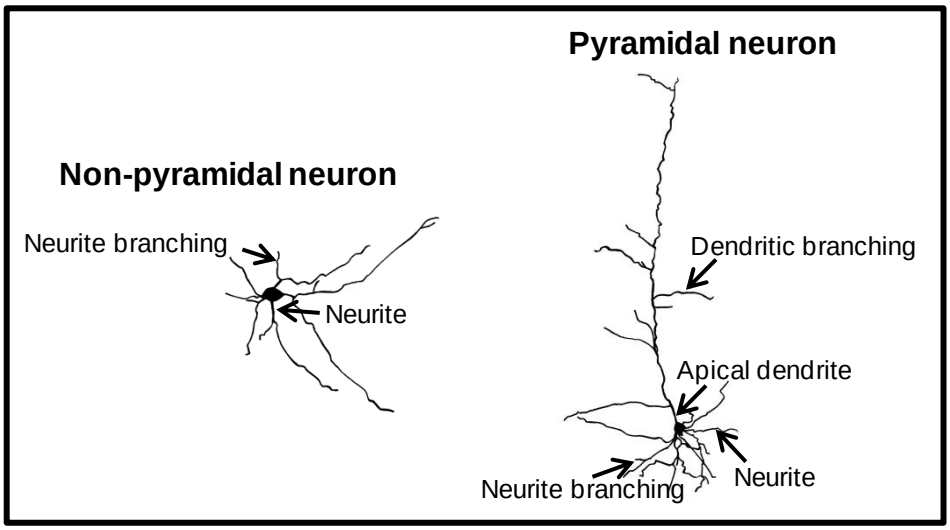

Figure 16. Nomenclature of pyramidal and non-pyramidal neurons branching.

2.2.4 Data analysis

The number of neurites, neurite branching or dendrite branching per pyramidal neuron or non-pyramidal neuron were presented as mean ± SEM and a Student's *t-test* (SigmaStat 3.5, Jandel Scientific) was run to identify significant differences between treatments ($p<0.05$).

3 Third block of experiments. Determining a relationship of RGS-mediated enhanced memory with neurotrophic factors

Neurotrophic factors are key to both neuronal growth, development of neural circuits, and learning and memory. Therefore, the aim of this section was to explore the possible role of neurotrophins in long-lasting memory enhancer effect of RGS14 gene treatment.

3.1 Experimental design

To test the implication of neurotrophic factors in RGS14-mediated memory enhancement, Wistar Han rats of 3-4 months old were treated in area V2 with either RGS or vehicle-lentivirus (from subsection III.1.2.2) by stereotaxic surgery (see subsection III.1.2.4 for details). These animals were housed and maintained as described in first block of experiments (subsection III.1.2.3). A scheme of experimental design is shown in figure 17.

(i) Neurotrophic factors in RGS-animals. After 21 days of injection, dissected brains of 2 animals treated with RGS and 2 with vehicle were used for the determination of mRNA levels of FGF-2, NGF and BDNF by quantitative reverse transcription polymerase chain reaction (qRT-PCR).

(ii) Effect of $RGS14_{414}$ treatment on brain-derived neurotrophic factor (BDNF). After a stereotaxic injection, a total of 16 animals were sacrificed at 4, 7, 14 and 21 days, where 2 RGS and 2 vehicle animals were included at each time point. BDNF protein levels were determined by Western blot (WB).

(iii) Dynamics of BDNF expression during object memory processing in RGS-animals. After 21 days of treatment, 8 rats of each treatment group were exposed to two identical objects for 3 minutes as detailed in section III.1.2.5.1, and then animals were sacrificed at 20 min, 40 min, 60 min and 24 h where 2 RGS and 2 vehicle animals were included at each time point. BDNF protein levels were analyzed by WB.

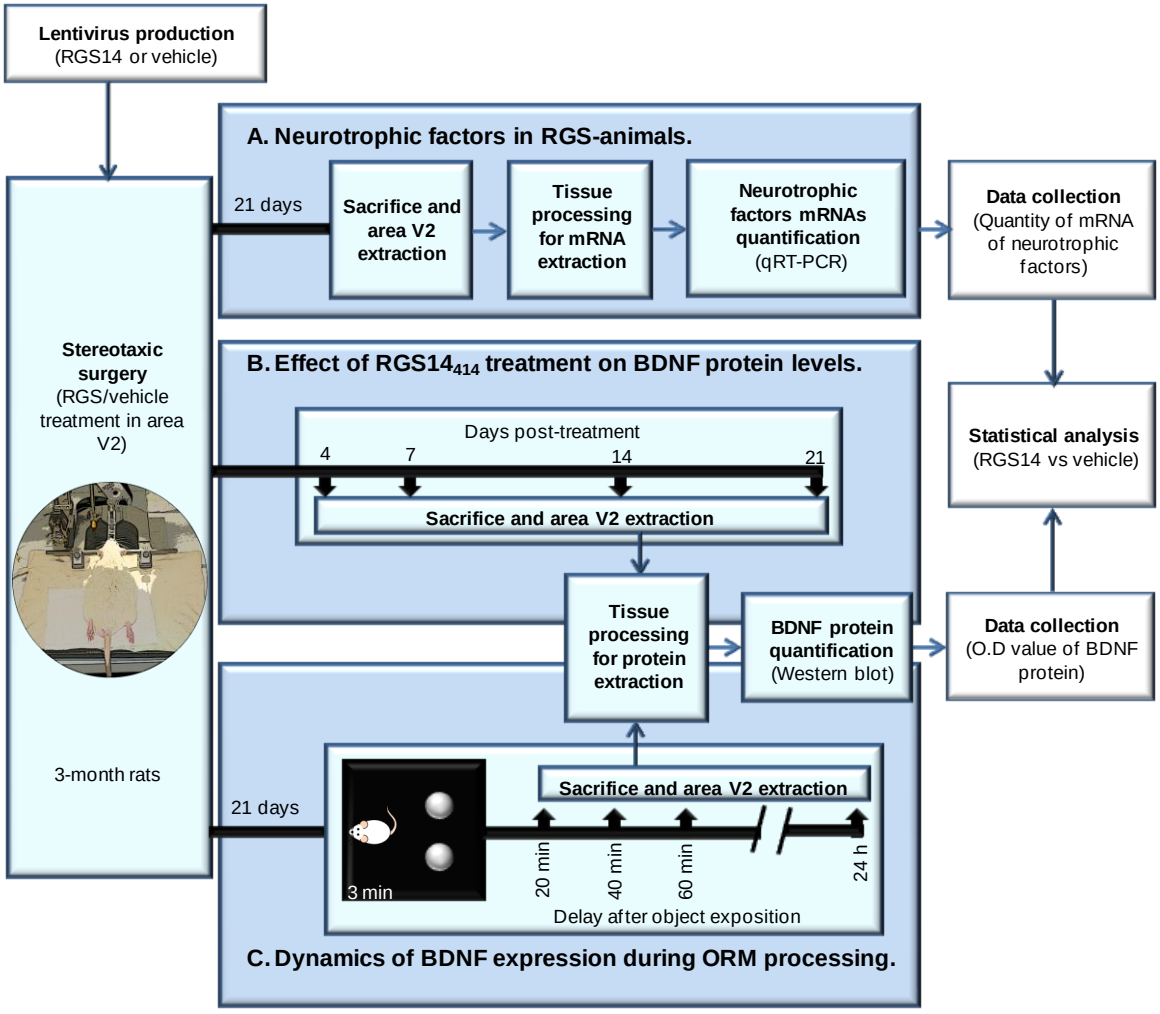

Figure 17. Scheme of experimental design.

3.2 Methods

3.2.1 Brain extraction

After deep anesthesia (see for details in subsection III.1.2.4), brains were dissected out and carefully area V_2 was extracted with a 4 mm punch (DH Material Médico, 94158BP-40F).

3.2.2 qRT-PCR

3.2.2.1 Extraction of total RNA

Punches of area V2 were collected in 1.5 ml tubes containing *RNAlater® RNA Stabilization Reagent* (Quiagen, 1018087) and stored at 15-25 ºC up to 7 days and then 2-8 ºC up to 4 weeks, if necessary. Tissue RNA extraction was performed with *RNeasy Tissue Mini*

kit (Quiagen, 74124) following manufacturers' protocol (appendix 1.D). RNA purity and concentration were determined by measuring absorbance at 260 and 280 nm in *Nanodrop1000*, v3.7 (Thermo Scientific). The concentration of RNA was determined using the formula of one unit at A260 is equal to 40 µg/ml of total RNA. A_{260}/A_{280} ratio of RNA samples was between 1.8 and 2, indicating a good purity grade of RNA.

3.2.2.2 **Reverse transcription (RT) of extracted RNA**

For removal of genomic DNA, extracted RNA samples were incubated with rDNase I enzyme at 37 ºC for 30 min (table 9) and then, enzyme was inactivated by heating at 75 ºC for 10 min. RNA samples were stored at 4 ºC.

Table 9. Reaction to remove the genomic DNA.

REAGENT	AMOUNT
10X DNAase Buffer (Ambion, AM2235)	1.4 µl
rDNase I (2 U/µl) (Ambion, AM2235)	0.2 U
RNA sample	1µg
Nuclease-Free water (Gibco, 10977)	Up to 14 µl
TOTAL VOLUME	**14 µl**

The RT reaction was performed with the *High Capacity RNA-to-cDNA kit* (Applied Biosystems, 4387406) as shown in table 10. The reaction was performed at 37 ºC for 30 min and reverse transcriptase was inactivated by heating at 95 ºC for 5 min. The cDNAs were stored at -20 ºC.

Table 10. Reverse transcription (RT).

REAGENT	AMOUNT
2X RT Buffer Mix	16 µl
20X RT Enzyme Mix	1.6 µl
RNA sample (resulting from genomic DNA digestion)	14 µl
Nuclease-Free water (Gibco, 10977)	0.4 µl
TOTAL VOLUME	**32 µl**

The cDNA concentration was estimated as above (in RNA extraction, III.3.2.2.1) using formula of one unit at A_{260} is equal to 33 µg/ml of ssDNA and A_{260}/A_{280} ratio of DNA samples was between 1.8 and 2.

3.2.2.3 **Primers design**

Forward and reverse primers (table 11) were designed with the use of software *Primer Express*, v2.0 (Applied Biosystems). Specificity of primers was checked by the software *Primer-Blast* (NCBI) (Ye et al 2012) and finally a qRT-PCR simulation was done by the software *Amplify 1*.2 (University of Wisconsin).

Table 11. qRT-PCR primer sequences.

GENE	GENBANK CODE	[1]SEQUENCE (5'→3')	AMPLICON LENGTH (bp)
BDNF	NC_005102.4	*Forward:* *AAGCAATATTTCTACGAGACCAAGTG* *Reverse:* *TACGATTGGGTAGTTCGGCATT*	110
FGF-2	NM_019305.2	*Forward:* *GACGGCTGCTGGCTTCTAAGT* *Reverse:* *TCCGTGACCGGTAAGTGTTG*	90
NGF	NM_001277055.1	*Forward:* *GCAGACCCGCAACATCACT* *Reverse: GGTGGAGGCTGGGTGCTAA*	90
***Ribosomal protein L19 (Rpl19)**	NM_031103.1	*Forward:* ATGCCAACTCTCGTCAACAG *Reverse:* AGGTGTTCTTCCGGCATCG	102

*Housekeeping gene.
[1]*Primers were synthesized by Sigma-Aldrich Company.*

3.2.2.4 **Determination of optimal primer concentration for qRT-PCR**

Three different concentrations of primers (0.45, 0.225 and 0.1125 µM) were tested in a qRT-PCR reaction (see section III.3.2.2.6 below) where each primer concentration was used with 3 different amounts of cDNA (640, 320 or 160 ng) from vehicle group as template. Optimal primer concentration was selected for qRT-PCR experiments based on following two criteria:

i) Primers concentration that represent lowest cycle threshold (Ct) values.

ii) Variations in Ct value between one concentration of cDNA to other are maintained to 1. Therefore, applying these criteria, we found that 0.45 µM primer concentration was optimum for all four genes that were subject to study.

3.2.2.5 **Creating standard curves**

Using optimal primer concentration, five serial dilutions of the DNA ranging 10^{-4} to 10^{-9} were processed for qRT-PCR to generate standard curve where DNA concentration was represented on X axis and corresponding Ct value on Y axis. A good linear relationship between Ct and the logarithm of DNA was considered when correlation coefficient (*r*) reached over 0.99. Furthermore, slope values (m) that reflect amplification coefficient, were very similar across the genes studied (F=1.01; p = 0.34). Figure 18 shows representative standard curves of BDNF and Rpl19.

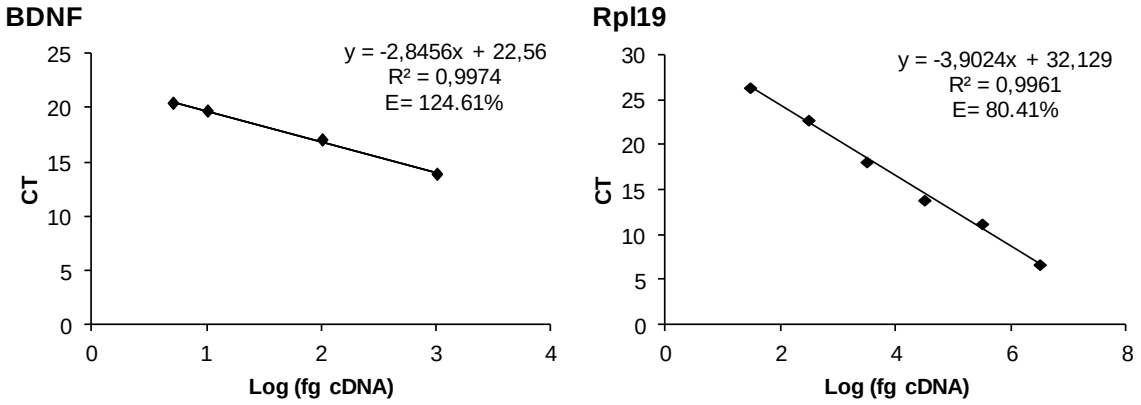

Figure 18. Standard curves.

3.2.2.6 **qRT-PCR reaction**

After primer optimization and standard curve analysis, we set out to perform qRT-PCR for the evaluation of differential gene expression between the brain tissues obtained from control and RGS14 treated rats. The qRT-PCR reactions were performed in thermocycler *7500 Real-Time PCR Systems* (Applied Biosystems), using the *Power SYBR® Green PCR Master Mix kit* (Applied Biosystems, Cat. No. 4367659) as it is detailed in table 12. Triplicates were run for each cDNA sample in a *MicroAmp®Optical 96-Well Reaction*

Plate with Barcode (Applied Biosystems, Cat. No. 4306737). In addition to housekeeping gene, negative control without cDNA was run at the same time. Once all reactive were added, plates were sealed with *qPCR Adhesive Clear Seals* (4titude, Cat. No. 4ti-0560) and centrifuged at 1000 rpm for 1 min at 4 ºC in the Centrifuge 5810R (Eppendorf) using the A-462 rotor, before placing it on the qRT-PCR thermocycler. The quantitative amplification conditions are shown in table 13.

Table 12. qRT-PCR reaction.

REAGENT	AMOUNT	CONCENTRATION
Power SYBR® Green PCR Master Mix (2X)	12 µl	1X
Reverse primer	8 µl	0.45 µM
Forward primer	8 µl	
cDNA	4 µl	640 ng
TOTAL VOLUME	**24 µl**	

Table 13. qRT-PCR amplification cycles and temperatures.

STEP		TEMPERATURE	TIME
Polymerase activation		95 ºC	10 min
40 cycles	**Denaturation**	95 ºC	15 s
	Primer annealing and extension	60 ºC	1 min
Dissociation reaction (1 cycle)		95 ºC	15 s
		60 ºC	1 min
		95 ºC	30 s
		60 ºC	15 s

3.2.3 Determination of BDNF protein level by Western blot

3.2.3.1 Brain homogenization and protein estimation

Brain punches of injection area V2 were dissected out (see III.3.2.1) and frozen immediately in dry ice and stored at -80 ºC. Brain tissues were thawed, weighted and homogenized in 2 ml of 0.01 M Tris-HCl buffer pH 7.4 (appendix 5.A.1) which included 1 % (v/v) protease inhibitor cocktail (Sigma-Aldrich, P8340) and 1 % (v/v) phosphatase inhibitor

cocktail (Sigma-Aldrich, P0044), using tissue homogenizing system (Glas col) and a 10 ml glass-Teflon homogenizer (Glas col). The homogenization was done in 3 cycles of 10 short steps, maintaining the homogenate in ice for 1 min between cycles to prevent heating. Protein concentration of homogenized samples was determined by Lowry method (Lowry et al 1951) (appendix 5.A.2). 50 µl aliquots were then lyophilized in SPD1010 SpeedVac System (Thermo Savant) for 45 min without heating and stored at -80 ºC until used.

3.2.3.2 **Denaturing polyacrylamide gel electrophoresis (SDS-PAGE) and protein transfer to membrane**

Loading buffer (Laemmli 1970 ; see appendix 5.A.3) was added to lyophilized samples to obtain 1 µg/µl protein concentration. The samples were heated at 95 ºC for 10 min twice in a thermostatic block heater TDB-100 (Boeco) to denature and dissolve the proteins. 2.5 µg and 5 µg of samples were run in 4–20 % Mini-PROTEAN® TGX™ precast polyacrylamide gels (Bio-Rad, 456-1096) using electrophoresis unit (Mini-PROTEAN 3 Cell, Bio-Rad). Sodium dodecyl sulfate polyacrylamide gel electrophoresis (SDS-PAGE) was run at 150 V (Power-Pac 300, Bio-Rad) with 1X Tris-Glycine-SDS 1X (TGS) running buffer (appendix 5.A.4). A 5 µl of protein ladder ranging between 10-250 kDa (*Precision Plus Protein ™ Dual Color S35* from Bio-Rad, 161-0374), were also loaded in gel. Separated proteins on polyacrylamide gel were transferred to a polyvinylidene difluoride (PVDF) membrane (Bio-Rad, 1704156) using the *Turbo Trans-Blot* apparatus (Bio-Rad) for 7 min at 25 V/ 3 A.

3.2.3.3 **Immunodetection**

Membranes were incubated with blocking solution prepared with 10 % (w/v) powdered skimmed milk and 2 % (w/v) BSA (Sigma-Aldrich, A3059) in PBS with Tween-20 (PBST) pH 7.4 (appendix 5.A.6) for 3 h at room temperature by gentle shaking. Membranes were washed 4 times in PBST for 5 min each and incubated overnight at 4 ºC with primary antibody, goat anti-BDNF (Santa Cruz Biotechnology Inc., sc-33904) (dilution 1:250) and as control of protein loading, monoclonal mouse α-tubulin antibody (Sigma Aldrich, T8203) (dilution 1:7500). Biotinylated secondary antibodies were from horse anti-goat (Vector Lab., BA9500) and goat anti-mouse (Vector Lab., BA-9200). Both primary and secondary antibodies were prepared in 5 % (w/v) powdered skimmed milk, 2 % (w/v) BSA and 0.1 % (w/v) sodium azide (Sigma Aldrich, S2002) in PBST. After incubation with primary antibody,

membranes were washed 4 times and incubated in secondary antibody at room temperature for 75 min. After washing, membranes were incubated with extravidin-peroxidase conjugate (Sigma-Aldrich, Cat. No. E2886) (dilution 1:2000 in PBST) for 50 min at room temperature. Finally, polypeptide bands corresponding to BDNF or α-tubulin were developed by 3,3'-*diaminobenzidine* (*DAB) Enhanced liquid substrate system* (Sigma-Aldrich, D3939) as a brown precipitate. High resolution images of dried blots were acquired with scanner Epson perfection V750 Pro. Densitometry analysis of bands was performed using *Quantity One version 4.3.6* software (Bio-Rad) and O.D. values were normalized with α-tubulin.

3.2.4 Data analysis

3.2.4.1 Analysis of qRT-PCR data

cDNA values corresponding to genes were normalized with housekeeping Rpl19 and percentage of change between vehicle and RGS groups were calculated as following:

$$[(Q_{\text{gene nor}}\,\text{RGS} - Q_{\text{gene nor}}\,\text{Vehicle}) \times 100 / Q_{\text{gene nor}}\,\text{Vehicle}]$$

The Q_{nor} were presented as the mean ±SEM and significant difference between RGS and vehicle were tested by paired t-test (SigmaStat 3.5 software, Jandel Scientific), accepting a confidence interval of 95 % ($p \leq 0.05$).

3.2.4.2 Analysis of Western blot data

The optical density of BDNF protein (RGS or vehicle) was normalized with α-tubulin ($O.D_{BDNF}$ / $O.D_{\alpha\text{-tubulin}}$). Subsequently, the percentage change of BDNF protein in RGS14 group related to the vehicle was calculated for each day post-treatment or each time post-object acquisition using the O.D normalized values (OD_{nor}) as following:

$$[(O.D_{BNFnor}\,\text{RGS} - O.D_{BDNFnor}\,\text{Vehicle}) \times 100 / O.D_{BDNFnor}\,\text{Vehicle}]$$

The values were expressed as mean ±SEM. Student's paired t-tests (SigmaStat 3.5; Jandel Scientific) comparing normalized O.D values of both treatment were carried out to identify Significant differences ($p \leq 0.05$).

4 Fourth block of experiments. Identification of proteins implicated in RGS-mediated enhanced memory processing

This section was designed to uncover molecular components implicated in RGS-mediated memory enhancer effect. Therefore, a proteomic study was performed with the idea to shed light on profile of proteins that are changing during this process.

4.1 Experimental design

Brain punches of area V2 were obtained at 4, 7 and 21 days after RGS or vehicle treatment and were processed for proteomic analysis. Differentially expressed proteins were identified and searched for correlation with memory. In particular, we have focused on 14-3-3ζ, a protein known to be involved in memory processing. Gene and protein levels were estimated by qRT-PCR and WB, respectively. An implication of this protein in ORM processing was also investigated. A summary of the experimental design is in figure 19.

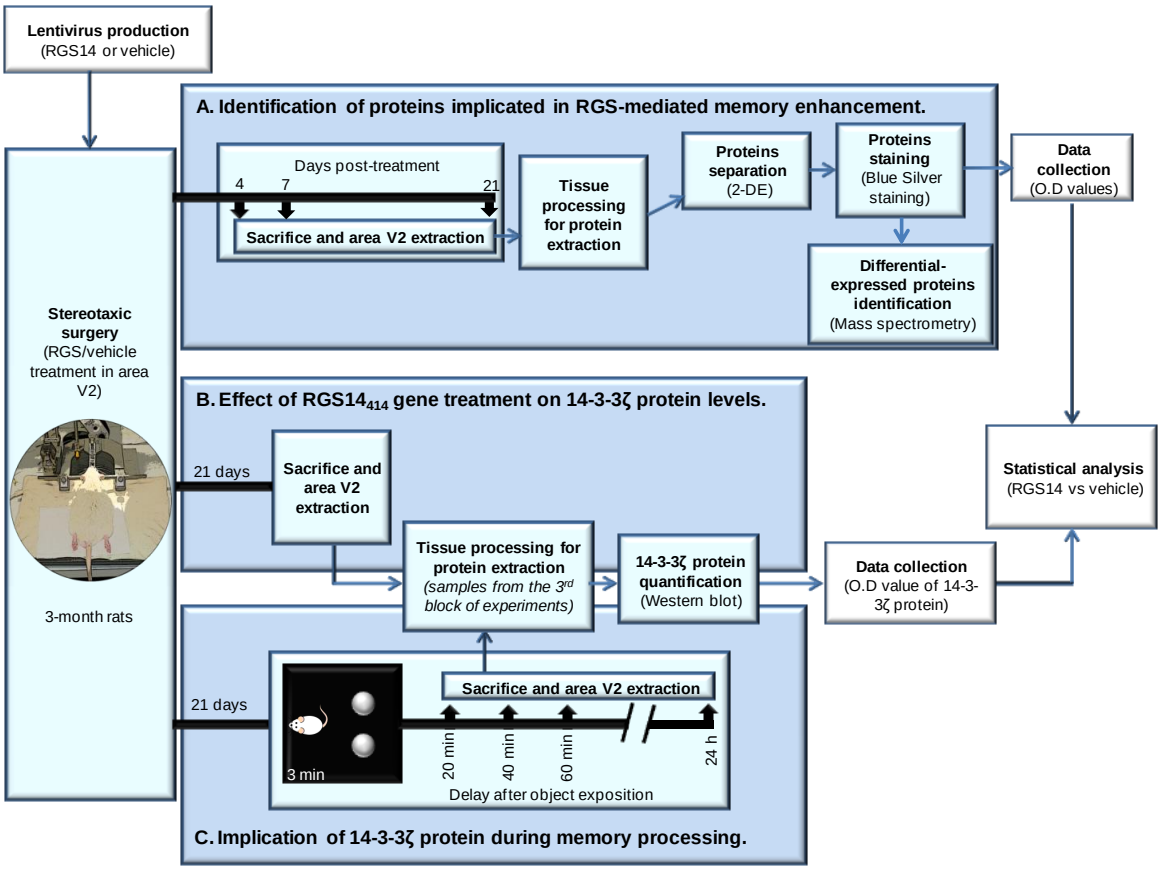

Figure 19. Scheme of experimental design.

4.2 Methods

4.2.1 Tissue homogenization and protein estimation

12 Wistar Han rats weighing 280-320 g were treated with RGS or vehicle-lentivirus (from subsection III.1.2.2) by stereotaxic surgery (see for details in subsection III.1.2.4). These animals were housed and maintained as described in first block of experiments (subsection III.1.2.3).

Animals were sacrificed at 4, 7 or 21 days after the injection and punches of area V2 were dissected out. For homogenization, brain tissues (approximately 100 mg) were thawed, weighted and homogenized in 100 µl of ice cold sample solubilization buffer (7 M urea, 2 M thiourea, 4 % CHAPS, 1 % dithioerythritol; see appendix 5.B.1) using 1 ml glass-Teflon homogenizer. Samples were then sonicated three times for 1 min at 4 ºC and leaving on ice for one minute between each sonication. Samples were centrifuged twice at 13,000 rpm for 15 min at 4 ºC (Beckman CS-15R, rotor F2402H), collecting the supernatant in a new clear 1.5 ml tube and discarding the pellet between each centrifugation. Protein concentration of supernatants were determined by Bradford method (Bradford 1976) (appendix 5.B.3) and aliquoted samples of 150 µg were stored at -80 ºC.

4.2.2 Two-dimensional electrophoresis (2-DE)

Proteins of samples were separated by two-dimensional electrophoresis (Bjellqvist et al 1982; Gorg et al 2009; O'Farrell 1975). During the first dimension, proteins are separated horizontally according to their isoelectric points (pI) using immobilized pH gradient (IPG) and applying an electric current. During the second dimension, proteins with same pI were further separated with SDS-PAGE according to their molecular weight.

4.2.2.1 Isoelectric Focusing: First dimension electrophoresis

Before proceeding, stored samples were thawed, gently vortex, sonicated for 1 min and centrifuged at 13,000 rpm (Beckman CS-15R, rotor F2402H) for 10 min at 4 ºC. Pellets were discarded, in case it was observed. First dimension of 2-DE was done using 7 cm IPG strips of an immobilized nonlinear gradient gel of pH 3-10 (Bio-Rad, Cat. No. 163-2002). A total of 100 µg of protein in 125 µl of 0.4 % ampholytes sample solubilization buffer (appendix 5.B.1) was applied in triplicates onto focusing trays (Protean IEF Cell tray from Bio-Rad) and then, IPG gel strips were carefully laid on the tray. After setting the cover,

focusing trays were placed on the Protean IEF Cell (Bio-Rad) to run isoelectrofocusing program (table 14). Before starting the isoelectrofocusing, wetted paper wicks (Bio-Rad, 165-4071) were placed on both electrodes at the end of each strip. To improve entry of higher molecular weight proteins into IPG gel matrix, an active rehydration was performed by applying 50 V low current for 14 h. The gel strips were covered with paraffin oil (Fisher Scientific, 0121-1) during rehydration.

Table 14. IEF program.

STEP		VOLTAGE	TIME
Active rehydration		50 V rapid	14 h
Isoelectric Focusing	**Step 2**	250 V rapid	30 min
	Step 3	4000 V linear	1 h
	Step 4	4000 V rapid	11000 Vhrs
Storage		100 V rapid	20 h *(stopped at 30 min-2h)*
		Total Vhrs	**13900-14200**

4.2.2.2 IPG gel strips equilibration

An equilibration protocol (reduction/alkylation reaction) was performed after first dimension to facilitate proteins transfer to second dimension (Gorg et al 1988). At the end of isoelectric focusing, strips were incubated in 10 ml of equilibration stock buffer (appendix 5.B.2) with 0.03 M dithioerythritol (Fluka, Cat. No. 43794) for 20 min with shaking at room temperature. The reduction reaction with dithioerythritol was followed by incubation in 10 ml of equilibration stock buffer with 0.136 M iodoacetamide (AppliChem Cat. No. A1666, 0100) for 20 min with shaking in darkness at room temperature, to alkylate sulfhydryl groups for avoiding point-streaking in SDS-PAGE.

4.2.2.3 SDS-PAGE: Second dimension electrophoresis

After equilibration step, strips were embedded onto 12 % polyacrylamide minigels (appendix 5.B.4). To fix the strip, support space on top of gel was filled with 0.5 % agarose and 0.05 % bromophenol blue in 1X TGS buffer (BioRad 161-0772). A hole on the upper left corner was made to load 3 µl of *BenchMark™ Pre-stained Protein ladder* (Bio-Rad, 10748010). Gel electrophoresis was carried out at 40 V for 15 min in Mini-Protean System (Bio-Rad) using 1X TGS buffer. The voltage was then increased to 120 V for 1 h 7 min.

4.2.3 Blue silver gel staining and analysis of protein spots

After second dimensional electrophoresis, each gel was incubated twice in 50 ml fixation solution prepared with 30 % (v/v) methanol and 10 % (v/v) acetic acid, for 30 min each time on rocker, and then once for 24 h. After rinsing 4 times with deionized water for 15 min, gels were stained in 0.12 % Brilliant Blue G-Colloidal dye solution (Candiano et al 2004 ;appendix 5.C.1) for overnight at room temperature. Excess of dye was removed by rinsing the gels 4 times in deionized water for 5 min. Finally, Gels were scanned with *Calibrated Imaging Densitometer Model GS-800* (Bio-Rad) and stored at 4 ºC in thermo sealed plastic bags with 0.02 % sodium azide solution. Acquired images were analyzed by using PDQuest Advanced 7.1.1 software (Bio-Rad). O.D. values of each spot were normalized and automatic spot density matching was then performed for initial evaluation. Furthermore, identified spots were confirmed by manual matching. Spots reflecting at least 2-fold change between RGS-treated and control animals were considered for further analysis and protein identification.

4.2.4 Identification of proteins

Proteins from excised gel spots are digested enzymatically to peptides and subjected to MALDI TOF-TOF Mass Spectrometer (Aebersold & Mann 2003). Obtained results are matched against protein sequence databases to identify the proteins.

4.2.4.1 **Excision of spots and destainig**

Identified protein spots were carefully and manually excised from gels and stored at 4 ºC. For elimination of Coomassie blue dye, excised gel spots were treated with 150 µl of destainig solution prepared with 30 % (v/v) acetonitrile and 50 mM ammonium bicarbonate (appendix 5.C.2) for 15 min at room temperature on rocker. This step was repeated until spots were completely transparent. Then, gel pieces were washed twice with 150 µl of deionized water. Finally, after removal of water, spots were dried in a SPD1010 Speed Vac System (Thermo Savant) for 1 h without heating.

4.2.4.2 **Tryptic digestion and peptide extraction**

Proteins in dried gels were digested with trypsin to generate small size polypeptides that can be identified by MALDI-TOF. The reaction was carried out by incubation of dried spot with 3 µl of 10 ng/µl trypsin (Sigma Aldrich, T6567) in 10 mM ammonium bicarbonate (NH_4HCO_3) buffer, pH 8.5 (appendix 5.D.1) for overnight in a wet atmosphere. After

completion of protein digestion, 10 µl of peptide extraction solution (50 % acetonitrile and 0.1 % trifluoroacetic acid; see appendix 5.D.2) were added to each gel spots and incubated in a parafilm sealed plate for 15 min at room temperature with gentle shaking.

4.2.4.3 **MALDI-TOF mass spectroscopy and identification of proteins**

Mass spectroscopy analysis of tryptic digest of gel spots were done by Dr. Konstantinos Vougas from the proteomic services of the Biomedical Research Foundation of Athens (www.bioacademy.gr/facility/proteomics). Peptide profiles were then compared with available data base systems to identify the protein of a selected gel spot.

4.2.5 Western blot analysis to elucidate a relationship of 14-3-3 ζ protein with RGS-mediated memory enhancement

Furthermore, area V2 homogenated samples from both conditions of the third block of experiments (see III.3.1) were used to detect 14-3-3 ζ protein. Western blot was carried out similar to as described in earlier section (III.3.2.3) except primary antibody. Polyclonal rabbit antibody against 14-3-3ζ was from Santa Cruz Biotechnology (sc-1019) and was used at 1:1000 dilution in primary antibody incubation reaction.

4.2.6 Data analysis

4.2.6.1 **Proteomic data analysis**

Student's t-tests were run by PDQuest Advanced 7.1.1 software, comparing O.D values of each spot from both treatments ($p \leq 0.05$).

4.2.6.2 **Western blot for 14-3-3ζ protein data analysis**

Analysis of data and statistical analysis to compare treatments were performed as described in previous section III.3.2.4.2 for BDNF protein results.

IV. RESULTS

1 $RGS14_{414}$ gene treatment prevents memory loss in aging and Alzheimer's disease

This study was performed to test whether $RGS14_{414}$ gene treatment can avert memory loss in aging rats and in AD-mice, two rodent models where memory loss has consistently been reported (Escribano et al 2009; Gamiz & Gallo 2012; Granholm 2010; Schiapparelli et al 2006). Both model groups received treatment prior to the appearance of ORM deficit and their memory capacity was monitored along their respective control animals.

1.1 Study in aging rats

In our studies, discrimination index (DI) value equal or above to 0.66 was considered that animals were able to retain the object information in memory. However, values below to this and close to 0.5 was treated as they we unable to do so. We observed that when normal rats of 3 months old were exposed to an object for 3 min, they were able to keep this information in memory after a delay of 45 min (0.719 ± 0.017); however, they were unable to retain this information until 24 h (0.495 ± 0.014, $p \leq 0.001$) (figure 20). In contrast to 3 months, rats of 18 months of age lost the capacity to retain information seen at delay of 45 minutes (0.507 ± 0.034. $p \leq 0.001$). Therefore, to test memory enhancer effect of RGS14 on prevention of this object recognition memory (ORM) loss, animals of 3 months old were treated with RGS gene and their ORM statuses were monitored at 5, 18, 20 and 22 months of age. As predicted, 2 months after treatment, no difference in ORM of 45 min between RGS-animals and vehicle-control was observed and RGS-animals behaved very similar to 3 months old non-treated rats (0.750 ± 0.016, bars of 5 months in figure 20) (vehicle vs. RGS14, $p=0.297$; 5 months RGS14 vs. 3 months control, $p=0.194$). However, after 15 months of treatment when animals reached 18 months, vehicle-control showed a significant loss in ORM (0.507 ± 0.035, $p \leq 0.001$), whereas animals treated with RGS14 derailed this memory loss (0.750±0.022). Furthermore, we observed that RGS14 treatment not only prevented memory loss in 18 months old rats, but also produced a robust enhancement in the ORM that was traceable after 24 h delay (0.744±0.023, $p \leq 0.001$). Non-treated 3 months old rats and vehicle-treated 18 months old rats do not have this capacity to retain object information in memory for 24h (3 months control without injection 24h bar and 18 months vehicle 24h bar). This boost in ORM to 24 h observed at 18 months of age in RGS-animals persisted even at 20

months of age (0.716±0.018, p≤0.001) and 22 months of age (0.688 ± 0.015, p≤0.001), a period until these animals were able to actively perform ORM test.

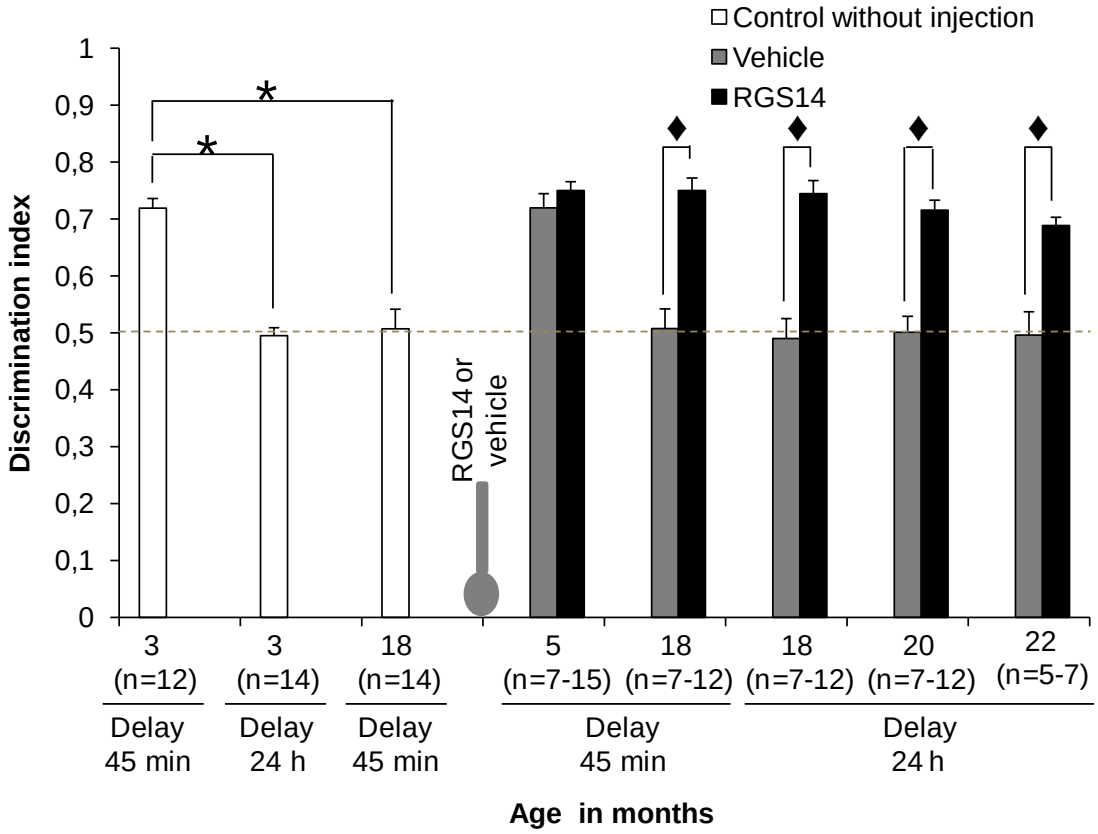

Figure 20. Prevention of ORM loss in aging rats by RGS14$_{414}$ gene treatment in area V2. Non-treated 3-months old control rats were able to recognize an object after a delay of 45 min, but this capacity was lost at the age of 18 months. A treatment with RGS14 gene to same animals not only prevented this ORM loss in 18 months old rats (18 months, delay 45 min), but also boosted the memory to such extent that these animals were able to retain information on an object even after 24 h (18 months; delay 24 h vs. 3 months; delay 24 h). In addition, the effect of treatment on memory persisted up to the age of 22 months. *n* indicates number of animals in each case. * and ♦ show significant intra- and inter-group differences, respectively (p≤0.001).

1.2 Study in Alzheimer´s disease mice

Previous studies have shown that J20 AD-mice suffer a significant ORM loss at 4 months of age (Escribano et al 2009). Therefore considering this time frame, we first tested memory status of these AD-mice at 2 and 4 months of age. We found that level of performance of 2 months old wild-type control mice (0.768 ± 0.039; bar of 2 months in figure 21) and AD-mice (0.754 ± 0.039; bar of 2 months in figure 21) on ORM task were very similar and both groups of animals showed normal ORM status (one-way ANOVA F1,18=0.0572; p=0.814). However, when AD-mice reached 4 months, a sharp drop in ORM was observed which fell to a level where they were unable to recall information on previously

seen objects (0.480 ± 0.039; one way ANOVA $F_{1,36}$=34.943, p<0.001) and in contrast, same age wild-type control mice were unaffected (0.780 ± 0.033) and they showed normal ORM similar to 2 months old mice.

To test preventive effect of RGS14 on ORM loss seen at 4 months of age, 2 months old AD-mice were either treated with RGS14 gene (AD + RGS) or vehicle in area V2 and their ORM status were evaluated at 4 and 7 months of age (bars of 4 and 7 months in figure 21). These RGS-treated AD-mice, when reached to 4 months of age (0.771 ± 0.020) and even to age of 7 months (0.696 ± 0.035) showed no sign of ORM loss, and in contrast, this memory loss was observed in same age untreated AD-mice (0.561 ± 0.0210, p<0.001 at 4 months; 0.421 ± 0.0754, p=0.01 at 7 months) as well as vehicle treated AD-mice (0.558 ± 0.0656; p<0.001 at 4 months; 0.429 ± 0.0764, p=0.013 at 7 months). This escape of RGS treated AD-mice from memory loss was long-lasting and these animals maintained their ORM status at same level as their wild-type control littermates (Tukey's HSD post-hoc test, p=0.811 at 4 months and p=0.993 at 7 months).

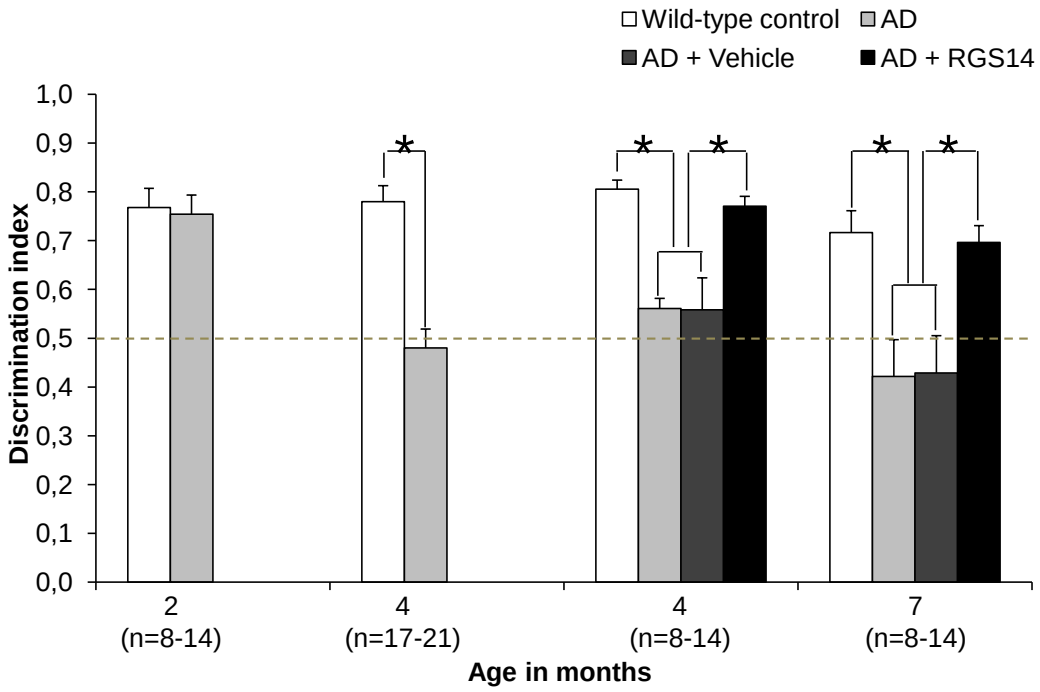

Figure 21. Prevention of ORM loss in AD-mice by $RGS14_{414}$ gene treatment in area V2. Non-treated 2 months old AD-mice, similar to wild-type animals, showed a normal ORM. However, AD-mice suffered a noticeable memory loss at 4 months of age. A treatment with RGS14 gene abrogated this memory loss. This effect of RGS treatment on memory was maintained until the age of 7 months. *n* indicates the number of animals in each case. * shows significant inter-group difference (p<0.05).

2 $RGS14_{414}$ gene treatment promotes cortical neuronal arborization

In first part of study, it was shown that the effect of $RGS14_{414}$ treatment on memory persisted for lifetime of rats. Therefore, we posit that this long-lasting effect is due to the permanent structural change in brain, which in turn facilitates information processing and memory formation. Hence, in this part of the study, brains of RGS14-treated rats were stained with Golgi-Cox silver staining and an analysis of neuronal arborization was done in treated area by counting neurites and dendritic branching.

An initial study of neuronal drawing of both pyramidal and non-pyramidal neurons of RGS-treated animals demonstrated a significant increase in overall neuronal arborization and that could be appreciated by just a visual examination (figure 22). RGS14 treatment produced a significant increase in neurites originating from cell body of pyramidal neurons (RGS 4.595 ± 0.190 versus vehicle 3.643 ± 0.181, $p \leq 0.001$) (pyramidal neurons, neurites in figure 23), whereas this effect was more pronounced in neurites of non-pyramidal neurons (RGS 6.069 ± 0.211 versus vehicle 3.673 ± 0.248 neurites per neuron, $p \leq 0.001$) (non-pyramidal neurons, neurites in figure 23). In contrast to neurites, RGS treatment caused a robust increase in dendritic branching of pyramidal neurons, leading to almost twice the number of vehicle treated control animals (RGS 6.646 ± 0.342 versus vehicle 3.357 ± 0.314, $p \leq 0.001$). The analysis of branching in neurites showed no difference in pyramidal neurons (RGS 1.494 ± 0.185 versus vehicle 1.714 ± 0.286, $p=0.5$) as well as in non-pyramidal neurons (RGS 1.914±0.249 versus vehicle 1.491±0.226, $p=0.212$). Therefore, these results suggest that RGS treatment poses prominent effect on dendritic branching of pyramidal neurons and on cell body neurites of non-pyramidal neurons (figure 23).

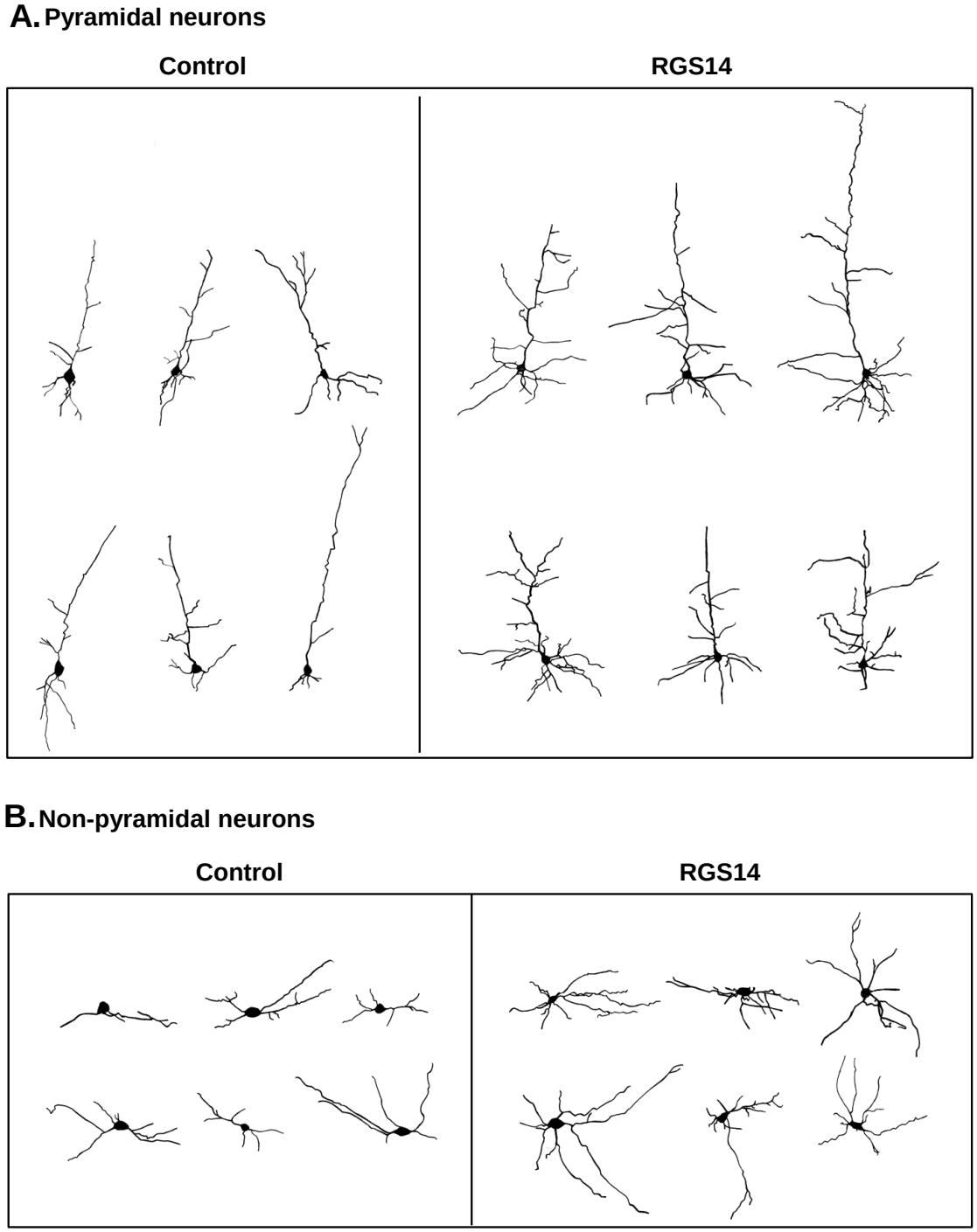

Figure 22. Drawings show examples of pyramidal neurons (A) and non-pyramidal neurons (B) from area V2 of RGS14 or vehicle treated animals. Neurons were drawn with the use of camera lucida and 10X objective.

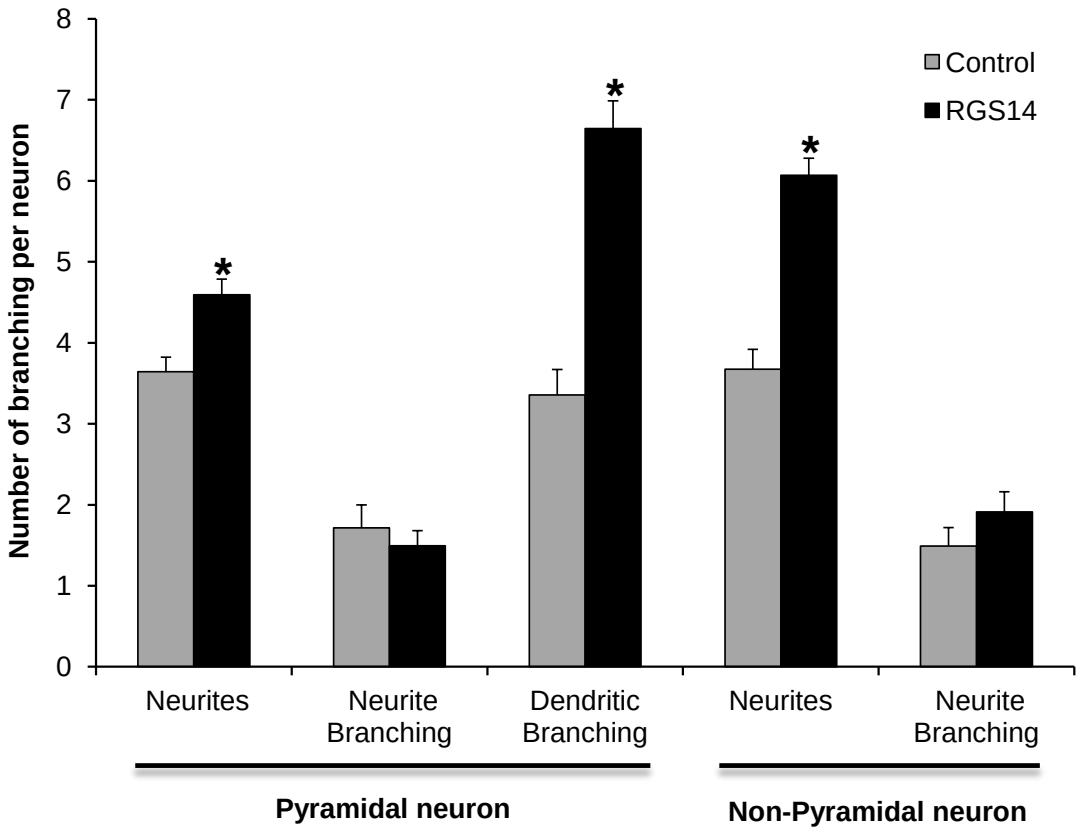

Figure 23. A dramatic increase in neuronal arborization after RGS14$_{414}$ gene treatment. Pyramidal neurons of treated animals showed a robust increase in number of neurites and of dendritic branching. However, the effect was more prominent in dendritic branching. In contrast to pyramidal neurons, the effect was more dominant in neurites of non-pyramidal neurons. * reflects a significant change from control ($p \leq 0.001$).

The effect of RGS14$_{414}$ gene treatment on dendritic branching of pyramidal neurons and neurites of non-pyramidal neurons were further analyzed to demonstrate the dimension of effect on neuronal arborization (Figure 24). Therefore, total number of pyramidal and non-pyramidal neurons studied was classified on the basis of their branching numbers. The plots in Figure 24 show that there was a big shift in number of branching of both dendrites of pyramidal neurons and neurites of non-pyramidal neurons. In vehicle-treated control animals, dendritic branching per neuron ranged between 0-8, however this jumped to 1-15 in RGS14-treated rats (Figure 24.A). A 50 % of total pyramidal neurons from control group represented between 3-4 branching and only 18 % showed more than 4 dendritic branching, whereas in RGS-animals, one of every two pyramidal neurons showed 6-9 dendritic branching and more than 62 % presented more than 6 branching. On the other hand, non-pyramidal neurons of RGS group showed greater arborization in neurites. Because more than 90 % of these neurons

represented 4-8 neurites per neuron and only 42 % in control group animals. A 56 % of non-pyramidal neurons from control group had 3 or less neurites (figure 24.B).

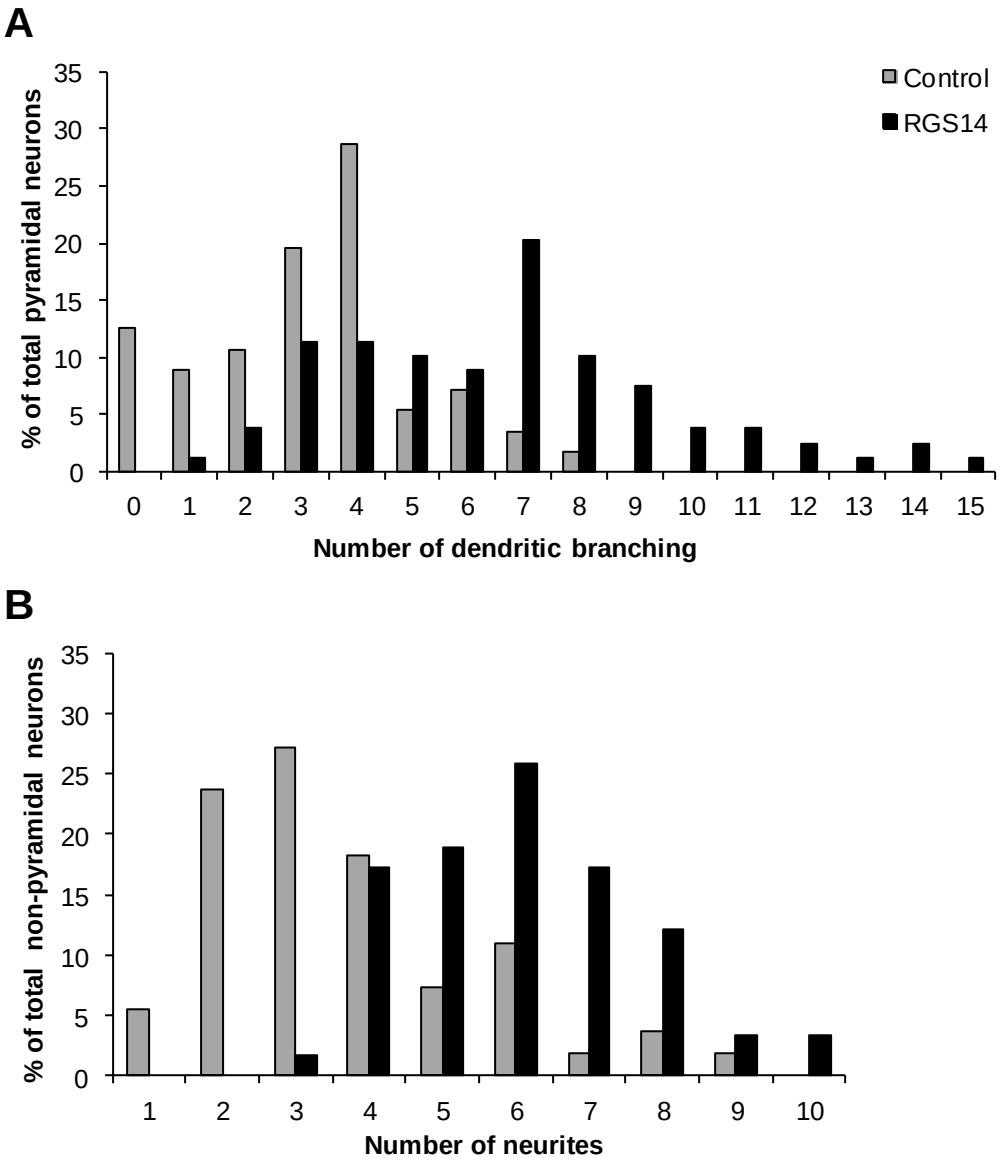

Figure 24. RGS14$_{414}$ gene treatment led to high neuronal arborization in both pyramidal and non-pyramidal neurons. In **(A),** effect of RGS treatment was so drastic that it led to a big shift in dendritic branching. This boost in dendritic branching reached from 0-8 neurite per neuron in control group to 1-15 in RGS group. **(B)** shows the extent of effect of treatment on neurites of non-pyramidal neurons where more than 90 % was seen between 4-8 neurites as compared to 2-4 neurites in control.

3 $RGS14_{414}$ gene treatment boosts expression of brain derived neurotrophic factor (BDNF)

The role of neurotrophic factors in memory and neuronal proliferation is well known. Therefore, here, with the goal to find a possible mechanism that might provide an explanation for this massive neuronal arborization seen in RGS-treated animals, we first evaluated mRNA levels of neurotrophic factors, such as BDNF, FGF and NGF, shown to be implicated in episodic memory and neuronal growth (Kopec & Carew 2013), and then was further confirmed at protein level by Western blot method. In addition, we have also explored whether RGS14-regulated BDNF participates during ORM processing or not.

3.1 A selective increase in both mRNA and protein levels of BDNF

qRT-PCR analysis revealed that mRNA levels of BDNF in RGS-treated animals was 2.4 fold higher compared to vehicle-treated control animals (RGS14, 0.340 ± 0.015 vs. vehicle, 0.147 ± 0.006, $p \leq 0.001$) (figure 25). However in contrast to BDNF, there was no effect on mRNA levels of other two neurotrophic factors: NGF and FGF-2. Therefore, it seems that RGS treatment produces a strong but selective effect on mRNA levels of BDNF.

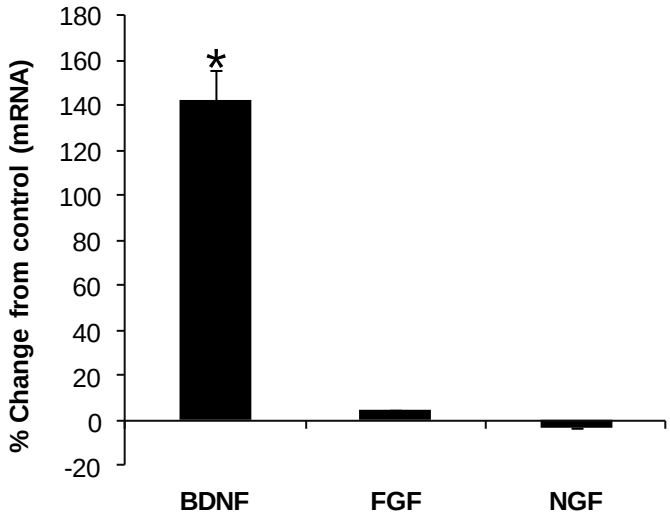

Figure 25. $RGS14_{414}$ gene treatment induced a selective increase in BDNF mRNA. qRT-PCR analysis shows that RGS14 gene treatment boosted BDNF mRNA levels but not of FGF and NGF mRNAs. Data presented are from 5 experiments. * indicates significant difference ($p < 0.001$).

Considering the effect of RGS treatment on BDNF mRNA levels, we next examined the effect of this treatment on BDNF protein levels. To this purpose, we extracted brains at 7, 14 and 21 days after RGS14 gene treatment and processed them for Western blot analysis.

Housekeeping protein, α-tubulin, was used as loading control for normalization of BDNF values. Plot of O.D. values of protein bands from figure 26.A shows a slight increment in BDNF after 7 (19.96 ± 2.72 %) and 14 (24.81 ± 3.17 %) days of RGS14 treatment (figure 26.B). However, the effect was more prominent after 21 days of treatment when BDNF protein was 71.25 ± 7.77 % higher than vehicle-treated control (paired Student's t-test, t0.025.2=5.142; p=0.036) (figure 26.B). This hefty increase in BDNF protein after 21 days of treatment coincides well with the period when emergence of enhancement in ORM has been observed in RGS-animals (Lopez-Aranda et al, 2009).

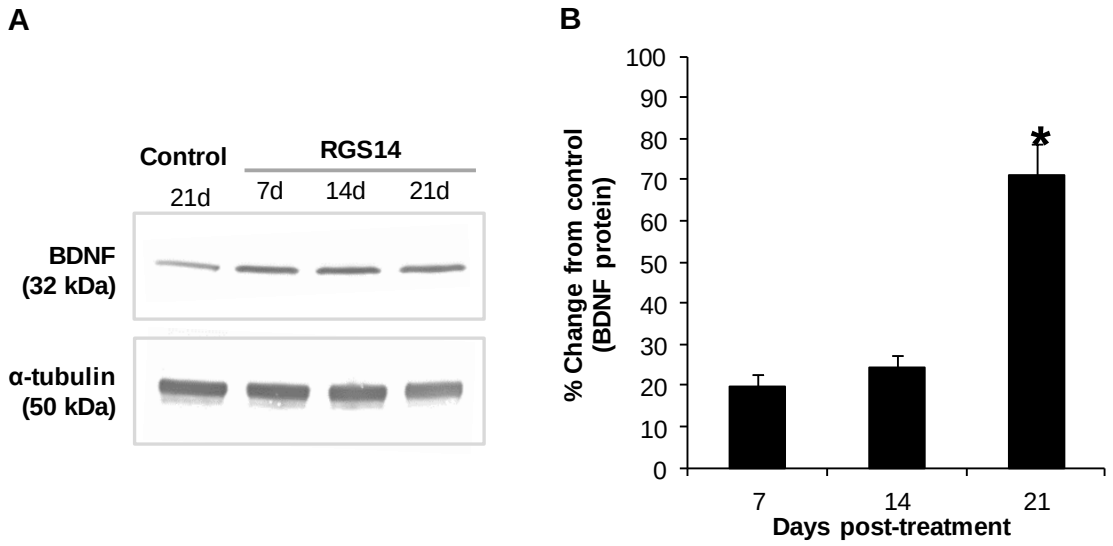

Figure 26. RGS14$_{414}$ gene treatment induced a noticeable increase in BDNF protein. (A) is an example of Western blot showing expression of BDNF protein after 7, 14 and 21 days of RGS14 gene treatment. **(B)** represents an analysis of normalized O.D. values of Western blot. Results suggest an increase in BDNF protein expression after RGS14 treatment that reached to maximum level after 21 days of treatment. Data presented are from 3 experiments. * indicates significant difference of normalized O.D. values from control group (p=0.036).

3.2 A dynamic BDNF protein expression during ORM processing

The coincidence of increase in BDNF protein and enhancement in ORM after 21 days of treatment suggests an involvement of this neurotrophic factor in ORM processing. Therefore, rats after 21 days of treatment were exposed to an object for 3 min and their brains were extracted after delay of 20, 40, 60 minutes and 24 h, with the idea to investigate a correlation between both. Normalized O.D. values of BDNF in figure 27.A are graphically represented in figure 27.B. An increase of 71.43 ± 7.89 % in BDNF protein levels was seen

after 20 min of object exposition (paired Student's t-test, t0.025, 3=-8.887; p=0.003), and this level was similar to animals of 21 days after treatment but without object exposure (figure 26.B). These data indicate that expression of BDNF remains unchanged in first 20 min of object information processing in brain. However, this neurotrophic factor appears to be significantly down-regulated after 40 (23.51 ± 5.99 %, p=0.012) and 60 (37.12 ± 3.49 %, p=0.009) minutes of object exposure. Moreover, after 24 h of object exposure, BDNF protein level started to normalize, however it still remained lower than unexposed RGS-animals. This dynamic BDNF protein expression observed during ORM processing indicates an implication of this neurotrophic factor in the formation of memory in our RGS-animals.

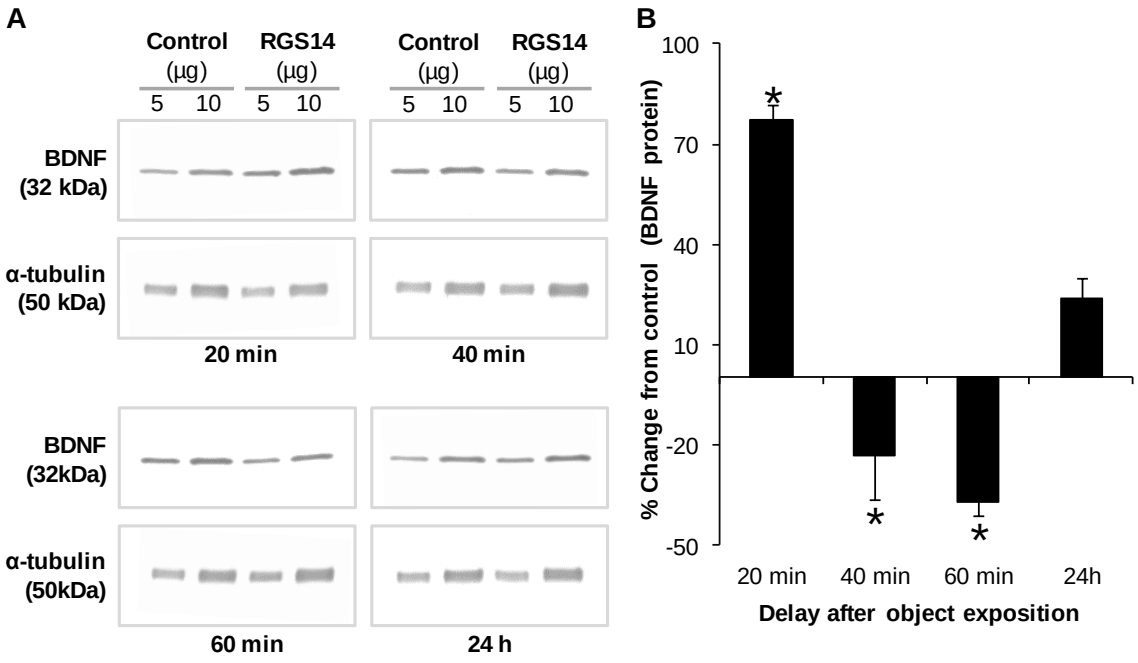

Figure 27. A dynamic BDNF protein expression pattern during ORM processing. (A) is an example of BDNF protein Western blot from RGS and control animals who were exposed to an object and their brains were processed after 20, 40, 60 min and 24 h. 5 µg and 10 µg of total protein were loaded from each time point. In **(B)**, a higher level of BDNF was observed after 20 min of object exposure and that was down-regulated after 40 and 60 min. However after 24 h, there was normalization in the level of this protein. Data presented are from 4 experiments. * reflect significant change from control ($p \leq 0.05$).

4 An implication of 14-3-3ζ protein in RGS-mediated memory enhancement

It remains unknown how BDNF expression is up-regulated in RGS-animals, a step that we believe is primarily responsible for neuronal arborization and enhanced memory processing. Here, we set out to investigate proteins that are responding to the RGS14 gene treatment with a goal to shed light on underlying mechanism of RGS-mediated memory enhancement. Therefore, we used proteomic analysis to identify proteins that react to RGS treatment and are associated with ORM.

4.1 Proteomic profiling revealed an elevated expression of 14-3-3ζ in RGS-treated animals

The differential expression analysis between RGS and vehicle treated animals was performed at 4, 7 and 21 days after the treatment, and the results of some proteins that have shown a strong relation to treatment are summarized in table 15. After evaluation, we found that one protein named 14-3-3ζ (indicated in bold in table 15) was responding to the treatment in a very different manner than others. There was a progressive and consistent increase in 14-3-3ζ protein levels (figure 28.B). This increase was even evident at the visual analysis of protein spots in 2-DE gel image (figure 28.A). After 7 days of treatment, this protein level was 2.8 fold higher than vehicle control and after 21 days, it reached to 3.7 fold (table 15 and figure 28.B). This time frame of elevated expression of 14-3-3ζ coincides very well with the appearance of memory enhancement seen in RGS-animals.

Table 15. Differential protein expression after RGS14 treatment.

Protein name	Accession name / number	Ratio		
		4d	7d	21d
14-3-3ζ	**1433Z_RAT / P63102**	**0.75**	**2.83**	**3.74**
ATP synthase subunit alpha	ATPA_RAT / P15999	0.96	1.27	0.73
ATP synthase subunit beta	ATPB_RAT / P10719	1.62	6.63	3.36
Dihydropyrimidinase-related protein 2	DPYL2_RAT / P47942	0.80	1.07	0.68
Glyceraldehyde-3-phosphate dehydrogenase	G3P_RAT / P04797	1.12	0.71	0.75
Neurofilament light polypeptide	NFL_RAT / P19527	0.87	1.03	0.59
Pyruvate kinase isoensymes M1/M2	KPYM_RAT / P11980	0.78	1.40	1.20
Tropomyosin alpha-3-chain	TPM3_RAT / Q63610	6.52	0.57	0.60
Tubulin β-2A chain + tubulin β-2B chain	TBB2A_RAT / P85108 TBB2B_RAT / Q3KRE8	0.33	0.85	0.42

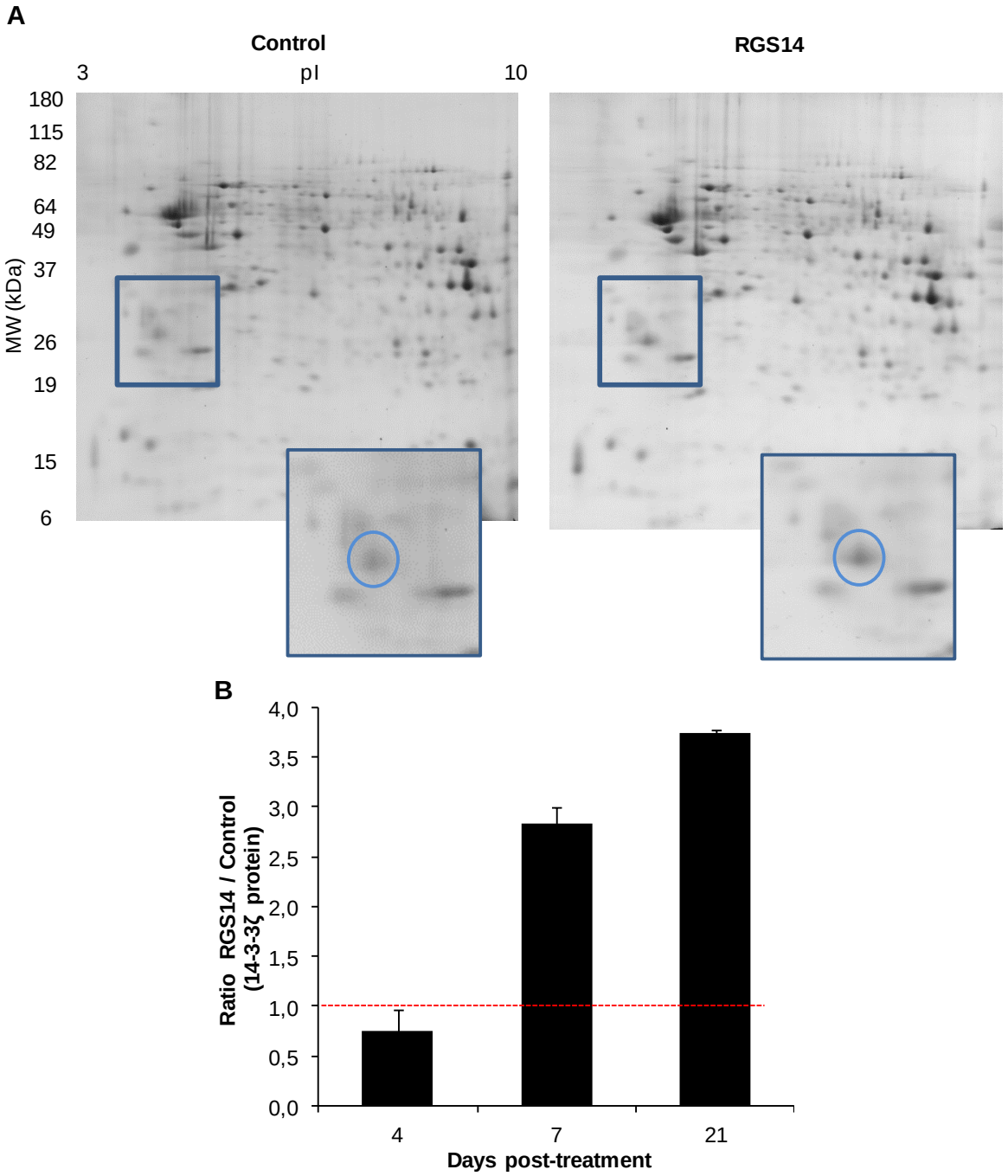

Figure 28. RGS14$_{414}$ gene treatment induces an increase in 14-3-3ζ protein. (A) is a representative 2-DE gel from a proteomic study showing spot corresponding to 14-3-3ζ protein (blue circle) where high expression of this protein is evident. **(B)** is normalized O.D. from 2-DE gel showing a progressive increase in 14-3-3ζ protein after 4, 7 and 21 days of RGS treatment, which coincided with BDNF expression. Data presented are from 4 experiments.

This RGS14-mediated increase in 14-3-3ζ protein level observed by 2-DE technique and protein spot analysis, was further confirmed by Western blot in two independent experiments at 21 days after treatment (figure 29). An example of Western blot and corresponding normalized O.D. values of 14-3-3ζ immunoreactive bands as percentage of change from

vehicle control is represented in figure 29.B (grey bars indicate the values of each experiment and the black bar is mean of both). When 2.5 µg of total protein was loaded on an acrylamide gel, a 191 % increase in 14-3-3ζ protein expression was observed and when total protein loaded was 5 µg, increase in this protein expression was 117 %. However, average of both concentrations was 154 ± 52 % from vehicle control (figure 29.B). Although the results of 2-DE analysis was slightly higher (3.74 ± 0.04 fold change from control) than Western blot (2.55 ± 0.37 fold-change from control), it is important to underline that a noticeable rise in 14-3-3ζ protein was observed in RGS-rats by both methods.

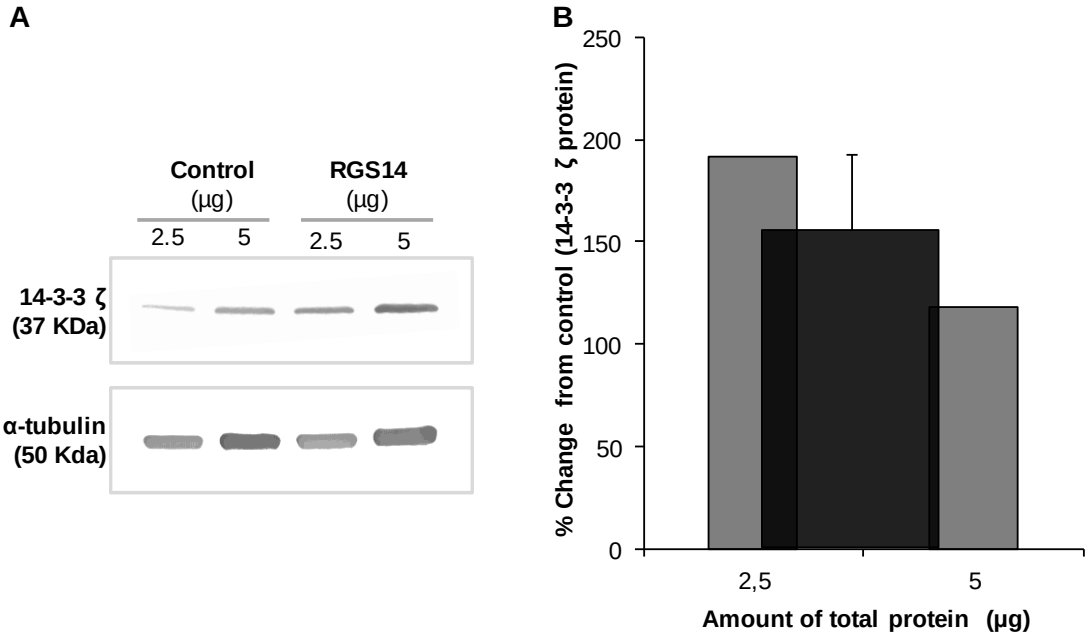

Figure 29. RGS14 treatment induces the expression of 14-3-3ζ protein. (A) shows a representative Western blot. Similar to 2-DE gels, an increase in 14-3-3ζ protein expression was also observed. **(B)** is a plot of results obtained from (A). An up regulation of 14-3-3ζ protein expression was observed after a treatment with RGS14 gene. Grey bars show the results from 2.5 and 5 µg of total protein that was loaded in 2 experiments, and black bar is mean of both.

4.2 Participation of 14-3-3ζ protein in ORM processing

Coincidence of elevated 14-3-3ζ protein expression with the emergence of enhancement in ORM of RGS-animals led us to think that this protein similar to BDNF is involved in the mechanism that facilitate memory enhancement seen in RGS-treated animals. To understand the implication in ORM, brain samples of RGS-treated animals were collected after 20, 40, 60 minutes and 24 h of object exposure and were analyzed by Western blot for the determination of 14-3-3ζ protein levels. Figure 30.A shows an example of Western blot

and figure 30.B represents normalized O.D. values in percentage of change from vehicle control. Results from four independent experiments showed a dynamic regulation of 14-3-3ζ protein during ORM processing. Protein expression of 14-3-3ζ after 20 min of object exposure was the same as vehicle control; however, we observed an increase of 43.19 ± 12.86 % at 40 min and 37.66 ± 4.04 % at 60 min. This increase in 14-3-3ζ protein was normalized after 24 h. The vital change in protein level during ORM processing indicates the implication of 14-3-3ζ.

To our surprise, when an overlap of protein expression profile during ORM processing of BDNF (figure 27.B) and 14-3-3ζ (figure 30.B) was done, we found that BDNF was high at 20 min, but it went down at 40 and 60 minutes and then, it was normalized after 24h. In contrast, 14-3-3ζ expression was normal at 20 min and it reached to highest at 40 and 60 minutes and then, returned to normal level at 24h. Together, these data indicate that during ORM processing, there is synergy between these two proteins. When BDNF level is down, 14-3-3ζ protein level is high in such manner that it suggests that they might be involved in direct or indirect regulation of one or other in animals treated with RGS14 gene.

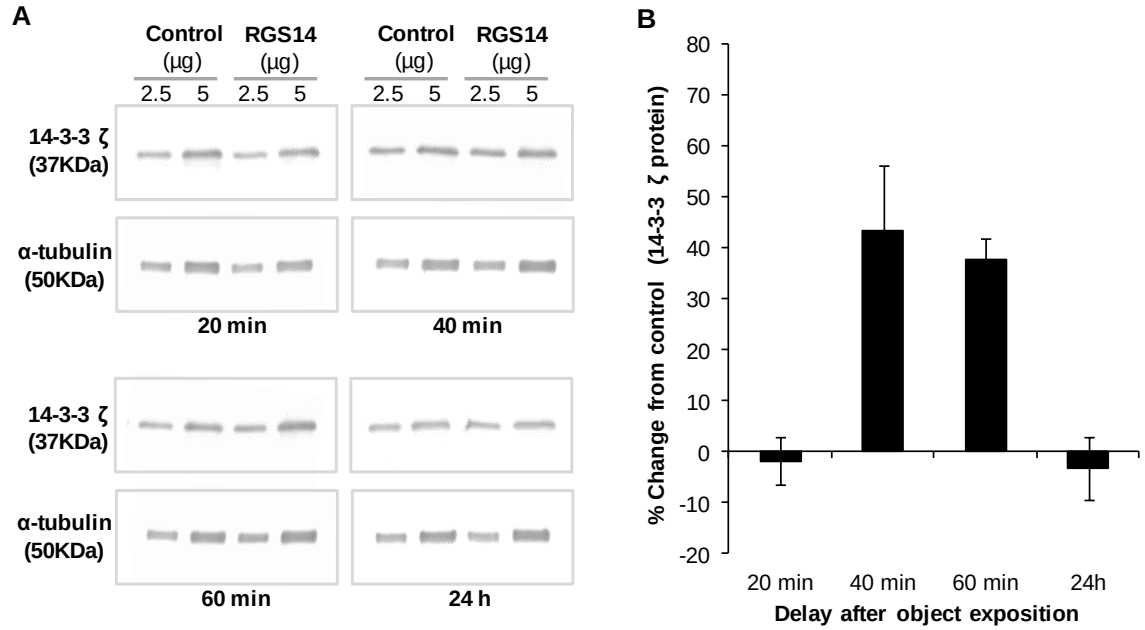

Figure 30. 14-3-3ζ protein is implicated in ORM processing. (A) shows an example of Western blot representing expression pattern of 14-3-3 ζ during ORM processing. **(B)** exhibits up-regulation of 14-3-3ζ protein seen after 40 and 60 min of object exposure. However, there was no change at 20 min and 24 h. Data presented are from 3 experiments.

V. DISCUSSION

Memory loss is one of the mental disorders that affect large proportion of human population. In addition to aging, memory dysfunctions have often been observed in most of the neurological and neurodegenerative diseases, including schizophrenia, Parkinson´s disease, and Alzheimer´s disease. The cost associated with cure and care of patients with memory impairments has been a tremendous social burden and in future, this is expected to soar dramatically due to progressive increase in life expectancy of aging population. According to United Nation report in World Population Ageing 2013, over 30 % of population in developed countries will be 65 years or older by 2040. Furthermore, Alzheimer Report 2014 indicated that dementia associated with memory loss is one of the main causes of dependence and disability in aged individuals. Thus, there is impending need to find remedy against this mental disorder. Memory enhancers are seen as good candidate. However, memory enhancers or other compounds tested so far have failed to show effect in clinical trials (Knafo & Venero 2015). Therefore, current thesis work was designed to counteract this problem by investigating whether memory loss can be prevented prior to its appearance. Our results demonstrate that prevention of an episodic memory loss is attainable by $RGS14_{414}$ gene treatment in rodent models of aging and Alzheimer´s disease, and furthermore show that the activity associated with prevention of ORM loss is regulated through 14-3-3ζ-BDNF pathway.

1 Prevention of memory loss

$RGS14_{414}$ is a potent memory enhancer and a treatment with this gene produces a conversion of an ORM which is expected to last for 45 min in normal animals, into long-lasting long-term memory (Lopez-Aranda et al 2009). Now, we found that the effect on memory of just a single treatment of $RGS14_{414}$ can persist for whole lifetime of rats. Normal as well as vehicle treated rats showed a significant ORM loss at 18 months of age; however, animals treated with $RGS14_{414}$ gene at 3 months of age did not show this loss at 18 months of age and their memory remained intact till the age of 24 months, a period until when animals were able to perform on ORM test. In addition to normal aging rats, effect of memory enhancer treatment in AD-mice, a model of Alzheimer´s disease, produced a similar effect. AD-mice showed an ORM loss at the age of 4 months. However, when these animals were subjected to treatment with $RGS14_{414}$ gene at the age of 2 months, a period when memory was intact and was similar to their wild-type siblings, they showed not only a prevention in ORM loss observed at 4 months of age but also they were able to maintain normal memory

after 6 months of the treatment. Together the results from both models suggest that $RGS14_{414}$ treatment produces a permanent effect and that this treatment paradigm can serve as a feasible alternative for the remedy of episodic memory dysfunction, kind of memory mainly affected in aging and many neurological diseases (Dickerson & Eichenbaum 2010; Tromp et al 2015). Though our data are at preclinical stage and it needs to be tested in clinical trials, they confirm the potential of this memory enhancer as candidate drug against memory loss in human.

2 BDNF in neuronal arborization and ORM

Previously, it was shown that $RGS14_{414}$ treatment produces a long-term memory enhancement (Lopez-Aranda et al 2009) and this characteristic of RGS is also evident in results obtained from experiments on prevention of ORM loss in two different conditions. RGS treatment not only prevented the memory loss, but also maintained the ORM intact for long-term. Our initial interpretation was that this long-lasting effect of $RGS14_{414}$ gene treatment was due to permanent structural change in brain. A neuronal arborization analysis of both pyramidal and non-pyramidal neurons in brain of $RGS14_{414}$-treated rats exhibited robust rise in branching of both classes of neurons. What more astounding was the increment in number of branching from the apical dendrites of pyramidal neurons, reaching to almost three times of the control animals. These apical dendrites of pyramidal neurons are fundamental in the formation of connections with other cortical layers and with other brain areas. We believe that $RGS14_{414}$ treatment mediated increase in neuronal connections leads to facilitation of higher information flow (Eyal et al 2014), and that ultimately causes enhancement in memory. To further understand of underlying mechanism by which $RGS14_{414}$ induces neuronal arborization, we investigated into neurotrophins. A large body of evidence in literature relates neurotrophins with neuronal survival, branching, and axonal and dendritic growth in an activity-dependent manner (see Park & Poo 2013 for review).

We observed that RGS14 treatment induces a selective increase in BDNF and not in other neurotrophins, such as FGF2 and NGF. BDNF and its receptor is one of the most abundant neurotrophins in the central nervous system in both rodents and humans (Aid et al 2007; Maisonpierre et al 1990; Timmusk et al 1994; Webster et al 2002). In fact, this neurotrophic factor is essential for neuronal development, function and synaptic plasticity (Hong et al 2008; Poo 2001). The role of BDNF in neuronal arborization, in regulation of dendritic outgrowth and branching, and in increase of pyramidal and non-pyramidal cells, has been well described (Horch 2004; Horch et al 1999; Jin et al 2003; Wirth et al 2003). In addition,

BDNF expression is necessary for the maintenance of dendritic structure and size of cortical neurons at 3 weeks of age when levels of BDNF rise dramatically (Gorski et al 2003). BDNF shapes the dendritic network by increasing cypin level through the activation of protein kinase and transcription-dependent signaling pathways. Their activation promotes CREB binding to the cAMP response element (CRE) of cypin promoter (Kwon et al 2011). Cypin protein was related to a dendrite branching increase in hippocampal neurons (Akum et al 2004). Altogether these evidence indicate that $RGS14_{414}$-mediated augment in BDNF might not only cause neuronal arborization, but could also maintain them. It is argued that the permanent structural change is associated with neuronal arborization and subsequently newer synaptic connections in brain (Bailey & Kandel 1993; Purves & Hadley 1985; Yang et al 2009). This structural change ultimately provides an infrastructure required for long-lasting long-term effect of $RGS14_{414}$ gene treatment.

The role of BDNF in learning and memory has been widely studied and its implication in formation of both short- and long-term memory is very well demonstrated (Alonso et al 2002; Bekinschtein et al 2008b; Bekinschtein et al 2014; Romero-Granados et al 2010). BDNF activates transcriptional mechanism through different signaling pathways leading to synthesis of proteins (Panja & Bramham 2014) that favor memory formation. Some of these pathways are ERK (Arthur et al 2004; Ying et al 2002), CAMKII, PIK3 (Alder et al 2003; Bogush et al 2007), and mammalian target of rapamycin (mTOR) (Slipczuk et al 2009). In addition, BDNF downstream signaling modulates synaptic plasticity by imposing structural and functional alterations of synapses, a process that underlie long-term potentiation (LTP) (Bramham & Messaoudi 2005; Maren 2005; Panja & Bramham 2014; Rioult-Pedotti et al 1998; Whitlock et al 2006) and long-term depression (LTD) (Kemp & Manahan-Vaughan 2007; Massey & Bashir 2007; Mizui et al 2015; Woo et al 2005). Both LTP and LTD are the best known mechanism of synaptic plasticity implicated in memory formation and consolidation. BDNF likely modulates LTP through TrkB downstream signaling (Minichiello et al 2002), which is required for the consolidation of hippocampal-dependent learning and the maintenance of that memory (Bekinschtein et al 2007; Lee et al 2004). Considering all these evidence, we believe that RGS-mediated increase in BDNF on one hand, promotes structural change that provides infrastructure needed for faster information flow and on other hand, during ORM processing, it facilitates memory consolidation by modulating signaling cascade. Our results showing dynamic expression pattern during ORM processing that overlapped with memory consolidation, further support the idea of BDNF involvement in formation of long-term memory in RGS-animals.

3 Regulation of BDNF levels by 14-3-3ζ

Considering that BDNF is a key to RGS-mediated memory enhancement as well as to prevention of memory loss, we next investigated how BDNF concentration is governed in RGS-animals. In studies of expression profiling of RGS-treated animals, 14-3-3ζ protein displayed a relationship coherent to RGS-mediated ORM enhancement. We have determined that a memory enhancement in RGS-animals generally appears between 17-20 days after the treatment (Lopez-Aranda et al 2009), a time period when highest level of 14-3-3ζ protein was observed in these animals. The 14-3-3ζ protein is a scaffold protein and has been found abundant in brain. It interacts with many proteins, intercedes in several signaling pathways and participates in learning and memory (see Aitken 2006 for review). Mutation in leonardo gene of Drosophila, which is a homologous of vertebrate 14-3-3ζ, showed significant decrease in olfactory learning (Philip et al 2001; Skoulakis & Davis 1996; 1998) and substantial impairment in synaptic plasticity (Broadie et al 1997). More recently, a study using mutant mice with deletion of 14-3-3ζ displayed reduced spatial memory and ORM (Cheah et al 2012; Qiao et al 2014).

Recent studies have demonstrated that interaction of receptor for activated protein kinase 1 (RACK1) with 14-3-3ζ is essential for its nuclear translocation (Neasta et al 2012) where RACK1-14-3-3ζ complex binds at promoter IV region of BDNF and promotes an increase in BDNF gene transcription (He et al 2010; Yaka et al 2003) (figure 31). These observations suggest that 14-3-3ζ might regulate the elevated level of BDNF seen in $RGS14_{414}$ gene treated animals. Additionally, boost in BDNF expression by overexpression of 14-3-3ζ further support this idea. Therefore, it seems that RGS-mediated surge in 14-3-3ζ causes elevated BDNF synthesis needed for neuronal arborization and enhanced ORM.

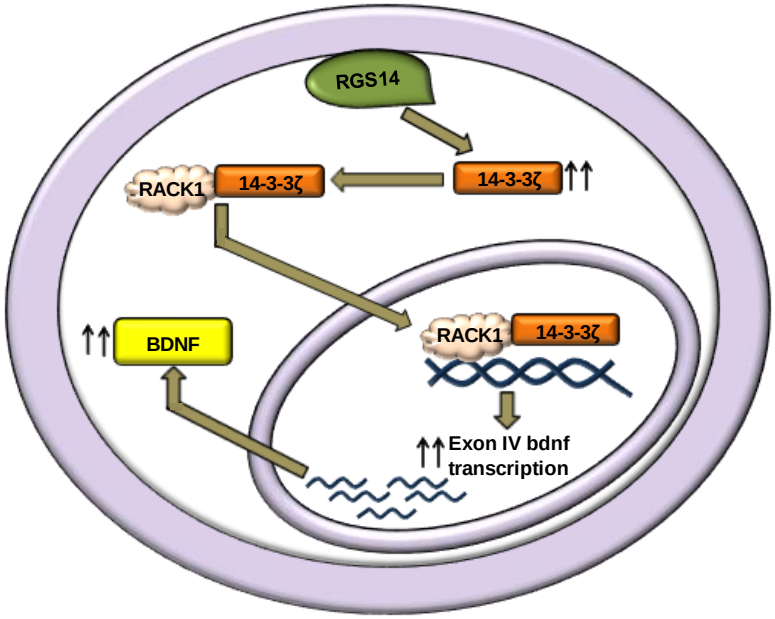

Figure 31. A model showing RGS14$_{414}$-mediated increase in BDNF. 14-3-3ζ binds RACK1 and help to shuttle from cytoplasm to nucleus, where 14-3-3ζ-RACK1 complex interacts with exon IV of BDNF and promotes its transcription. RGS-mediated increase in 14-3-3ζ plays a crucial role in upregulated synthesis of BDNF.

An evaluation of expression pattern of both BDNF and 14-3-3ζ at different time intervals of ORM processing showed a complementary expression in such manner that when there was lower level of BDNF, a surge in 14-3-3ζ protein was observed (figure 32). These findings indicate the implication of 14-3-3ζ in regulation of BDNF expression during memory processing in RGS-rats.

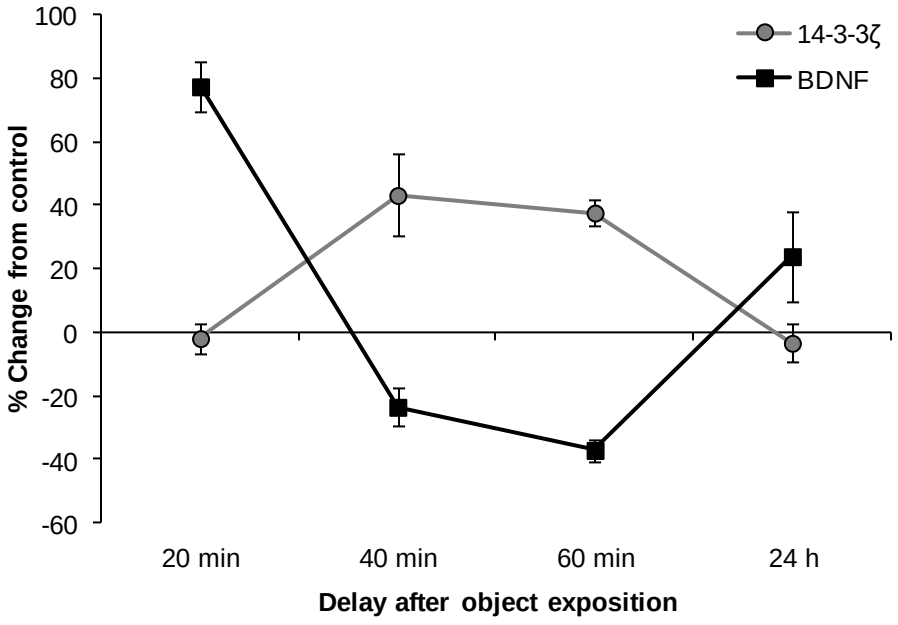

Figure 32. . Synergic expression of 14-3-3ζ and BDNF during ORM processing in RGS-animals. A relative expression pattern analysis of these two proteins suggests that 14-3-3ζ might be involved in regulation of BDNF in RGS14-treated animals.

4 RGS-14-3-3ζ-BDNF pathway in aging and Alzheimer´s disease

It is well documented in literature that BDNF at both mRNA and protein levels are significantly reduced in normal aging and in AD (Connor et al 1997; Hock et al 2000; Michalski & Fahnestock 2003; Narisawa-Saito et al 1996; Peng et al 2005) (Caccamo et al 2010; Christensen et al 2008; Francis et al 2012; Peng et al 2009; Shin et al 2014). In fact, many therapeutic strategies targeting to ameliorate cognitive impairment are associated with BDNF up-regulation (Blurton-Jones et al 2009; Caccamo et al 2010; Iwasaki et al 2012). Recent studies showed that direct BDNF infusion or gene delivery into entorhinal cortex of dementia models reversed synaptic loss, partially normalized aberrant gene expression, improved cell signaling, and restored learning and memory (Iwasaki et al 2012; Nagahara et al 2013; Nagahara et al 2009). Additionally, treatment with other natural products and small molecules that can induce endogenous BDNF expression has been discovered to ameliorate cognitive dysfunction (Li et al 2015; Shin et al 2014; Teng et al 2014; Zuccato & Cattaneo 2009). In addition to BDNF, differential gene expression studies have demonstrated a substantial decrease in 14-3-3ζ in normal aging and in AD (Miller et al 2008). Our results demonstrating prevention of memory loss in rodent models of aging and AD by $RGS14_{414}$ gene treatment might be mediated through restoration in BDNF and 14-3-3ζ protein levels and normalization in 14-3-3ζ–BDNF pathway. Though how RGS14 causes an increase in 14-3-3ζ protein levels remains an issue of current investigation of this laboratory, we have demonstrated from current work that $RGS14_{414}$ gene treatment is a viable strategy against memory loss.

VI. CONCLUSIONS

1. A single treatment of $RGS14_{414}$ gene in rodent models of aging and Alzheimer´s disease not only prevented a memory loss but also maintained the memory level long after the treatment.

2. $RGS14_{414}$ treatment induced robust neuronal arborization and permanent structural change. This structural reorganization in brain overrides the faulty functions responsible for memory loss and further facilitates enhanced memory information processing.

3. The expression pattern of BDNF during ORM processing overlapped with the time frame observed for memory consolidation. Therefore, high BDNF levels in RGS-animals may be key to RGS-mediated memory enhancement.

4. A synergic expression pattern of both BDNF and 14-3-3ζ during memory processing in brain suggest the implication of 14-3-3ζ-BDNF pathway. Thus, high level of 14-3-3ζ in RGS-animals may induce high expression of BDNF needed for neuronal arborization, its maintenance and enhanced memory processing in RGS-animals.

5. Our data suggest that $RGS14_{414}$ gene treatment could serve as a therapeutic strategy for the treatment of episodic memory loss in patients.

VII. RESUMEN

1 INTRODUCCIÓN Y OBJETIVOS

1.1 Regulador de la señalización de la proteína G 14 (RGS14) y su implicación en la memoria

La señalización de las proteínas G comienza con la unión del ligando a un receptor acoplado a dicha proteína G heterotrimérica (GPCR) (Albert & Robillard 2002; Neves et al 2002). La activación de GPCR promueve la liberación de guanosín difosfato (GDP) y la consiguiente unión de guanosín trifosfato (GTP) para la activación de la subunidad Gα. Esta activación modula la disociación/reorganización del complejo heterotrimérico permitiendo la interacción de las subunidades Gα y Gβγ con sus efectores y desencadenando así las cascadas de señalización intracelular correspondientes. La subunidad Gα que presenta una actividad GTPasa, rápidamente inicia su propia inactivación a través de la hidrólisis de GTP volviendo así a su estado de reposo (Gα-GDP), uniéndose a la subunidad Gβγ y reasociándose con GPCR (Gilman 1987; Hamm 1998; Hepler & Gilman 1992; Oldham & Hamm 2008) (ver figure 1, pág. 3). Este ciclo GTPasa de activación/desactivación de las proteínas G está regulado por los más de 30 miembros que constituyen la familia de reguladores de la señalización de las proteínas G (RGS) (Ishii & Kurachi 2003; Koelle 1997). RGS14 pertenece a esta familia de proteínas que comparten un dominio RGS de 120-130 aminoácidos en el extremo amino terminal. Este dominio les confiere actividad GTPasa (actividad GAP) sobre la subunidad G_α activada (G_α-GTP) de las proteínas G heterotriméricas acelerando e interrumpiendo la señalización intracelular mediada por GPCR (De Vries et al 2000; Hollinger & Hepler 2002; Ross & Wilkie 2000; Woodard et al 2015). Dado que las proteínas RGS se unen selectivamente a distintas isoformas de las subunidades G_α, pueden modular de manera específica la señalización de distintos receptores GPCR (Arshavsky & Pugh 1998; Berman & Gilman 1998; Berman et al 1996; De Vries & Farquhar 2002; Hepler 1999; Hollinger & Hepler 2002; Neubig & Siderovski 2002; Ross & Wilkie 2000; Tesmer et al 1997). Concretamente, la proteína RGS14 se une a la subfamilia de $G_{\alpha i/o}$ para promover la hidrólisis del GTP (Cho et al 2000; Hollinger et al 2001; Traver et al 2000; Traver et al 2004).

No obstante, la proteína RGS14 cuenta con otros dominios funcionales además del dominio RGS: un dominio C-terminal regulador de proteínas G (GPR; también conocido como GoLoco) de ≈ 20 aa y dos dominios centrales en tándem de unión a Ras (RBD), RBD1 y RBD2 de ≈ 70 aa cada uno (Kimple et al 2001; Siderovski et al 1999) (ver figure 2, pág. 5).

A través del dominio GPR, RGS14 se une selectivamente a las isoformas inactivas $G_{\alpha i1}$-GDP o $G_{\alpha i3}$-GDP inhibiendo la disociación del GDP (actividad GDI) y por tanto la activación de dichas subunidades. Esta función además mantiene a la proteína RGS14 próxima a la membrana plasmática (Kimple et al 2001; Mittal & Linder 2004; Shu et al 2007). La fosforilación de la proteína RGS14 en la treonina 497 mediante la proteína quinasa A (PKA) favorece su actividad GDI (Hollinger et al 2003). Además, a través de su dominio RBD1, RGS14 se une a las proteínas H-Ras y Rap2 permitiendo así la participación de RGS14 en las vías de señalización de H-Ras (Formstecher et al 2005; Kiel et al 2005; Mittal & Linder 2006; Shu et al 2010; Traver et al 2000; Willard et al 2009; Wohlgemuth et al 2005). Hasta el momento, no se conocen moléculas de unión al dominio RBD2.

El hecho de ser una proteína multidominios, hace que RGS14 se considere una proteína de andamiaje que podría estar integrando distintas vías de señalización intracelular (Brown et al 2015; Vellano et al 2013; Zhao et al 2013) y por tanto participar en diversas funciones celulares. Esta idea se ha visto respaldada por el patrón de expresión dinámico en el tiempo y en el espacio que presenta RGS14 a través de la totalidad del cerebro, e incluso en los distintos compartimentos celulares (Evans et al 2014; Lopez-Aranda et al 2006; Shu et al 2007). Experimentos de Northen blot (Snow et al 1997), estudios de hibridación *in situ* (Grafstein-Dunn et al 2001) y de reacción en cadena de la polimerasa cuantitativa (qPCR) (Larminie et al 2004) demostraron de forma independiente la presencia de mRNA de RGS14 en tejidos de cerebro de rata y humano. De igual modo, estudios de inmunohistoquímica (Lopez-Aranda et al 2006) y experimentos de inmunoblot (Hollinger et al 2001) han demostrado que la proteína RGS14 se localiza de forma abundante en el cerebro de rata y mono. En el cerebro adulto de ratón, el mRNA de RGS14 así como la proteína RGS14 se encuentran de forma predominante en las neuronas hipocampales de CA2, específicamente en espinas y dendritas (Lee et al 2010). Recientemente, un análisis anatómico detallado de la localización de RGS14 en el cerebro de ratón ha demostrado la existencia de altos niveles tanto de mRNA como de proteína RGS14 durante el desarrollo posnatal, presentando un patrón de expresión dinámico localizado en el hipocampo y la corteza olfatoria primaria en el cerebro de ratón adulto (Evans et al 2014).

El gen para RGS14 humana (GenBank, NP_006471.2) codifica una proteína de 566 aminoácidos ($RGS14_{566}$, Uniprot, O43566-7). Hasta el momento, se han descrito tres

variantes mediante *splicing* alternativo, sin embargo, aún no han sido completamente caracterizadas. La isoforma 3 de la proteína RGS14 de 414 aminoácidos ($RGS14_{414}$, Uniprot, O43566-5), objeto de estudio de este trabajo de tesis, se codifica en un gen de 1245 pares de bases (bp) (GenBank, AY987041) y ha sido clonado en nuestro laboratorio a partir de la genoteca de cDNA de corteza cerebral humana (Lopez-Aranda et al 2006) (ver figure 2, pág. 5). La secuencia de esta isoforma ($RGS14_{414}$) difiere de la original ($RGS14_{566}$) en que presenta una deleción de los 153 primeros aminoácidos, una inserción de una lisina en la posición 352 además de un cambio del aminoácido valina, que se encuentra en la posición 416. Por tanto, considerando no solo la ausencia del dominio RGS, que es crucial para la actividad GAP, sino también la presencia de diferencias significativas a través de la secuencia completa, se sugiere que $RGS14_{414}$ podría estar interviniendo en funciones cerebrales no asociadas a la hidrólisis del GTP.

Un estudio comportamental *in vivo* realizado en nuestro laboratorio puso de manifiesto el papel de esta isoforma en la mejora de la memoria de reconocimiento de objetos (ORM) (Lopez-Aranda et al 2009). La memoria de reconocimiento es uno de los ejemplos más estudiados de memoria declarativa. Proceso por el cual se identifica un objeto, una persona, un lugar o un evento que se ha visto previamente (Diana et al 2007; Yonelinas 2001; Yonelinas et al 2010). A lo largo de los años, se ha demostrado que el lóbulo medio temporal (MTL) juega un papel central en el procesamiento de la ORM. Sin embargo, las diferentes subregiones del MTL contribuyen de un modo diferente en dicho proceso (Aggleton & Brown 2006; Aggleton et al 1997; Bachevalier et al 2015; Barbosa et al 2012; Barker et al 2007; Barker & Warburton 2011; Bussey et al 2000; Bussey et al 1999; Eichenbaum et al 2007; Hunsaker et al 2008; Lee et al 2005; Meunier et al 1993; Mumby & Pinel 1994; Yonelinas et al 2002). No obstante, además del MTL, otras regiones cerebrales se han visto implicadas en el procesamiento de la ORM, tales como la corteza prefrontal (PFC) (Morici et al 2015) y la corteza visual secundaria (V2) (Lopez-Aranda et al 2009). La estimulación del área V2 mediante la sobreexpresión de $RGS14_{414}$ dio lugar a un importante aumento de la capacidad mnemónica en ratas. Este efecto sobre la ORM fue de tal magnitud que en nuestras condiciones experimentales una ORM normal, de una duración de hasta 45 min (memoria a corto plazo), se convirtió en una memoria a largo plazo que pudo ser registrada incluso después de varios meses (Lopez-Aranda et al 2009). Además, la eliminación selectiva de las neuronas del área V2 conllevó tanto la pérdida completa de la ORM normal como de la potenciación de la ORM mediada por esta proteína. Esto demuestra no sólo la capacidad potenciadora de esta molécula, sino también la importancia de V2, un área localizada fuera

del lóbulo medio temporal (MTL), en el procesamiento de este tipo de información. Por otro lado, se demostró que el tratamiento con la proteína $RGS14_{414}$ aumentó la capacidad de carga, es decir, que en nuestras condiciones experimentales los animales tratados con el gen de $RGS14_{414}$ mostraron la capacidad de retener la información de hasta 6 objetos a diferencia de los animales normales sin tratamiento que fueron incapaces de reconocer más de 3 objetos (Lopez-Aranda et al 2009).

Estos hallazgos sugieren que la proteína $RGS14_{414}$ podría ser un buen candidato terapéutico para tratar la pérdida de memoria episódica asociada al envejecimiento (Anderson et al 2008; Friedman et al 2010; Luo et al 2007; Nilsson 2003; Peters & Daum 2008; Wang et al 2012; Westerberg et al 2013; Westerberg et al 2006; Wolk et al 2011; Yonelinas & Levy 2002) y a las enfermedades neurológicas y neurodegenerativas, tales como la enfermedad de Alzheimer (Ally et al 2009; Wolk et al 2011). En base a ello, el **primer objetivo** de este trabajo de tesis ha sido evaluar el posible efecto preventivo del tratamiento con el gen $RGS14_{414}$ sobre el déficit de memoria en dos modelos de roedores que presentan dicho déficit, rata envejecida y ratón transgénico de la enfermedad de Alzheimer. Con ello se pretende probar la viabilidad de este tratamiento como potenciador de la memoria no solo en condiciones normales, tal y como se había descrito hasta el momento, sino también en condiciones patológicas. Seguidamente, en este trabajo de tesis, nos propusimos dilucidar el mecanismo que subyace a la mejora de la memoria inducida por la proteína $RGS14_{414}$.

1.2 Importancia de la plasticidad estructural y los factores neurotróficos en la formación de la memoria

Se piensa que el alto nivel de plasticidad estructural que presenta el cerebro de mamífero con respecto al de especies inferiores es clave para codificar y almacenar información a largo plazo sobre las experiencias vividas (Bailey et al 2015; Bosch et al 2014; Fu & Zuo 2011). De hecho, diversos estudios han relacionado fallos en la capacidad de remodelación neuronal con la pérdida de memoria observada en el envejecimiento y en la enfermedad de Alzheimer (Badhwar et al 2013; Bloss et al 2011; Selkoe 2002; Spires-Jones & Knafo 2012). Teniendo en cuenta que las proyecciones dendríticas suponen la mayor parte de la sustancia gris y su implicación en la mayoría de los contactos sinápticos de las distintas áreas corticales y subcorticales (Hofer et al 2009; Restivo et al 2009; Roberts et al 2010; Xu et al 2009; Yang et al 2009), la plasticidad estructural dendrítica debe ser clave para el

procesamiento de la información en el cerebro. En este sentido, se piensa que el refuerzo de los contactos sinápticos a través de las dendritas debido a procesos electrofisiológicos y moleculares en el interior de las neuronas, es el principal responsable en la adquisición y consolidación de la memoria a largo plazo (Bailey & Kandel 1993; Yang et al 2009). Así, en los procesos de aprendizaje y memoria diversos trabajos han demostrado cambios en la longitud en el cuello de las espinas dendríticas y en su volumen, pérdida o generación de prolongaciones dendríticas, así como la propia generación de nuevas dendritas (Lamprecht & LeDoux 2004; Segal 2005).

Por esta razón, considerando la implicación de la plasticidad estructural y de la proteína $RGS14_{414}$ sobre la capacidad mnemónica, pensamos que el tratamiento con el gen de $RGS14_{414}$ podría estar induciendo un aumento en la arborización neuronal en el cerebro que favorezca las conexiones neuronales y una mayor plasticidad estructural. Para probar esta hipótesis el **segundo objetivo** de este trabajo ha sido analizar el nivel de ramificación dendrítica de neuronas piramidales y no piramidales del área tratada con $RGS14_{414}$ en contraposición con el de animales controles.

En la literatura ha quedado bien documentada la implicación de los factores neurotróficos a través de sus cascadas de señalización en la arborización dendrítica de las neuronas (Kopec & Carew 2013; McAllister et al 1999). Los factores neurotróficos son moléculas secretadas que al unirse a sus receptores asociados a membrana activan distintas cascadas de señalización intracelular que en última instancia promueven la supervivencia celular, la neurogénesis, la sinaptogénesis, así como el nacimiento del axón y de nuevas dendritas y su maduración (Dijkhuizen & Ghosh 2005; Horch & Katz 2002; Ji et al 2005; Park & Poo 2013). Además, los factores neurotróficos se han visto implicados en la inducción de la plasticidad sináptica a largo plazo (Conner et al 2009; Chao 2003; Egan et al 2003; McAllister et al 1999; Poo 2001) y en la síntesis de proteínas (Tanaka et al 2008), actividades fundamentales para la formación de la memoria a largo plazo.

En base a ello como **tercer objetivo** de este trabajo nos planteamos estudiar la posible implicación de los factores neurotróficos en la mejora de la memoria mediada por la proteína $RGS14_{414}$. Dado que nos ha sido imposible estudiar todos los existentes (Kopec & Carew 2013), nos hemos centrados en dos neurotrofinas, el factor de crecimiento nervioso (NGF) y el factor neurotrófico derivado del cerebro (BDNF), así como en el factor de crecimiento de fibroblastos 2 (FGF2). Estas tres moléculas han sido clásicamente bien estudiadas por su abundancia en el cerebro (Aid et al 2007; Bean et al 1991; Eckenstein et al 1991; Gonzalez et al 1995; Grothe & Janet 1995; Korsching et al 1985; Large et al 1986; Levi-Montalcini &

Angeletti 1968; Maisonpierre et al 1990; Timmusk et al 1994), su relación con la plasticidad estructural (Alleva & Aloe 1989; Comeau et al 2007; Gorski et al 2003; Horch 2004; Horch et al 1999; Jin et al 2003; Szebenyi et al 2001; Wirth et al 2003) y sináptica (Barrett 2000; Bramham & Messaoudi 2005; Conner et al 2009; Chao & Bothwell 2002; Dechant & Barde 2002; Lu 2003; Miller & Kaplan 2001; Poo 2001; Tongiorgi 2008; Tongiorgi & Baj 2008; Zhao et al 2007), así como su implicación en los procesos de aprendizaje y memoria (Alonso et al 2002; Andero et al 2014; Bekinschtein et al 2008a; Bekinschtein et al 2014; Conner et al 2009; Gomez-Pinilla et al 1998; Gutierrez et al 1997; Intlekofer et al 2013; Koponen et al 2004; Linnarsson et al 1997; Mizuno et al 2000; Romero-Granados et al 2010; Tyler et al 2002; Woolf et al 2001).

Finalmente, para completar este trabajo de tesis como **cuarto objetivo** nos planteamos llevar a cabo un proyecto de proteómica con el fin de identificar nuevas proteínas implicadas en el mecanismo molecular subyacente a la mejora de la memoria mediada por la proteína $RGS14_{414}$.

2 MATERIALES Y MÉTODOS

2.1 *Primer bloque experimental.* Efecto del tratamiento del gen RGS14$_{414}$ sobre la prevención de la pérdida de memoria episódica que aparece en la enfermedad de Alzheimer y en el envejecimiento

Con la finalidad de probar el posible efecto preventivo sobre la pérdida de memoria del gen RGS14$_{414}$, llevamos a cabo este primer bloque de experimentos (resumen en la figura 1). Dado que la pérdida de memoria ha sido bien estudiada en los casos de envejecimiento y enfermedad de Alzheimer (Drag & Bieliauskas 2010), en este trabajo de tesis hemos utilizado ratas macho Wistar Han (Charles River) modelo de envejecimiento, así como ratones transgénicos J20 (Jackson Laboratory) modelo de enfermedad de Alzheimer.

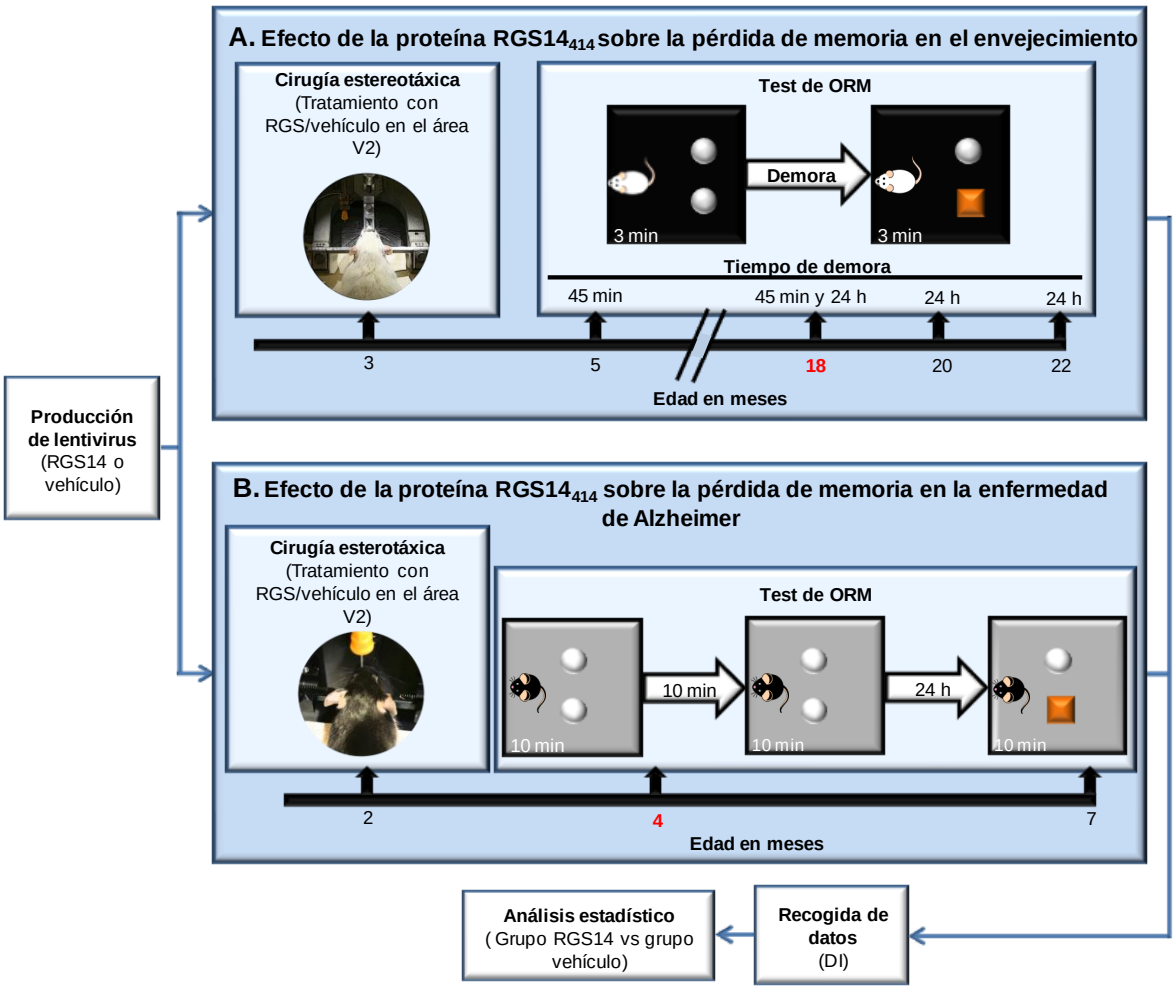

Figura 1. Esquema del diseño experimental (en rojo se muestra la edad a la cual cada modelo pierde la memoria).

Previamente al estudio de envejecimiento, se estableció en nuestro modelo la edad de aparición del déficit de memoria como consecuencia del propio paso del tiempo, sometiendo a un grupo de 12 ratas a la prueba de reconocimiento de objetos a distintas edades. Una vez demostrado que nuestro modelo experimental presentaba una pérdida significativa de la memoria a los 18 meses, se procedió a tratar a los animales antes de la aparición del déficit cognitivo con el gen de $RGS14_{414}$. Para ello se perfundió una solución de lentivirus que contenían el gen $RGS14_{414}$ o el vector vacío (vehículo, individuos controles) en el área V2 de ratas de 3 meses de edad mediante la técnica de cirugía estereotáxica. Posteriormente, su ORM se evaluó a las edades de 5, 18, 20 y 22 meses (figura 1.A).

En el estudio sobre la pérdida de memoria en un modelo de la enfermedad de Alzheimer, utilizamos ratones transgénicos de la línea J20 que sobreexpresan la proteína precursora de β-amiloide humana con las mutaciones sueca (K670N/M671L) e indiana (V717F) bajo el control del promotor de la cadena B del factor de crecimiento derivado de plaquetas (PDGF-β) (Mucke et al 2000); responsables ambas mutaciones de la variante familiar de la enfermedad de Alzheimer en humanos. Mediante un estudio previo y en base a trabajos anteriores (Escribano et al 2009; Schiapparelli et al 2006), confirmamos la edad a la que este modelo comenzaba a presentar un déficit cognitivo. Para ello, se emplearon 12 animales *wild-type* de la cepa C57BL/6J y 8 ratones transgénicos, cuya ORM se evaluó a los 2 y 4 meses de edad. Seguidamente, ratones transgénicos de 2 meses de edad, se trataron con lentivirus del gen RGS14 o con lentivirus vehículo en el área V2 mediante cirugía estereotáxica y su capacidad mnemónica se evaluó mediante el test de reconocimiento de objetos a las edades de 4 y 7 meses (figura 1.B).

Producción de lentivirus

El gen de $RGS14_{414}$ (GenBank, AY987041) se clonó en el plásmido comercial pLVX-DsRed-Monomer-C1 (Clontech, 632153) aprovechando las secuencias diana de restricción para las endonucleasas EcoRI y XhoI. Este vector permite la coexpresión constitutiva de nuestro gen de interés con la proteína fluorescente DsRed-Monomer, facilitando así su posterior identificación. Las secuencias diana de corte para ambas endonucleasas se añadieron a los extremos del gen $RGS14_{414}$ mediante una reacción en cadena de la polimerasa (PCR) (ver *table* 1,2,3, págs. 23, 24) y posteriormente tras confirmar la presencia del fragmento de DNA con el tamaño adecuado mediante un gel de agarosa éste se purificó por gel usando el kit *Wizard® SV gel and PCR Clean-Up System* (Promega, A9281). Se llevó a cabo una

reacción de restricción con las endonucleasas XhoI y EcoRI de New England Biolab tanto del gen como del vector para generar extremos cohesivos entre ambos que facilitasen su unión (ver *table* 4, pág. 26). El DNA del gen se insertó en el del vector, ambos previamente purificados por gel, mediante una reacción de ligación usando la enzima ligasa T4 (Life Technologies, 1524) de acuerdo con el protocolo del fabricante (ver *table* 5, pág. 26). Finalmente, el DNA recombinante se amplificó por transformación mediante shock térmico en bacterias competentes (One Shot® Omni Max^{TM} 2 T1® Chemically Competent *E.coli*; Life Technologies, C8540-03) de acuerdo con el protocolo del kit. Las bacterias que incorporaron con éxito el DNA se seleccionaron en medio LB-agar con ampicilina a una concentración de 100 µg/ml. El DNA de cuatro colonias se purificó por la técnica de miniprep usando el kit *StratPrep plasmid miniprep* (Agilent technologies, 4007661) (*appendix 1*.C.2) y mediante una reacción de restricción con las enzimas XhoI y EcoRI, se comprobó la existencia no sólo del vector, sino también del inserto de interés (*figure 9*.A, pág. 30). Mediante la reacción de maxiprep usando el kit de Promega *Wizard® Plus Maxiprep DNA Purification System* (A7270) (*appendix* 1.C.3) se generó una mayor cantidad de nuestro DNA recombinante de interés que nuevamente fue evaluado mediante una reacción de restricción con las enzimas XhoI y EcoRI (figure 9.B, pág. 30). Células de la línea 293T (Clontech, 632180) (ver *appendix* 2) en su sexto subcultivo se transfectaron con el DNA del plásmido vacío (para generar lentivirus vehículo) y con el DNA recombinante de $RGS14_{414}$ (lentivirus $RGS14_{414}$) mediante el *Lenti-XTM Packaging System* (Clontech, 631247) de acuerdo con el protocolo aportado por el fabricante (*table* 7, pág. 31). Las células se incubaron durante 48 h para favorecer la producción de lentivirus cambiando el medio a las 24 h. El medio que contenía los lentivirus tanto del stock RGS14 como de vehículo, se recogió cuidadosamente y se centrifugó a 500 x g durante 15 min a 4 ºC y el sobrenadante resultante se filtró a través de un filtro polisulfónico de 0,45 µm de tamaño de poro, con el fin de eliminar cualquier resto celular.

La solución de lentivirus se concentró mediante ultracentrifugación (Ichim & Wells 2011) a 25.000 rpm durante 90 min a 4 ºC en tubos Ultra-Clear (Beckman Coulter, 344058) en una ultracentrífuga XL-90, rotor SW29. El sobrenadante se descartó y el pellet donde se encontraban los lentivirus se resuspendió cuidadosamente en 150 µl de suero salino estéril. Finalmente, se hicieron alícuotas de 3,5 µl de las soluciones stock de lentivirus que se almacenaron a -80 ºC hasta su uso.

Para determinar, el título de las soluciones de lentivirus, se utilizaron las células HT1080 (ATCC, CCL-121) (ver *appendix* 2) una línea celular comercial derivada de fibrosarcoma humano. 2 x 10^5 células en su cuarto subcultivo, se sembraron en cada uno de los pocillos de una placa de 6 pocillos y se dejaron reposar durante 24 h para favorecer su adhesión. Entonces, diluciones seriadas en base 10 en un rango entre 10^{-3} a 10^{-7} de las soluciones de lentivirus se añadieron a cada uno de los pocillos, agregando medio sin lentivirus como control a uno de ellos. Tras incubar las células durante 48 h en la solución de lentivirus, las células transfectadas se seleccionaron añadiendo al medio el antibiótico puromicina (Clontech, 631306) a una concentración de 1 µg/µl ya que el vector pLVX contiene el gen de resistencia a dicho antibiótico ($Puro^r$). Las células se mantuvieron durante 10 días renovando el medio cada 48 h. Finalmente, las colonias supervivientes se tiñeron con cristal violeta al 1 %. El título de lentivirus en términos de unidades formadoras de colonias (CFU) se estimó mediante el recuento de las colonias supervivientes en el pocillo sometido a la solución de lentivirus más diluida en la que pudieron visualizarse colonias (*figure* 10, pág. 33). El título de los stocks de lentivirus $RGS14_{414}$ y vehículo fue de 1,75 x 10^7 CFU/ml y 2,75 x 10^6 CFU/ml respectivamente.

Cirugía estereotáxica

4000 CFU en 2 µl (en el caso de ratas) o 2000 CFU en 1 µl (en el caso de ratón) de la solución de lentivirus RGS14 se perfundieron intracranealmente mediante cirugía estereotáxica (Cetin et al 2006; Cooley & Vanderwolf 2005; Fornari et al 2012) usando el estereotáxico de rata (Stoelting), al cual se le acopló un adaptador para el caso de ratón (Cunningham mouse, Harvard Apparatus) y una bomba de infusión (11 Plus, Harvard Apparatus) a un flujo de 10 µl/h. Las coordenadas del área V2 (ver *table* 8, pág. 34) se tomaron de *The Rat Brain in Stereotaxic Coordinates* (Paxinos & Watson 1998) y del *The Mouse Brain in Stereotaxic Coordinates* (Paxinos & Franklin 2001). Antes de proceder con la cirugía los animales se anestesiaron profundamente mediante inyección intraperitoneal (i.p) de una dosis de ketamina de 75 mg/kg (Imagelne 1000; Merial Laboratorios) y medetomidina (Domtor; Pfizer) a una dosis de 1 mg/kg en el caso de rata y de 0,5 mg/kg en el caso de ratón. Durante el proceso, los animales se mantuvieron sobre una manta eléctrica para evitar la hipotermia y sus ojos se mantuvieron lubricados. Después del procedimiento quirúrgico, durante 5 días consecutivos los animales se trataron con antibiótico (Dermocan, Fatro) vía tópica y con 150 µl del analgésico Meloxicam i.p (Metacam 5 mg/ml, Boehringer Ingelheim).

Test de reconocimiento de objetos

Para evaluar la memoria episódica de los roedores se llevó a cabo la prueba de reconocimiento de objetos (figura 2). El test de ORM se basa en la tendencia natural de los roedores por explorar la novedad (Ennaceur & Delacour 1988), de manera que la tarea consiste en una primera fase de adquisición, en la que los animales se exponen a dos objetos idénticos y transcurrido un tiempo de demora, se exponen a un objeto completamente nuevo en contraposición con el familiar. Si el animal recuerda el objeto familiar explorará más el objeto nuevo, mientras que si no lo recuerda dedicará un tiempo similar a la exploración de ambos objetos. El protocolo del test de ORM para rata (figura 2.A) fue descrito previamente por López-Aranda y col. (Lopez-Aranda et al 2009) y la tarea de ORM para ratón (figura 2.B) por otros grupos (Escribano et al 2009; Schiapparelli et al 2006).

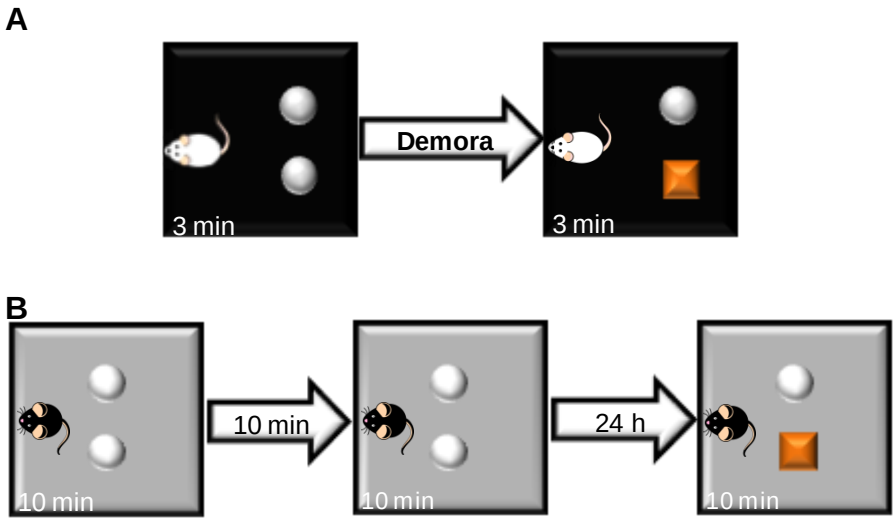

Figura 2. Test de ORM para rata (A) y para ratón (B).

Antes de llevar a cabo la tarea, con el fin de eliminar el estrés de los animales y por consiguiente favorecer la exploración a los objetos durante la prueba, se llevó a cabo un protocolo de manipulación sobre el brazo del investigador durante 8 min, 5 días consecutivos. Seguidamente y durante 3 días consecutivos, los animales se habituaron al campo abierto vacío donde se realiza el test (una caja negra cuadrada de madera de 100 x 100 x 50 cm en el caso de la rata, y una caja gris cuadrada de 50 x 35 x 50 cm de Harvard Apparatus para ratón); 12 min en el caso de las ratas y 10 min en el caso de los ratones. Los objetos usados para la prueba se muestran en el *appendix* 3 y el tiempo de exploración de los objetos se estimó como el tiempo que el animal permanecía con la nariz pegada a ellos. El índice de discriminación (DI) se calculó como: DI=N/(N+F), donde N indica el tiempo de exploración del objeto nuevo y F el tiempo de exploración del objeto familiar. En nuestro experimento, consideramos que

valores de DI por encima de 0,66 indican que el animal es capaz de retener la información del objeto familiar en su memoria. Los valores de DI se presentaron como la media ± SEM y mediante un análisis estadístico a través del programa SigmaStat 3.5 (Jandel Scientific) entre los distintos grupos, se detectaron las posibles diferencias significativas inter o intra grupos aceptando una probabilidad de error del 5%. En el caso del estudio de envejecimiento los grupos se compararon mediante la prueba t de Student, mientras que para el estudio de Alzheimer se usó el ANOVA de una vía con la consiguiente prueba post-hoc HSD de Tukey.

Inmunohistoquímica

La expresión de la proteína $RGS14_{414}$ en el área V2 del cerebro de roedores se confirmó mediante la técnica de inmunohistoquímica (*figure* 14, pág. 38) utilizando un anticuerpo específico para nuestra proteína producido en conejo (NBP1-31174, dilución 1:500; Novus biological). Tras la perfusión transcardíaca del animal, el cerebro lavado y fijado con PLP se extrajo, se crioprotegió en una solución de sacarosa al 30 % y se congeló para la obtención de secciones coronales de 30 µm de grosor del área tratada. Sobre las secciones se llevó a cabo la inmunohistoquímica de fluorescencia siguiendo un protocolo similar al descrito previamente en (Lopez-Aranda et al 2009). El anticuerpo secundario anti-conejo usado fue producido en cabra y conjugado con el fluorocromo Alexa fluor® 488 (Life technologies, A11008; dilución 1:1000). Para conocer más detalle de la técnica consultar el *appendix* 4.

2.2 *Segundo bloque experimental.* Determinación de la correlación entre la mejora de la ORM mediada por la proteína $RGS14_{414}$ y la arborización neuronal

Dado que el efecto potenciador de la memoria mediado por la proteína $RGS14_{414}$ perdura en el tiempo, pensamos que esta proteína podría estar provocando cambios estructurales permanentes, concretamente un aumento en la arborización neuronal, que favorezca la conexión en el cerebro y facilite el procesamiento de la información en el mismo. Con la finalidad de comprobar esta hipótesis, diseñamos este bloque experimental en el que se visualizó y analizó el grado de arborización de neuronas piramidales y no piramidales del área V2 tratada con $RGS14_{414}$ en contraposición de aquellas en animales tratados con vehículo (figura 3).

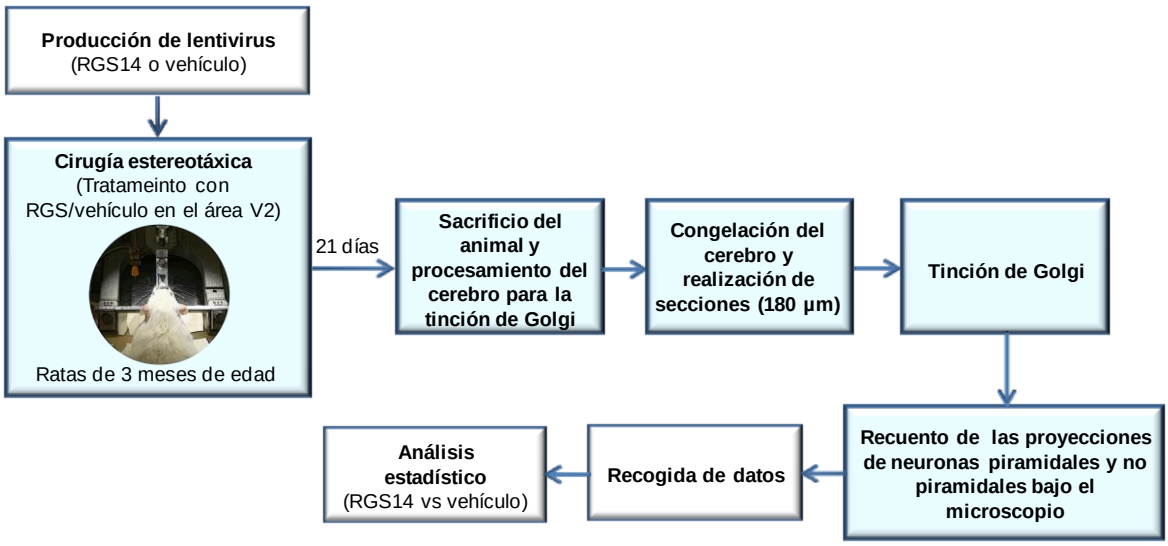

Figura 3. Esquema resumen del 2º bloque de experimentos.

Ratas de la cepa Wistar Han de 3-4 meses se trataron con la solución de lentivirus de $RGS14_{414}$ y de vehículo en el área V2 mediante cirugía estereotáxica (ver primer bloque experimental apartado VII.2.1) incluyendo 4 animales por grupo. Transcurridos 21 días desde el tratamiento, los animales profundamente anestesiados se decapitaron, obteniéndose y procesándose el área V2 para la tinción de Golgi-Cox que se llevó a cabo usando el kit *Rapid GolgiStain* (FD Neurotechnologies, Inc, PK401), de acuerdo con el protocolo suministrado por el fabricante. Una vez procesado el tejido, se sumergió durante 1 min en una solución de isopentano pre-enfriado a -70 ºC (Sigma Aldrich, M32631) y se congeló rápidamente a -80ºC. Tras realizar secciones de 180 µm de grosor al criostato y montarlas sobre el portaobjetos, las rodajas se tiñeron y deshidrataron por inmersión en una batería de soluciones de etanol en gradación creciente:50 %, 75 %, 95 %, 100 % (v/v) y se cubrieron con cubreobjetos usando unas gotas de medio de montaje Permount (Fisher Scientific, SP15-100).Finalmente, usando el microscopio DM IRE2 (Leica Micosystems) y el programa Leica MM AF versión 1.6.0 (Leica Microsystems) se realizó un recuento de las neuritas, así como de las proyecciones que emergían desde las neuritas tanto de neuronas piramidales como de células no piramidales del área tratada. Además, en el caso de las neuronas piramidales, también se analizó el número de ramificaciones que se proyectaban desde la dendrita apical (*figure* 16, pág. 41). Un total de 55 y 56 neuronas piramidales y no piramidales respectivamente se contaron en las secciones de los animales tratados con vehículo; mientras que de las secciones procedentes de animales tratados con RGS14 se contaron 79 y 56 respectivamente. El número de neuritas, de ramificaciones neuríticas o de ramificaciones en la dendrita apical por cada neurona piramidal o no piramidal se presentó como la media ± SEM y mediante un análisis estadístico t de

Student (SigmaStat 3.5, Jandel Scientific) se identificaron las posibles diferencias significativas entre el tratamiento con $RGS14_{414}$ y el tratamiento control con vehículo aceptando una probabilidad de error igual o inferior al 5 % ($p \leq 0,05$).

2.3 *Tercer bloque experimental.* Determinación de la relación entre la mejora de la memoria mediada por $RGS14_{414}$ y los factores neurotróficos.

Considerando que los factores neurotróficos juegan un papel clave en la arborización dendrítica, así como en el desarrollo de los circuitos neuronales y en los procesos de aprendizaje y memoria, diseñamos este bloque experimental con el fin de estudiar la posible implicación de estas moléculas en el mecanismo que subyace a la mejora de la ORM mediada por la proteína RGS14 (figura 4).

Ratas de la cepa Wistar Han de 3 meses de edad se trataron con la solución de lentivirus que contenían el gen de $RGS14_{414}$ o el vehículo (ver apartadoVII.2.1) mediante cirugía estereotáxica (ver apartadoVII.2.1). Los animales tratados se dividieron en 3 grupos:

(i) Estudio de los factores neurotróficos en los animales RGS. Transcurridos 21 días desde el tratamiento 2 animales por grupo (vehículo o RGS) se sacrificaron para determinar los niveles de mRNA de los factores neurotróficos FGF-2, NGF y BDNF mediante qRT-PCR.

(ii) Estudio del efecto de $RGS14_{414}$ sobre los niveles proteicos de BDNF. Los animales tratados se sacrificaron a los 4, 7, 14 y 21 días (2 animales por grupo para cada día post-tratamiento) y sus cerebros se procesaron para medir los niveles de BDNF mediante la técnica de Western blot (WB).

(iii) Estudio del patrón de expresión del gen bdnf durante el procesamiento de la memoria de reconocimiento de objetos en el modelo animal RGS. Después de 21 días desde el tratamiento, 8 animales por tratamiento se expusieron a dos objetos idénticos durante 3 min como se detalla en el apartado VII.2.1. Los animales se sacrificaron a los 20, 40, 60 min y 24 h desde el momento de la adquisición para analizar los niveles de BDNF en cada intervalo mediante WB.

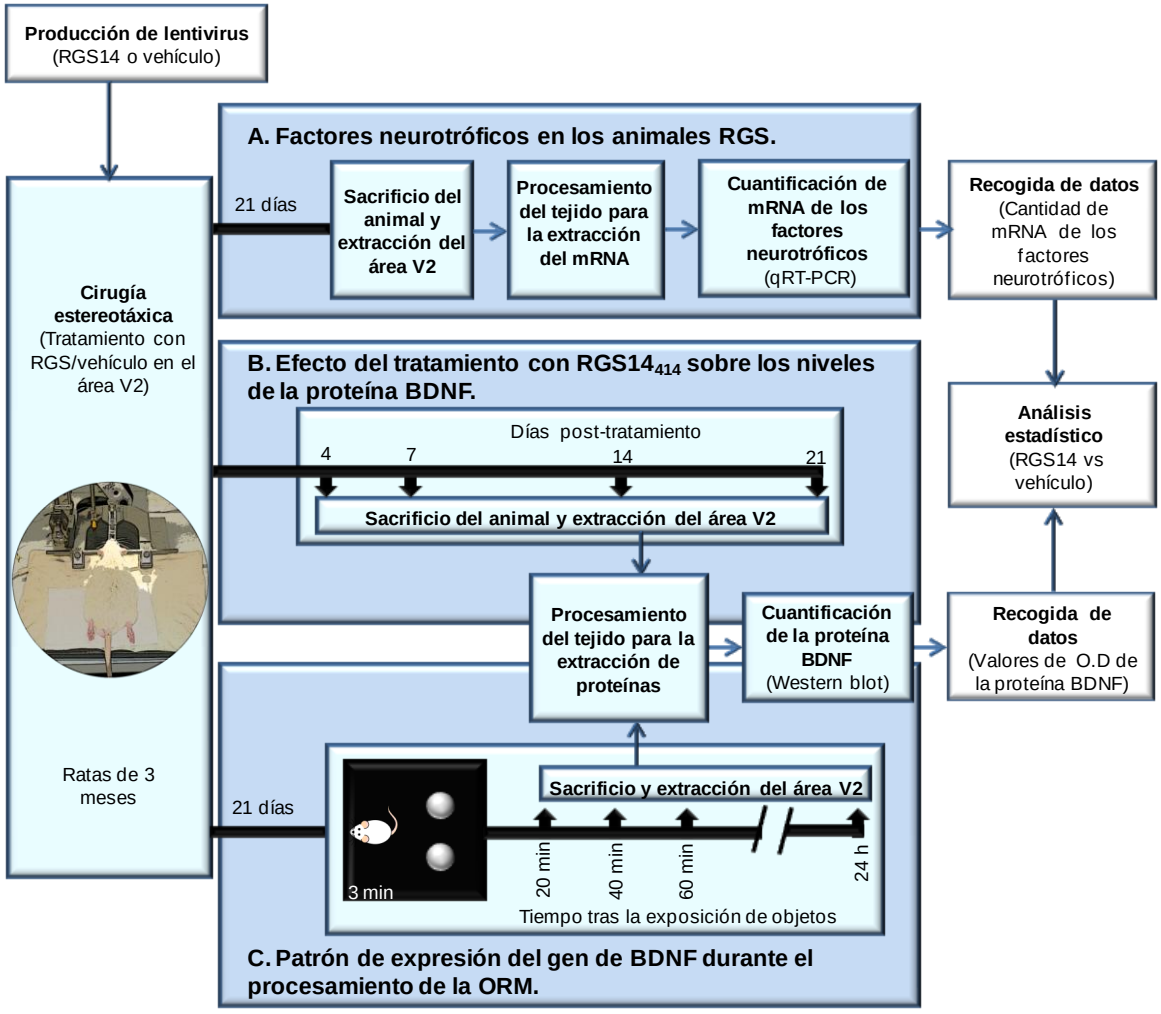

Figura 4. Esquema del diseño experimental.

Para la extracción del área V2 empleada en los experimentos arriba mencionados, los animales se anestesiaron profundamente usando ketamina y medetomidina (ver sección VII.2.1) y se decapitaron. Una vez extraído cuidadosamente el cerebro en fresco, se diseccionó el área V2 con un punch de 4 mm (DH Material Médico, 94158BP-40F).

qRT-PCR

Las muestras se almacenaron en 10 µl de *RNAlater® RNA Stabilization Reagent* (Quiagen, 1018087) por cada mg de tejido en tubos de 1,5 ml a temperatura ambiente hasta su uso. El RNA total de los tejidos se aisló utilizando el *RNeasy Tissue Mini kit* (Quiagen, 74124) de acuerdo con el protocolo proporcionado por el fabricante (ver *appendix* 1.D) y se cuantificó midiendo la absorbancia a una longitud de onda de 260 nm en el espectrofotómetro *Nanodrop1000*, v3.7 (Thermo Scientific). Con el fin de eliminar cualquier resto de DNA genómico, las muestras de RNA se sometieron a la enzima rDNasa I (Ambion,

AM235) siguiendo las recomendaciones del fabricante (*table* 9, pág. 44). Una vez inactivada la endonucleasa, se procedió con la reacción de transcripción inversa para convertir el RNA en un formato más estable, cDNA. La retrotranscripción se llevó a cabo mediante el kit *High Capacity RNA-to-cDNA* (Applied Biosystems, 4387406) durante 30 min a 37 ºC (*table* 10, pág. 44). Al final de la reacción, la enzima se inactivó a 95 ºC durante 5 min, y la concentración de cDNA se estimó de nuevo espectrofotométricamente.

Los cebadores usados en la reacción de qRT-PCR (ver secuencia en la tabla 1) se diseñaron mediante el programa *Primer Express*, v.2.0 (Applied Biosystems) y su especificidad se comprobó utilizando el programa *Primer-Blast* (NCBI) (Ye et al 2012). Finalmente, se llevó a cabo una simulación de la reacción de qRT-PCR usando esta pareja de cebadores con el programa *Amplify 1*.2 (University of Wisconsin).

Tabla 1. Secuencia de los cebadores empleados en las reacciones de qRT-PCR.

GEN	CÓDIGO (GENBANK)	[1]SECUENCIA (5'→3')	TAMAÑO AMPLICÓN (bp)
BDNF	NC_005102.4	*Sentido:* *AAGCAATATTTCTACGAGACCAAGTG* *Antisentido:* *TACGATTGGGTAGTTCGGCATT*	110
FGF-2	NM_019305.2	*Sentido:* *GACGGCTGCTGGCTTCTAAGT* *Antisentido:* *TCCGTGACCGGTAAGTGTTG*	90
NGF	NM_001277055.1	*Forward:* *GCAGACCCGCAACATCACT* *Antisentido:* *GGTGGAGGCTGGGTGCTAA*	90
***Proteína ribosomal L19 (Rpl19)**	NM_031103.1	*Sentido:* ATGCCAACTCTCGTCAACAG *Antisentido:* AGGTGTTCTTCCGGCATCG	102

*Gen de referencia *"Housekeeping"*. [1] *Los primers se sintetizaron por la empresa Sigma-Aldrich.*

Una vez seleccionadas las parejas de cebadores, se determinó su concentración óptima de uso realizando una reacción de qRT-PCR tal y como se explicará más adelante. Se probaron tres concentraciones distintas de cebadores (0,45; 0,225 y 0,1125 µM), con tres cantidades distintas de cDNA control (640, 320 y 160 ng). La concentración de 0,45 µM fue seleccionada para todas las parejas de cebadores ya que además de mantener una diferencia en el valor de Ct de uno entre las distintas cantidades de cDNA probadas, fue la que presentó un menor valor de Ct.

Para la obtención de las curvas estándar, se usó una solución de cDNA de concentración conocida, sobre la que se realizaron 5 diluciones seriadas en base 10 (rango entre 10^{-4} y 10^{-9}). Se llevó a cabo una reacción qRT-PCR usando la concentración óptima de los cebadores. Los valores de Ct se representaron frente al logaritmo de la cantidad de cDNA en femtogramos (*figure* 18, pág. 46), teniendo en consideración sólo aquellos valores de Ct que mantuvieron un correlación de 3,3 ciclos entre dos diluciones 1:10 consecutivas. Se admitieron los valores de curva estándar lineal con un $R^2 > 0,99$ y la eficiencia de amplificación para cada reacción (E) se calculó según la pendiente de la curva mediante la fórmula: $E = 10^{-1/pendiente}$

Elaboradas las curvas estándar para cada gen a estudiar, se realizó la reacción de qRT-PCR de las muestras problema utilizando el kit *Power SYBR® Green PCR Master Mix* (Applied Biosystems, 4367659). Se prepararon triplicados de cada una de las muestras, incluyendo controles negativos (sin muestra) en placas de 96 pocillos para reacciones ópticas *MicroAmp® Optical 96-Well Reaction Plate with Barcode* (Applied Biosystems, 4306737). Cada reacción se llevó a cabo en un volumen total de 24 µl incluyendo la concentración óptima de cebadores y 640 ng de cDNA usando el termociclador *7500 Real-Time PCR Systems* (Applied Biosystems) (*table* 12, pág. 47). Las condiciones térmicas de la amplificación y de la obtención de las curvas de disociación se detallan en la *table* 13 (pág. 47). Las curvas de disociación observadas mediante el programa 7500 V.2.0.6 demostraron que la amplificación había sido específica.

Para determinar la cantidad de RNA (cDNA) en las muestras se interpolaron los valores Ct obtenidos para cada gen en las curvas estándar correspondientes. La cantidad de RNA de los distintos genes (FGF-2, NGF y BDNF) obtenidas tanto para el grupo-RGS14 como para el grupo-vehículo se normalizaron con respecto a las alcanzadas para el gen Rpl19 (gen de referencia, "housekeeping") ($Cantidad_{gen}$ / $Cantidad_{Rpl19}$). Posteriormente, los valores normalizados para cada gen ($Cantidad_{gen\ nor}$) en ambos grupos, se usaron para determinar el porcentaje de cambio que presentaban estos genes a consecuencia del tratamiento con $RGS14_{414}$ con respecto al control (tratamiento vehículo) mediante la fórmula siguiente:

$$[(Cantidad_{gen\ nor}RGS - Cantidad_{gen\ nor}Vehículo)/ Cantidad_{gen\ nor}\ Vehículo] \times 100$$

Finalmente, para detectar posibles diferencias significativas entre los valores normalizados de RNA de ambos tratamientos (RGS versus vehículo) se realizó la prueba estadística t de Student para muestras apareadas usando el programa estadístico SigmaStat 3.5 (Jandel Scientific) y aceptándose un nivel de confianza del 95 %.

Western Blot

Los niveles proteicos de BDNF se evaluaron mediante la técnica de Western blot. Así, el tejido del área V2 se homogeneizó mediante un homogeneizador (Glas-Col) en 2 ml de tampón Tris-HCl 0,01 M, pH 7,4 (*appendix* 5.A.1) que incluía un cocktail de inhibidores de proteasas al 1 % (v/v) (Sigma-Aldrich, P8340) y un cocktail de inhibidores de fosfatasas al 1 % (v/v) (Sigma-Aldrich, P0044). Una vez, estimada la concentración total de proteínas mediante el método de Lowry (Lowry et al 1951) (*appendix* 5.A.2), las muestras se liofilizaron en el *SPC1010 SpeedVac System* (Thermo Savant) y se resuspendieron en tampón de carga (1X) (Laemmli 1970) (*appendix* 5.A.3) para obtener una concentración final de 1 µg/µl. Tras desnaturalizar las proteínas por calor a 95 ºC durante 10 min, se cargaron 2,5 y 5 µg de proteína total de cada muestra junto al marcador de peso molecular *Precision Plus Protein™ ladder* (Bio-Rad, 161-0374) en un gel de poliacrilamida-SDS en gradiente 4-20 % (Bio-Rad, 456-1096). La electroforesis en gel de poliacrilamida en condiciones desnaturalizantes (SDS-PAGE) para separar las proteínas en función del peso molecular se llevó a cabo aplicando un potencial eléctrico de 150 V en el tampón Tris-Glicina-SDS (TGS) (*appendix* 5.A.4). Tras la separación, las proteínas se transfirieron a una membrana de PVDF (Bio-Rad, 1704156) usando el sistema de transferencia *Turbo Trans-Blot (*Bio-Rad) al aplicar una corriente de 25 V durante 7 min.

Una vez finalizada la transferencia, las membranas se incubaron en una solución de bloqueo (leche desnatada en polvo al 10 % (p/v) y BSA al 2 % (Sigma-Aldrich, A3059) en tampón PBS-Tween) (*appendix* 5.A.6) durante 3 h a temperatura ambiente en agitación. Después de cuatro lavados cortos de 5 min en PBS-Tween, las membranas se incubaron con los anticuerpos primarios correspondientes durante toda la noche a 4 ºC y en agitación. Los anticuerpos primarios usados fueron: el anticuerpo policlonal de cabra anti-BDNF (Santa Cruz Biotechnology Inc., sc-33904; dilución 1:250) y el anticuerpo monoclonal de ratón anti-α-tubulina (Sigma Aldrich, T8203; dilución 1:7500) empleado como control de carga. Tras breves lavados, las membranas se incubaron durante 75 min a temperatura ambiente con los respectivos anticuerpos secundarios biotinilados (dilución 1:500): anti-IgG de cabra producido en caballo (Vector Lab., BA9500) y anti-IgG de ratón producido en cabra (Vector Lab., BA9200). Tanto los anticuerpos primarios como secundarios se prepararon en una solución que contenía leche desnatada al 5 %, BSA al 2 % y azida sódica al 0,1 % en PBST. Tras eliminar el exceso de anticuerpo secundario con breves lavados, las membranas se incubaron en una solución de extravidina conjugada con la enzima peroxidasa (Sigma-

Aldrich, E2886) a una dilución 1:2000 en PBS-Tween durante 50 min a temperatura ambiente. Finalmente, las bandas correspondientes a las proteínas BDNF y α-tubulina se revelaron con 3,3'-diaminobenzidina (DAB) *Enhanced liquid substrate system* (Sigma-Aldrich, D3939).

Tras el secado, las membranas se digitalizaron en el escáner *Epson perfection V750 Pro* para el posterior análisis densitométrico de las bandas usando el programa *Quantity One versión 4.6.3* (Bio-Rad). Los valores de densidad óptica de las bandas de la proteína BDNF obtenidos tanto para el grupo RGS4 como para el grupo vehículo en las distintas condiciones experimentales se normalizaron con respecto a los obtenidos para la proteína α-tubulina (control de carga) ($O.D_{BDNF}$ / $O.D_{\alpha\text{-tubulina}}$). Posteriormente, los valores de densidad óptica normalizados ($O.D_{BDNF\ nor}$) en ambos grupos, se usaron para calcular el porcentaje de cambio de los niveles de esta neurotrofina con respecto al grupo control de acuerdo con la siguiente fórmula:

$$[(O.D_{BNFnor}\ RGS - O.D_{BDNFnor}\ Vehículo) \times 100 / O.D_{BDNFnor}\ Vehículo]$$

Posteriormente los valores de $O.D_{nor}$ obtenidos para cada tratamiento se expresaron como la media ± SEM. El posterior análisis de significancia se calculó mediante la prueba t de Student para muestras apareadas usando el programa estadístico SigmaStat 3.5 (Jandel Scientific) y aceptándose una probabilidad de error igual o inferior al 5 % ($p \leq 0,05$).

2.4 *Cuarto bloque experimental*. Identificación de proteínas implicadas en el procesamiento de la mejora de la memoria mediada por el tratamiento con $RGS14_{414}$

Finalmente, en la búsqueda del mecanismo molecular desencadenado por la proteína $RGS14_{414}$ en el cerebro, diseñamos un proyecto de proteómica (resumido en la figura 5) para identificar proteínas implicadas en dicho proceso y que por consiguiente fuesen importantes para el procesamiento y almacenamiento de la información en el cerebro.

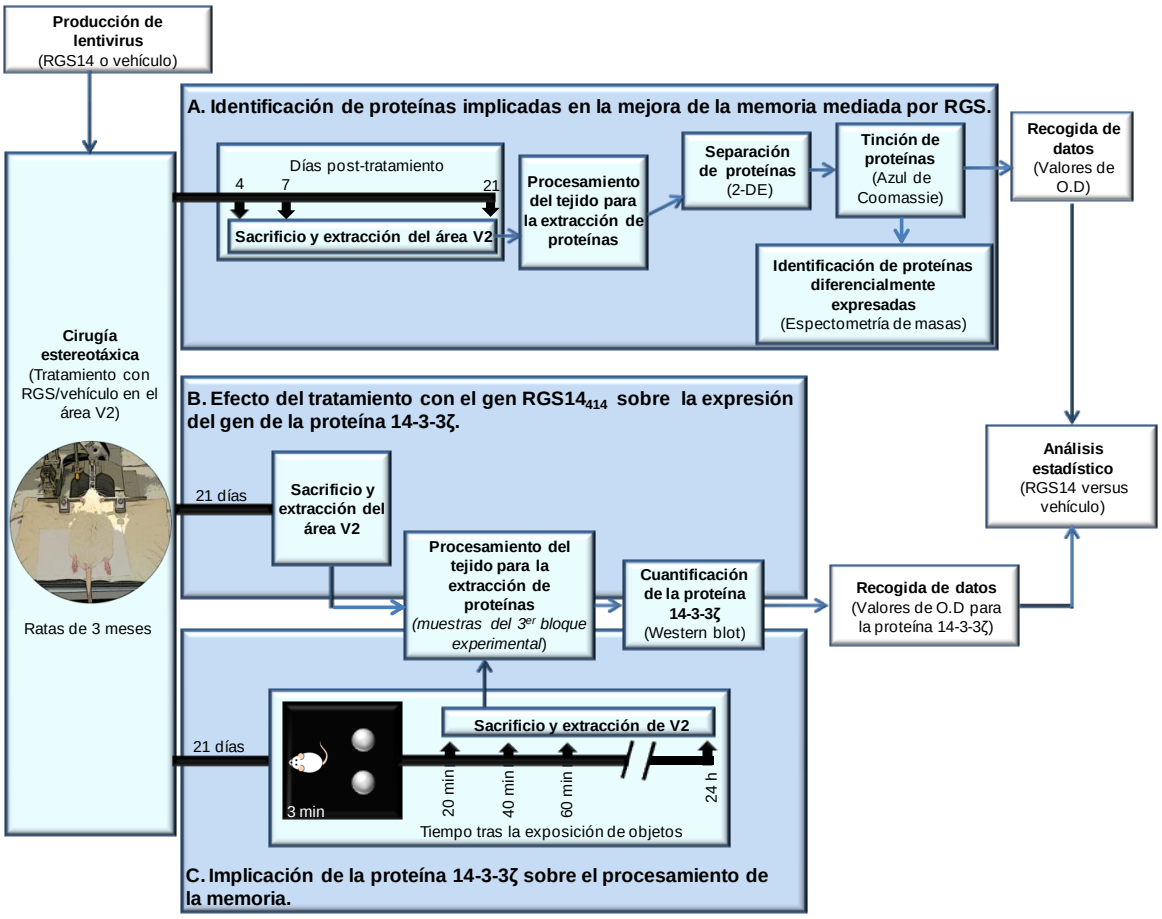

Figura 5. Esquema del diseño experimental.

El área de la corteza cerebral V2 de animales tratados con RGS14 o vehículo, se extrajo a los 4, 7 y 21 días tras el tratamiento como se explicó en el apartado VII.2.3 y el tejido se procesó para el análisis de proteómica (figura 5.A). La posterior documentación bibliográfica acerca de aquellas proteínas que presentaron un patrón de expresión cambiante en concordancia temporal con los efectos del tratamiento de RGS14, condujo nuestra atención hacia la proteína 14-3-3ζ. Varios trabajos *in vivo* han demostrado una correlación entre esta proteína y la memoria (Broadie et al 1997; Cheah et al 2012; Skoulakis & Davis 1996). Los altos niveles de 14-3-3ζ observados a los 21 días del tratamiento se confirmaron mediante Western blot (figura 5.B) y finalmente se investigó también la implicación de esta molécula en el procesamiento de la ORM de un modo similar a como hicimos con la proteína BDNF (figura 5.C).

Estudio de proteómica

Las muestras de tejido cerebral del área V2 obtenidas a distintos días del tratamiento se homogeneizaron en 100 µl del tampón de solubilización de la muestra (urea 7 M, tiourea 2 M, CHAPS 4 %, DTE 1 %; ver *appendix* 5.B.1) a 4 ºC. Con el fin de favorecer la liberación

de proteínas, las muestras se sonicaron 3 veces durante 1 min a 4 ºC. La concentración de proteínas totales de cada una de las muestras se estimó mediante el método de Bradford (ver *appendix* 5.B.3; Bradford 1976). La separación de las proteínas se llevó a cabo mediante la técnica de electroforesis bidimensional (2-DE) cargando en cada experimento 100 µg de proteínas totales. Durante la primera dimensión (isoelectroenfoque) se separaron las proteínas horizontalmente en base a un punto isoeléctrico (pI) sobre un gel en una tira de 7 cm con gradiente no lineal de pH entre 3-10 inmovilizado (IPG; Bio-Rad, 163-2002). El isoelectroenfoque (IEF) se llevó a cabo en el *Protean IEF Cell* de Bio-Rad aplicando el programa que se detalla en la *table* 14 (pág. 52).

Una vez finalizado el protocolo de IEF, se llevó a cabo una reacción de reducción/alquilación para facilitar la transferencia de proteínas de la primera a la segunda dimensión. Para ello las tiras se incubaron durante 20 min en agitación a temperatura ambiente en 10 ml de tampón de equilibrado (ver *appendix* 5.B.2) con DTE a 0,03 M primero, y con iodoacetamida a 0,136 M después. Tras este paso intermedio de equilibrado, las proteínas con el mismo pI se separaron verticalmente de acuerdo con su peso molecular mediante SDS-PAGE en minigeles de poliacrilamida al 12 % (ver *appendix* 5.B.4) en tampón TGS 1X (Bio-Rad, 161-0772) usando el *Mini-Protean System* (Bio-Rad). Esta segunda dimensión se llevó a cabo aplicando un voltaje de 40 V durante los primeros 15 min e incrementándolo posteriormente a 120 V durante aproximadamente 1 h. Además, junto a las muestras se cargaron 3 µl del marcador de peso molecular *BenchMark Pre-stained Protein ladder* (Bio-Rad, 10748010). Las proteínas separadas en el gel se fijaron en 50 ml de solución fijadora (metanol 30 % y ácido acético al 10 %) durante 24 h y posteriormente se tiñeron mediante la tinción Blue Silver (ver *appendix* 5.C.1; Candiano et al 2004). El exceso de colorante se eliminó con lavados breves en agua y los geles se escanearon en el *Calibrated Imaging Densitometer Model GS-800* (Bio-Rad). Las imágenes obtenidas se analizaron mediante el programa PDQuest Advanced 7.1.1 (Bio-Rad). Aquellos puntos correspondientes a proteínas que presentaron unos valores de O.D al menos dos veces superior o inferior con respecto al control se procesaron para su identificación mediante espectrometría de masas. Inicialmente se destiñeron con una solución de acetonitrilo al 30 % y bicarbonato de amonio 50 mM y se liofilizaron mediante un sistema de vacío. A continuación se llevó a cabo una digestión tríptica con tripsina para generar un patrón de polipéptidos de menor tamaño de cada proteína. El perfil de polipéptidos de cada proteína se identificó mediante la técnica de MALDI-TOF realizada por el servicio de proteómica del *Biomedical Research Foundation* en Atenas (www.bioacademy.gr/facility/proteomics).

Western blot

Los niveles de la proteína 14-3-3ζ se detectaron usando un anticuerpo policlonal específico producido en conejo (Santa Cruz Biotechnology, sc-1019) a una dilución 1:1000 mediante la técnica de Western blot (ver apartado VII.2.3). Las muestras usadas fueron las mismas del 3er bloque experimental. El análisis de datos y la estadística se llevó a cabo de un modo similar al explicado en el 3er bloque experimental para el análisis de la proteína BDNF.

3 RESULTADOS

3.1 El tratamiento con el gen $RGS14_{414}$ previene la pérdida de memoria asociada al envejecimiento y a la enfermedad de Alzheimer

Previamente, se había demostrado el potente y perdurable efecto de la proteína RGS14 sobre la memoria de reconocimiento de objetos en ratas normales (Lopez-Aranda et al 2009). En base a ello, se pensó en la molécula $RGS14_{414}$ como un candidato terapéutico para prevenir la pérdida de memoria en condiciones patológicas. En este trabajo de tesis hemos testado la viabilidad de $RGS14_{414}$ como terapia preventiva del déficit de memoria episódica descrito en dos modelos de roedores que presentan dicho déficit, rata envejecida y ratón transgénico de la enfermedad de Alzheimer. (Escribano et al 2009; Gamiz & Gallo 2012; Granholm 2010; Schiapparelli et al 2006). Para ello, ambos modelos se trataron con el gen de $RGS14_{414}$ en el área V2 mediante una inyección- intracerebral antes de la aparición del déficit en la ORM, y su capacidad mnemónica fue testada a lo largo del tiempo junto a sus respectivos grupos controles utilizando la prueba de reconocimiento de objetos.

Estudio en el modelo de envejecimiento

El resultado del estudio del efecto de la proteína RGS14 sobre la pérdida de memoria episódica en el modelo de rata envejecida se puede observar gráficamente en la *figure* 20 (pág.58). Se consideró que un animal era capaz de recordar un objeto al que había sido expuesto con anterioridad, cuando se obtenía un valor del índice de discriminación (DI) igual o superior a 0,66. En base a este criterio, se observó que ratas jóvenes de tres meses de edad que se habían expuesto a un determinado objeto durante 3 min, tuvieron la capacidad recordarlo 45 min después, mostrando una clara preferencia por el objeto nuevo (0,719 ± 0,017); sin embargo estos animales fueron incapaces de discriminar entre el objeto familiar y el nuevo después de 24 h (0,495 ± 0,014; $p \leq 0,001$). Estos datos demuestran la capacidad de la rata joven para formar memoria a corto plazo pero no a largo plazo en nuestras condiciones normales de experimentación. A diferencia de las ratas de 3 meses de edad, las ratas de 18 meses de edad perdieron la capacidad de recordar el objeto después de 45 min (0,507 ± 0,034. $p \leq 0,001$). Una vez demostrado el déficit nemónico que sufre nuestro modelo de envejecimiento en condiciones normales, se pasó a estudiar el posible efecto preventivo de la proteína RGS14 sobre la pérdida de memoria. Así, un grupo de animales jóvenes de 3 meses de edad se trató con el gen $RGS14_{414}$ y otro con vehículo (control) en el área V2. Su capacidad de reconocer un objeto familiar a corto y a largo plazo se evaluó a los 5, 18, 20 y

22 meses de edad. Como era de esperar, a los 2 meses del tratamiento, cuando los animales se encontraban aún en edad adulta, no se observaron diferencias significativas entre el grupo RGS y el grupo vehículo en un test de ORM de 45 min, mostrando un comportamiento similar al grupo de ratas de 3 meses sin tratar (grupo RGS, 0,750 ± 0,016 versus grupo vehículo, 0,719 ± 0,022; p=0,297; grupo RGS de 5 meses versus grupo control de 3 meses, p=0,194). Sin embargo, cuando los animales tratados alcanzaron los 18 meses de edad, se observó que mientras que el grupo vehículo mostró una pérdida significativa de la ORM (0,507 ± 0,035), el grupo tratado con RGS14 no presentó este déficit cognitivo (0,750 ± 0,022; RGS versus vehículo p≤0,001). Además del efecto preventivo sobre el déficit de memoria, RGS14 manifestó una importante potenciación de la capacidad mnemónica. Así, el grupo RGS14 a los 18 meses de edad mostró la capacidad de reconocer un objeto después de 24 h (0,744 ± 0,023), mientras que ni el grupo vehículo de la misma edad (0,490 ± 0,035; p≤0,001), ni el grupo de ratas jóvenes de 3 meses expresaron dicha capacidad (0,495 ±0,014) (ver en *figure* 20, pág. 58). Este aumento del tiempo de retención de la información observado a los 18 meses de edad en el grupo RGS14, persistió en el tiempo incluso a los 20 (0,716 ± 0,018, p≤0,001) y a los 22 meses (0,688 ± 0.015, p≤0.001), edad hasta la cual los animales fueron capaces de llevar a cabo el test de ORM de manera activa.

Estudio en el modelo de la enfermedad de Alzheimer

Trabajos previos han demostrado que los ratones transgénicos J20 modelo de la enfermedad de Alzheimer (ratones AD) utilizados en este estudio presentan una pérdida de la ORM a partir de los 4 meses de edad (Escribano et al 2009), lo cual se mantiene en concordancia con los resultados obtenidos en este trabajo (ver *figure* 21, pág.59). De manera que a los 2 meses de edad, ratones del grupo *wild-type* control y del grupo transgénico AD se comportaron de manera similar, presentando valores de DI superiores a 0,66 y por tanto mostrando la capacidad de reconocer un objeto familiar (WT 0,768 ± 0,039 versus AD 0,754 ± 0,039; one-way ANOVA $F_{1,18}$=0,057; p=0,814). Sin embargo, cuando el grupo AD alcanzó los 4 meses de edad, la capacidad mnemónica de estos animales disminuyó de manera drástica con respecto al grupo *wild-type*, que mantuvo su nivel de ORM (AD 0,480 ± 0,039 versus WT 0,780 ± 0,033; one-way ANOVA $F_{1,36}$=34,943, p≤0,001). De manera similar al estudio de envejecimiento, para probar el efecto preventivo de la proteína RGS14 sobre la pérdida de memoria asociada a la enfermedad de Alzheimer, ratones AD de 2 meses de edad (antes de la aparición del déficit cognitivo) se trataron con el gen $RGS14_{414}$ (AD-RGS) o con

vehículo (AD-vehículo) en el área cortical V2. La ORM de ambos grupos se evaluó a los 4 y a los 7 meses de edad junto a un grupo de animales *wild-type* (control positivo) y un grupo de ratones transgénicos sin tratar (control negativo) (ver *figure* 21, pág.59). El grupo de animales AD-RGS no presentó muestras de déficit en la ORM ni a los 4 meses (0,771 ± 0,020) ni a los 7 meses de edad (0,696 ± 0,035) a diferencia de lo que ocurrió en el grupo de animales transgénicos sin tratar (0,561 ± 0,021, $p \leq 0.001$ a los 4 meses; 0,421 ± 0,0754, p=0,01 a los 7 meses) y en el grupo AD-vehículo (0,558 ± 0,065; p<0,001 a los 4 meses; 0,429 ± 0,076, p=0,013 a los 7 meses), los cuales tal y como era de esperar se mostraron incapaces de retener información en el cerebro a largo plazo en nuestras condiciones experimentales. El efecto preventivo de RGS14 sobre la aparición del déficit de memoria en los ratones AD se mantuvo en el tiempo, de forma que estos animales presentaron un nivel de la ORM similar al grupo control *wild-type* (Tukey HSD post-hoc test, p=0,811 a los 4 meses y p=0,993 a los 7 meses).

3.2 El tratamiento con el gen $RGS14_{414}$ promueve la arborización dendrítica de neuronas corticales

Como se ha demostrado previamente en nuestro laboratorio (Lopez-Aranda et al 2009) e incluso en el primer bloque de resultados de esta tesis doctoral, un único tratamiento con el gen de $RGS14_{414}$ produce un efecto potenciador sobre la memoria, el cual puede llegar a mantenerse a los largo de toda la vida de las ratas. Por lo tanto, postulamos que este efecto perdurable podría ser debido a cambios estructurales que facilitasen el procesamiento de la información y la formación de la memoria como consecuencia del tratamiento. Para probar dicha hipótesis, los cerebros de ratas tratadas con el gen RGS14 o con vehículo se sometieron a la tinción de Golgi para analizar la arborización neuronal dendrítica en el área V2 (zona tratada) a los 21 días del tratamiento, es decir, cuando se observa el efecto sobre la memoria. El resultado se muestra en la *figure* 23, pág. 62.

Tanto las neuronas piramidales como las no piramidales de los animales tratados con $RGS14_{414}$ presentaron un incremento en la arborización neuronal con respecto al tratamiento con vehículo, apreciable incluso en un simple examen visual de neuronas dibujadas usando la cámara lúcida (*figure* 22, pág. 61). El tratamiento con RGS14 produjo un aumento significativo en el número de neuritas que emergen de cada célula piramidal (RGS 4,595 ± 0,190 versus vehículo 3,643 ± 0,181; $p \leq 0,001$), mientras que su efecto fue más pronunciado sobre el número de neuritas de células no piramidales (RGS 6,069 ± 0,211 versus vehículo 3,673 ± 0,248 neuritas por neurona; $p \leq 0,001$). No obstante, el tratamiento con $RGS14_{414}$

provocó un mayor efecto en el nivel de ramificación de la dendrita apical de neuronas piramidales, en las cuales se observan el doble de prolongaciones que en los animales tratados con vehículo (RGS 6,646 ± 0,342 versus vehículo 3,357 ± 0,314; p≤0.001). Sin embargo, no se encontraron diferencias significativas en el grado de ramificación de las neuritas de neuronas piramidales (RGS 1,494 ± 0,185 versus vehículo 1,714 ± 0,286; p=0,5), ni de células no piramidales (RGS 1,914 ± 0.249 versus vehículo 1,491 ± 0,226; p=0,212). En resumen, estos resultados sugieren que el tratamiento con el gen $RGS14_{414}$ está implicado en la arborización neuronal, favoreciendo especialmente la arborización de la dendrita apical en las neuronas piramidales, así como aumentando el número de neuritas tanto de células piramidales como de las no piramidales (*figure* 23, pág. 62). El efecto producido por la proteína RGS14 *in vivo* fue analizado con mayor detalle en la caso de la arborización de la dendrita apical de las neuronas piramidales y en el número de neuritas de las células no piramidales, categorías en las que el tratamiento provocó un efecto más prominente. De este modo, el número total de neuronas piramidales y no piramidales estudiadas se clasificaron en base a su grado de ramificación dentro de las categorías anteriormente mencionadas. Las gráficas de la *figure* 24 (pág. 63) muestran que se produjo un aumento en el porcentaje de neuronas tanto piramidales como no piramidales con un mayor grado de ramificación. En los animales controles tratados con vehículo, la dendrita apical de neuronas piramidales analizadas presentó entre 0-8 prolongaciones dendríticas, sin embargo, se observó un rango de entre 1-15 en el caso de neuronas piramidales de ratas tratadas con $RGS14_{414}$ (*figure* 24.A). Además, el porcentaje de neuronas con un mayor grado de ramificación fue más alto en el caso del tratamiento con RGS14. Así, mientras que el 50 % del total de las células piramidales analizadas en el grupo control presentó 3-4 proyecciones desde su dendrita apical y sólo el 18 % mostró más de 4; en los animales tratados con RGS14, una de cada dos neuronas piramidales presentó entre 6-9 dendritas de esta categoría y más del 62% mostraron más de 6 ramificaciones. Por otro lado, el 90 % de las neuronas no piramidales del grupo RGS expresaron entre 4-8 neuritas por neurona, unos valores que supusieron tan sólo el 42 % en el grupo control; de hecho el 56 % de las neuronas no piramidales del grupo control presentaron 3 o un número inferior de prolongaciones en sus somas (*figure* 24.B).

3.3 El tratamiento con el gen $RGS14_{414}$ aumenta la expresión de BDNF

Considerando el efecto potenciador de la memoria mediado por $RGS14_{414}$ a través del aumento de la arborización dendrítica, y el importante papel que juegan los factores

neurotróficos en ambos procesos (ver apartados VII.3.1 y VII.3.2), pensamos que estos factores de crecimiento podrían estar implicados en el mecanismo molecular que subyace a la proteína $RGS14_{414}$. De este modo, decidimos comprobar los niveles de mRNA y proteína de distintos factores neurotróficos FGF2, NGF y BDNF en nuestro modelo RGS. Además, estudiamos la implicación de BDNF en el procesamiento de la ORM.

Incremento selectivo en los niveles de mRNA y proteína BDNF

El análisis de qRT-PCR reveló que a los 21 días tras el tratamiento, la cantidad de mRNA de BDNF en los animales tratados con $RGS14_{414}$ fue 2,4 veces mayor que en los animales controles tratados con vehículo (cantidades de mRNA en fg normalizadas con el gen *housekeeping* Rlp-19; RGS14, 0,340 ± 0,015 versus vehículo, 0,147 ± 0,006; $p \leq 0,001$) . Sin embargo, no se observó ningún cambio significativo con respeto al control en el caso de los otros dos factores neurotróficos analizados, NGF y FGF-2 (*figure* 25, pág. 64). Por lo tanto, podríamos decir que el tratamiento con RGS14 produce de manera selectiva un aumento en los niveles de mRNA del factor de crecimiento BDNF.

Considerando el efecto del tratamiento con RGS14 sobre los niveles de mRNA de BDNF, evaluamos si el aumento en mRNA se tradujo en un aumento de su expresión proteica utilizando para ello un anticuerpo específico. Tras 7, 14 y 21 días desde el tratamiento con RGS14 o vehículo, los cerebros de los animales se procesaron para el análisis por Western blot. Los niveles de la proteína α-tubulina se usaron como control de carga para la normalización de los datos. En la *figure* 26.A (pág., 65) se muestra un ejemplo de las bandas resultantes de la inmunodetección de BDNF. Los valores de densidad óptica (O.D) normalizados tanto del tratamiento RGS14 como del control demostraron un ligero aumento no significativo en la proteína BDNF a los 7 (19,96 ± 2,72 %) y a los 14 días (24,81 ± 3,17 %) tras el tratamiento. Sin embargo, el efecto en la expresión se acentuó a los 21 días, cuando los animales tratados con RGS14 presentaron un 71,25 ± 7,77 % más de proteína BDNF que el grupo control (prueba t de Student para muestras dependientes, $t_{0,025;2}=5,142$; $p=0,036$) (*figure* 26.B, pág. 65). Este considerable aumento en los niveles de BDNF a los 21 días desde el tratamiento con RGS14 coincide con el momento en el cual se observa la aparición del efecto potenciador de la ORM en animales RGS (López-Aranda et al, 2009 ; *figure* 20, pág. 58, *figure* 21, pág. 59).

Expresión dinámica de la proteína BDNF durante el procesamiento de la ORM

La coincidencia temporal del incremento de BDNF y del efecto de la potenciación de la ORM a los 21 días tras el tratamiento sugiere que esta neurotrofina podría estar desempeñando un papel en el procesamiento de la memoria de reconocimiento de objetos. Para estudiar la posible correlación entre ambos sucesos, 21 días después del tratamiento, las ratas se expusieron a dos objetos idénticos durante 3 minutos y transcurridos 20, 40, 60 min así como 24 h desde la adquisición se estimaron los niveles de la proteína BDNF mediante WB (*figure* 27.A, pág. 66). El porcentaje de cambio con respecto al control se calculó según los valores de O.D. normalizados (ver *figure* 27.B). A los 20 min, se observó un incremento significativo del 71,43 ± 7,89 % (prueba t de Student para muestras dependientes, $t_{0,025;3}$=-8,887; p=0,003), similar a la mostrada a los 21 días tras el tratamiento sin nuevas exposiciones a los objetos (*figure* 26.B, pág. 65). Estos datos parecen indicar que los niveles de BDNF permanecen sin cambios durante los primeros 20 min del procesamiento de la ORM. Sin embargo, la expresión se reguló a la baja de manera significativa con respecto al control a los 40 min (23,51 ± 5,99 %, p=0,012) y a los 60 min (37,12 ± 3,49 %, p=0,009) desde el momento de la adquisición. Después de 24 h, los niveles de la proteína BDNF parecían comenzar a normalizarse sin mostrar diferencias significativas con respecto al control (p=0,436). Esta dinámica en los niveles de expresión de la proteína BDNF durante el procesamiento de la ORM indica su implicación en la formación de la memoria en los animales RGS.

3.4 Implicación de la proteína 14-3-3ζ en la potenciación de la memoria mediada por $RGS14_{414}$

Finalmente, en el intento de esclarecer el mecanismo intracelular que conlleva al aumento de BDNF mediado por $RGS14_{414}$, se planteó un estudio de proteómica que nos permitiese identificar nuevas proteínas implicadas en el proceso.

El perfil del análisis de proteínas reveló un aumento en la expresión de la proteína 14-3-3ζ en los animales tratados con RGS14

Se realizó un minucioso análisis de las proteínas diferencialmente expresadas como consecuencia del tratamiento con RGS14 con respecto al control (vehículo) a los 4, 7 y 21 días desde la inyección. En la *table* 15 (pág. 67) se resumen algunas proteínas que parecieron presentar una fuerte relación con el tratamiento. Después de evaluar con más detalle los

resultados, encontramos que la proteína 14-3-3ζ (indicada en negrita en la *table* 15) presentaba una dinámica de expresión en concordancia temporal con el aumento de la memoria mediada por $RGS14_{414}$. Así, 7 días después del tratamiento con $RGS14_{414}$ los animales presentaron unos niveles de la proteína 14-3-3ζ 2,8 veces superior a los tratados con vehículo, alcanzando su máximo nivel a los 21 días tras la inyección, cuando los niveles de 14-3-3 ζ llegaron a ser hasta 3,7 veces el valor del control (*table* 15; *figure* 28.B, pág. 68). Este acusado incremento a los 21 días desde el tratamiento, visible incluso sobre el gel 2-DE (*figure* 28.A), coincidió no sólo con el aumento de BDNF (*figure* 25, pág. 64; *figure* 26, pág. 65), sino también con el momento de aparición de la potenciación de la memoria en los animales RGS14 (Lopez-Aranda et al 2009 ; *figure* 20, *figure* 21 del presente trabajo).

El acusado incremento de la proteína 14-3-3ζ mediado por $RGS14_{414}$ observado mediante la técnica de 2-DE a los 21 días desde el tratamiento se confirmó mediante Western blot (*figure* 29, pág. 69). Los valores de O.D. normalizados correspondientes a las bandas inmunoreactivas para 14-3-3ζ (ejemplo de las bandas en la *figure* 29.A) se representan en la *figure* 29.B como el porcentaje de cambio con respecto al control (las barras en gris muestran los valores de 2 experimentos y la barra negra la media de ambos). Cuando en el gel se cargaron 2,5 µg de proteína total, se observó un aumento del 191 % en los niveles de la proteína 14-3-3 ζ de animales RGS con respecto al control siendo dicho incremento algo menor (117%) cuando se cargaron 5 µg. Sin embargo, la media de ambos experimentos muestra un aumento del 154 ± 52 % con respecto al control. Aunque los resultados obtenidos por la técnica 2-DE fueron ligeramente más elevados (3,74 ± 0,04 veces mayor que el control) que los obtenidos por la técnica de Western blot (2,55 ± 0,37 cambio con respecto al control), es importante subrayar un notable aumento de la proteína 14-3-3ζ de más del doble en las ratas RGS por ambos métodos.

Participación de la proteína 14-3-3ζ en el procesamiento de la ORM

La coincidencia temporal del efecto de la proteína RGS14 sobre el aumento de la ORM y del incremento de la proteína 14-3-3ζ, nos condujo a pensar que esta proteína que surgió en nuestro estudio podría estar involucrada en el mecanismo molecular que conlleva a una facilitación en el almacenamiento de la información en el cerebro desencadenado por la proteína RGS14. Para comprender la implicación de la proteína 14-3-3ζ en el procesamiento de la ORM, se llevó a cabo un experimento similar al empleado para el estudio de BDNF. Tras 21 días desde el tratamiento con el gen RGS14 o con vehículo, los animales se

expusieron a dos objetos idénticos durante 3 min y a los 20, 40, 60 min y a las 24 h de la fase de adquisición se extrajo el área V2, donde se analizaron los niveles de la proteína 14-3-3ζ mediante Western blot. En la *figure* 30.A (pág 70) se muestra un ejemplo de las bandas obtenidas al usar un anticuerpo específico para la proteína; y en la *figure* 30.B se representan los valores de O.D. normalizados como el porcentaje de cambio con respecto al control. El resultado de cuatro experimentos independientes demostró la existencia de un patrón de expresión dinámico de la proteína 14-3-3ζ durante el procesamiento de la ORM. A los 20 min de la adquisición, no se observaron cambios en los niveles de 14-3-3ζ con respecto al control. Sin embargo, se observó un 43,19 ± 12,86 % y un 37,66 ± 4,04 % más de la proteína 14-3-3ζ en los animales RGS que en el control a los 40 y a los 60 min desde la exposición a los objetos respectivamente. A las 24 h, los niveles de 14-3-3ζ tendieron a normalizarse. El pico de expresión de la proteína 14-3-3ζ en los animales tratados con RGS14 parece indicar la implicación de esta proteína en el procesamiento de la ORM.

Sorprendentemente, al solapar el perfil de expresión de la proteína BDNF (*figure* 27.B) y de la proteína 14-3-3ζ (*figure* 30.B) durante el procesamiento de la ORM, encontramos que ambas proteínas parecen presentar una actividad sinérgica entre ellas *figure* 32, pág. 77). En este sentido, cuando los niveles de BNDF se mostraron bajos (a los 40 y 60 min desde la adquisición), los niveles de la proteína 14-3-3ζ se mostraron altos; y cuando los valores de BDNF eran altos, la expresión de 14-3-3ζ se mantuvo igual en los animales RGS con respecto a los tratados con vehículo. No obstante, a las 24 h no se observaron diferencias con respecto al vehículo de ninguna de las dos proteínas. Estos datos conjuntamente sugieren que 14-3-3ζ y BDNF podrían estar involucradas en la regulación de la expresión de una proteína sobre la otra proteína de una manera directa o indirecta como consecuencia del tratamiento con el gen $RGS14_{414}$.

4 DISCUSIÓN

La pérdida de memoria es un trastorno mental que afectan a una gran proporción de la población humana. Fallos en la memoria se han visto asociados al envejecimiento, así como a diversas enfermedades neurológicas y neurodegenerativas, entre las que se incluyen la esquizofrenia, la enfermedad de Parkinson y la enfermedad de Alzheimer. El coste asociado a la cura y el cuidado de este tipo de pacientes con un alto grado de dependencia ha supuesto una importante carga económica y social. Además, se estima que en el futuro el número de personas con este problema se incremente de manera drástica debido al aumento de la esperanza de vida con el consiguiente envejecimiento de la población. De acuerdo con el informe *World Poplation Ageing 2013* de las Naciones Unidas, más del 30 % de la población en los países desarrollados tendrá 65 años o más para el año 2040. Además, el *Alzheimer Report 2014* indicó que la demencia asociada con la pérdida de memoria es una de las principales causas de dependencia e incapacidad en los individuos de avanzada edad. Por lo tanto, existe una necesidad inminente de encontrar un remedio contra el déficit de memoria. En este sentido el hallazgo de potenciadores de la memoria podría ser una buena solución para este problema. Sin embargo, los potenciadores de la memoria u otros compuestos testados hasta ahora han fallado en las fases clínicas y preclínicas a pesar de sus esperanzadores resultados en animales de experimentación (Knafo & Venero 2015).

Este trabajo de tesis ha sido diseñado para contrarrestar este problema, investigando si la pérdida de memoria se puede prevenir antes de su aparición. Nuestros resultados han demostrado que la prevención de la pérdida de memoria episódica podría ser viable mediante el tratamiento con el gen $RGS14_{414}$ en dos modelos de roedores que presentan dicho déficit, rata envejecida y ratón transgénico de la enfermedad de Alzheimer. Además muestran que la actividad asociada con la prevención de la pérdida de la ORM está regulada por la vía de 14-3-3ζ-BDNF.

4.1 Prevención de la pérdida de memoria.

$RGS14_{414}$ es un potente potenciador de la memoria y el tratamiento con este gen en el área V2 produce la conversión de una ORM normal de 45 min, en una memoria a largo plazo de más de 24 h (Lopez-Aranda et al 2009) que puede mantenerse durante toda la vida de los animales. Ratas normales, así como aquellas tratadas con vehículo presentaron una pérdida significativa de la ORM a los 18 meses de edad; sin embargo, los animales tratados con el gen

$RGS14_{414}$ a los 3 meses de edad no mostraron esta pérdida a los 18 meses y su memoria permaneció intacta hasta los 22 meses de edad, período hasta el cual los animales fueron capaces de llevar a cabo el test de ORM.

Además, el tratamiento con el gen $RGS14_{414}$ también fue efectivo sobre la pérdida de memoria asociada a la enfermedad de Alzheimer que presenta un modelo de ratón transgénico de la enfermedad. Los ratones AD mostraron una pérdida de la ORM a partir de los 4 meses de edad. Así el tratamiento con el gen $RGS14_{414}$ a la edad de 2 meses, antes de la aparición del déficit cognitivo, no sólo evitó la aparición de la pérdida de memoria a los 4 meses de edad, sino que además, permitió que estos animales mostrasen un nivel de memoria similar al *wild-type* después de los 6 meses de edad.

Conjuntamente, los resultados obtenidos en ambos modelos sugieren que el tratamiento con $RGS14_{414}$ produce un efecto permanente que podría ser factible como un remedio preventivo contra la aparición de los fallos de memoria episódica, un tipo de memoria que se ve principalmente afectada durante el envejecimiento y en muchas enfermedades neurológicas (Dickerson & Eichenbaum 2010; Tromp et al 2015). A pesar de que nuestros resultados son a un nivel de investigación básica y requieren ser validados en humanos con ensayos clínicos, confirman que la molécula $RGS14_{414}$ podría ser un fármaco potencial contra la pérdida de memoria en humanos.

4.2 Papel de la proteína BDNF en la arborización neuronal y en la ORM en el modelo RGS

Previamente, se ha mostrado que el tratamiento con $RGS14_{414}$ facilita la formación de la memoria a largo plazo (Lopez-Aranda et al 2009) y este efecto ha quedado patente en los resultados obtenidos en los experimentos de prevención de la pérdida de ORM realizados en este trabajo de tesis. El tratamiento con RGS no sólo previno el déficit cognitivo, sino que además su efecto se mantuvo en el tiempo, manteniendo una ORM intacta a edades más avanzadas. La interpretación inicial de estos resultados nos llevó a pensar que el efecto duradero del tratamiento con el gen $RGS14_{414}$ podría deberse a una mayor plasticidad estructural como consecuencia de la aparición de cambios estructurales y permanentes en las neuronas. De este modo, el análisis de la arborización tanto de neuronas piramidales como de neuronas no piramidales de la zona del cerebro tratada con $RGS14_{414}$ exhibió un importante aumento en la arborización dendrítica en ambos tipos neuronales. Lo que resultó aún más sorprendente fue el incremento en el número de ramificaciones dendríticas que se proyectaban

desde la dendrita apical en las neuronas piramidales, casi triplicando el número que mostraron estas neuronas de animales controles. Las dendritas apicales de las neuronas piramidales son fundamentales en la formación de las conexiones con otras capas corticales e incluso con otras áreas del cerebro. De este modo, pensamos que el tratamiento con $RGS14_{414}$ provocó un incremento en las conexiones neuronales que condujo a facilitar el flujo y el procesamiento de la información (Eyal et al 2014), lo que consecuentemente causó una mejora en la memoria.

No obstante, con el fin de comprender el mecanismo por el cual la proteína $RGS14_{414}$ estaba induciendo dicha arborización dendrítica, investigamos los niveles de factores neurotróficos en el área V2 de animales tratados; ya que un gran número de evidencias en la literatura ha demostrado el papel de estos factores de crecimiento en la supervivencia neuronal, en el crecimiento axonal y dendrítico dependiente de actividad, así como en la arborización (ver Park & Poo 2013 para una revisión). Observamos que el tratamiento con $RGS14_{414}$ indujo un incremento selectivo en los niveles de la proteína BDNF, pero no de otros factores neurotróficos testados (NGF o FGF2).

BNDF, junto a su receptor, es uno de los factores de crecimiento más abundantes en el sistema nervioso central tanto en roedores como en humanos (Aid et al 2007; Maisonpierre et al 1990; Timmusk et al 1994; Webster et al 2002). De hecho, esta neurotrofina es esencial para el desarrollo neuronal y la plasticidad sináptica (Hong et al 2008; Poo 2001). Hasta el momento se ha escrito su papel en la arborización neuronal, o en la regulación del crecimiento y arborización dendrítica de neuronas piramidales y no piramidales (Horch 2004; Horch et al 1999; Jin et al 2003; Wirth et al 2003). Además, la expresión de BNDF es necesaria para el mantenimiento de la estructura y el tamaño de las dendritas de neuronas corticales a los 3 meses de edad, cuando los niveles de la proteína BDNF aumentan de manera drástica (Gorski et al 2003). Esta neurotrofina participa en la remodelación de la red dendrítica mediante el incremento de los niveles de cipina. De manera que BDNF trae la activación de la vía de señalización de las proteínas quinasas y las vías de señalización dependientes de la transcripción que promueven la unión de CREB al elemento de respuesta al cAMP (CRE) presente en el promotor de la cipina (Kwon et al 2011). La proteína cipina está relacionada con el incremento de la arborización dendrítica de las neuronas hipocampales (Akum et al 2004). Todas estas evidencias indican que el aumento de la proteína BDNF mediado por la proteína $RGS14_{414}$ podría no sólo causar un aumento en la arborización neuronal, sino también en su mantenimiento. Numerosos trabajos han argumentado que los cambios estructurales permanentes relacionados con el incremento de la arborización neuronal, contribuyen consecuentemente a la formación de nuevas conexiones sinápticas (Bailey &

Kandel 1993; Purves & Hadley 1985; Yang et al 2009). Este cambio estructural crea por tanto una infraestructura requerida para el efecto a largo plazo del tratamiento con el gen $RGS14_{414}$. El papel de la proteína BDNF en el aprendizaje ha sido bastante estudiada, al igual que su implicación en la formación de la memoria a corto y a largo plazo (Alonso et al 2002; Bekinschtein et al 2008b; Bekinschtein et al 2014; Romero-Granados et al 2010).

BDNF induce la transcripción de diferentes genes a través de la activación de diferentes vías de señalización que conducen a la síntesis de nuevas proteínas (Panja & Bramham 2014) las cuales favorecen la formación de la memoria. Algunas de estas vías de señalización incluyen ERK (Arthur et al 2004; Ying et al 2002), la CAMKII, el PIK3 (Alder et al 2003; Bogush et al 2007), y la diana de rapamicina en células de mamíferos (mTOR) (Slipczuk et al 2009). Además, esta neurotrofina modula la plasticidad sináptica gracias no sólo al incremento de la arborización dendrítica, sino también a los cambios funcionales de las sinapsis, un proceso que subyace a la potenciación a largo plazo (LTP) (Bramham & Messaoudi 2005; Maren 2005; Panja & Bramham 2014; Rioult-Pedotti et al 1998; Whitlock et al 2006) y a la depresión a largo plazo (LTD) (Kemp & Manahan-Vaughan 2007; Massey & Bashir 2007; Mizui et al 2015; Woo et al 2005). La LTP y la LTD son los mecanismos de plasticidad sináptica mejor conocidos que han sido implicados en la formación y consolidación de la memoria. BDNF probablemente modula la LTP a través de la cascada de señalización del receptor TrkB (Minichiello et al 2002), la cual es requerida para la consolidación del aprendizaje dependiente del hipocampo y el mantenimiento de dicha memoria (Bekinschtein et al 2007; Lee et al 2004). Considerando todas estas evidencias, pensamos que el incremento de BDNF mediado por el tratamiento con $RGS14_{414}$, por un lado, promueve cambios estructurales que favorecen la aparición de nuevos contactos sinápticos que permiten que la información fluya más rápidamente por el cerebro, y por otro lado, facilita la consolidación de la memoria durante el procesamiento de la ORM modulando distintas cascadas de señalización intracelulares que conducen a la síntesis de nuevas proteínas. En concordancia con todas estas evidencias, nuestros resultados muestran un patrón de expresión dinámico de BDNF durante el procesamiento de la ORM, el cual coincide con la consolidación de la memoria, apoyando la idea de la implicación de BDNF en la formación de la memoria a largo plazo en los animales tratados con $RGS14_{414}$.

4.3 Regulación de los niveles de la proteína BDNF mediante la proteína 14-3-3ζ

Considerando que BDNF es un elemento clave en la mejora de la memoria mediada por la proteína $RGS14_{414}$ no sólo en casos normales sino también ante el déficit cognitivo, continuamos investigando el mecanismo por el cual la proteína $RGS14_{414}$ podría estar induciendo el aumento de esta neurotrofina. En el estudio del perfil de expresión de proteínas en animales tratados con RGS, se identificó a la proteína 14-3-3ζ como un posible candidato mediador de este proceso. El patrón temporal de expresión de la proteína 14-3-3ζ pareció presentar una relación coherente en la mejora de la ORM mediada por la proteína $RGS14_{414}$. Así, en animales tratados con el gen $RGS14_{414}$, los niveles de expresión más altos de la proteína 14-3-3ζ se encontraron entre los 14-21 días desde el tratamiento, momento en el cual se había observado el efecto de $RGS14_{414}$ en la potenciación de la ORM (Lopez-Aranda et al 2009). La proteína 14-3-3ζ se ha encontrado de manera abundante en el cerebro de mamíferos y suele asociarse con otras muchas proteínas, tanto en forma dimérica o monomérica, interviniendo en varias vías de señalización y modulando distintas funciones celulares (Aitken 2006). Esta interacción en muchos casos requiere de la fosforilación de la proteína diana y en algunos incluso de la propia isoforma de 14-3-3 (Aitken 2006; Sluchanko et al 2012; Sluchanko & Gusev 2012). La proteína 14-3-3ζ participa en diversas funciones celulares que subyacen al aprendizaje y la memoria. La mutación en el gen leonardo de Drosophila, homólogo del gen para la proteína 14-3-3ζ en vertebrados, mostró una disminución significativa en la memoria olfativa de estos animales (Philip et al 2001; Skoulakis & Davis 1996; 1998) así como un fallo considerable en la plasticidad sináptica (Broadie et al 1997). Más recientemente, un estudio en ratones *knockout* para la proteína 14-3-3ζ demostró la importancia de la misma en la memoria espacial, en la ORM y en la memoria asociativa, además de incapacidad en la formación de LTP hipocampal (Cheah et al 2012; Qiao et al 2014). Estudios recientes, han demostrado que la interacción del receptor de la proteína quinasa C-1 activada (Adams et al 2011) con la proteína 14-3-3ζ es esencial para la translocación de dicha molécula al núcleo (Neasta et al 2012) donde el complejo RACK1-14-3-3ζ se une a la región IV del promotor del gen de BDNF y promueve un incremento en la transcripción de dicho gen (He et al 2010; Yaka et al 2003) (*figure* 31, pág. 77). Estas observaciones sugieren que el aumento de la proteína 14-3-3ζ podría regular los niveles de BDNF observados en los animales tratados con el gen $RGS14_{414}$. El resultado de nuestro trabajo apoya esta idea, ya que como consecuencia del tratamiento con $RGS14_{414}$ hemos observado un aumento de expresión del gen de BDNF, así como una sobreexpresión del gen

de 14-3-3ζ. Por lo tanto, podríamos decir que el aumento de la proteína 14-3-3ζ mediado por $RGS14_{414}$ elevó la síntesis de la proteína BDNF, molécula necesaria para el aumento de la arborización neuronal y la mejora de la ORM.

La evaluación del patrón de expresión del gen de BDNF y de 14-3-3ζ a distintos intervalos de tiempo durante el procesamiento de la ORM mostró una expresión complementaria de tal forma que cuando había niveles más bajos de BDNF, se observó un aumento en la proteína 14-3-3ζ y viceversa (*figure* 32, pág. 77). Estos hallazgos indican la implicación de la proteína 14-3-3ζ en la regulación de la expresión de BDNF durante el procesamiento de la ORM en ratas tratadas con la proteína $RGS14_{414}$.

4.4 Vía de RGS-14-3-3ζ-BDNF en el envejecimiento y en la enfermedad de Alzheimer

En la literatura se ha descrito una disminución significativa del BDNF, tanto a nivel de mRNA como de proteína, asociada al envejecimiento y a la enfermedad de Alzheimer (Caccamo et al 2010; Connor et al 1997; Christensen et al 2008; Francis et al 2012; Hock et al 2000; Michalski & Fahnestock 2003; Narisawa-Saito et al 1996; Peng et al 2009; Peng et al 2005; Shin et al 2014). De hecho, numerosas estrategias terapéuticas se han dirigido a disminuir los fallos cognitivos a través de aumentar los niveles de BDNF (Blurton-Jones et al 2009; Caccamo et al 2010; Iwasaki et al 2012). Estudios recientes mostraron que la infusión directa de la proteína BDNF o de su gen en la corteza entorrinal de modelos con demencia revirtió la pérdida sináptica, normalizó los niveles de expresión del gen, mejoró la señalización celular y restauró la capacidad de aprendizaje y memoria (Iwasaki et al 2012; Nagahara et al 2013; Nagahara et al 2009). Asimismo, los tratamientos con otros productos naturales y pequeñas moléculas que pueden inducir la expresión del gen de BDNF también han demostrado aminorar dichos fallos cognitivos (Li et al 2015; Shin et al 2014; Teng et al 2014; Zuccato & Cattaneo 2009). Además de BDNF, otros estudios de proteómica han demostrado una importante disminución en los niveles de la proteína 14-3-3ζ tanto en casos de envejecimiento como de la enfermedad de Alzheimer (Miller et al 2008), así como su implicación en el fallo cognitivo producido en otras enfermedades neurológicas (Shimada et al 2013; Umahara et al 2012). Concretamente un estudio *in vitro* demostró que la fosforilación de tau en el aminoácido serina mediante las proteínas quinasa A o B aumenta la afinidad de 14-3-3ζ por esta proteína hasta 14 veces, y la interacción de ambas proteínas supone la inhibición de la formación de agregados de tau para crear los ovillos neurofibrilares

y las placas neuríticas que caracterizan a la enfermedad de Alzheimer (Sadik et al 2009a; Sadik et al 2009b).

Nuestros resultados demostraron que la prevención de la pérdida de memoria en ambos modelos de roedores, rata envejecida y ratón transgénico de la enfermedad de Alzheimer podría estar mediada por la recuperación tanto de los niveles de la proteína BDNF como de la proteína 14-3-3ζ y consiguientemente por la normalización de la vía de señalización de 14-3-3ζ-BDNF. Aunque el mecanismo por el cual la proteína $RGS14_{414}$ incrementa los niveles de la proteína 14-3-3ζ sigue siendo parte del trabajo de nuestro laboratorio, en esta tesis doctoral se ha puesto de manifiesto que el tratamiento con el gen $RGS14_{414}$ podría ser una estrategia viable contra la pérdida de memoria.

VIII. REFERENCES

Adams DR, Ron D, Kiely PA. 2011. RACK1, A multifaceted scaffolding protein: Structure and function. *Cell Commun Signal* 9:22

Aebersold R, Mann M. 2003. Mass spectrometry-based proteomics. *Nature* 422:198-207

Aggleton JP, Brown MW. 2006. Interleaving brain systems for episodic and recognition memory. *Trends Cogn Sci* 10:455-63

Aggleton JP, Keen S, Warburton EC, Bussey TJ. 1997. Extensive cytotoxic lesions involving both the rhinal cortices and area TE impair recognition but spare spatial alternation in the rat. *Brain Res Bull* 43:279-87

Aid T, Kazantseva A, Piirsoo M, Palm K, Timmusk T. 2007. Mouse and rat BDNF gene structure and expression revisited. *J Neurosci Res* 85:525-35

Aitken A. 2006. 14-3-3 proteins: a historic overview. *Semin Cancer Biol* 16:162-72

Akum BF, Chen M, Gunderson SI, Riefler GM, Scerri-Hansen MM, Firestein BL. 2004. Cypin regulates dendrite patterning in hippocampal neurons by promoting microtubule assembly. *Nat Neurosci* 7:145-52

Albert PR, Robillard L. 2002. G protein specificity: traffic direction required. *Cell Signal* 14:407-18

Alder J, Thakker-Varia S, Bangasser DA, Kuroiwa M, Plummer MR, et al. 2003. Brain-derived neurotrophic factor-induced gene expression reveals novel actions of VGF in hippocampal synaptic plasticity. *J Neurosci* 23:10800-8

Alonso A, Zaidi T, Novak M, Grundke-Iqbal I, Iqbal K. 2001. Hyperphosphorylation induces self-assembly of tau into tangles of paired helical filaments/straight filaments. *Proc Natl Acad Sci U S A* 98:6923-8

Alonso M, Vianna MR, Depino AM, Mello e Souza T, Pereira P, et al. 2002. BDNF-triggered events in the rat hippocampus are required for both short- and long-term memory formation. *Hippocampus* 12:551-60

Allard S, Leon WC, Pakavathkumar P, Bruno MA, Ribeiro-da-Silva A, Cuello AC. 2012. Impact of the NGF maturation and degradation pathway on the cortical cholinergic system phenotype. *J Neurosci* 32:2002-12

Alleva E, Aloe L. 1989. Physiological roles of nerve growth factor in adult rodents: a biobehavioral perspective. *The International Journal of Comparative Psychology* 2:213-30

Ally BA, Gold CA, Budson AE. 2009. An evaluation of recollection and familiarity in Alzheimer's disease and mild cognitive impairment using receiver operating characteristics. *Brain Cogn* 69:504-13

Andero R, Choi DC, Ressler KJ. 2014. BDNF-TrkB receptor regulation of distributed adult neural plasticity, memory formation, and psychiatric disorders. *Prog Mol Biol Transl Sci* 122:169-92

Anderson ND, Ebert PL, Jennings JM, Grady CL, Cabeza R, Graham SJ. 2008. Recollection- and familiarity-based memory in healthy aging and amnestic mild cognitive impairment. *Neuropsychology* 22:177-87

Arshavsky VY, Pugh EN, Jr. 1998. Lifetime regulation of G protein-effector complex: emerging importance of RGS proteins. *Neuron* 20:11-4

Arthur JS, Fong AL, Dwyer JM, Davare M, Reese E, et al. 2004. Mitogen- and stress-activated protein kinase 1 mediates cAMP response element-binding protein phosphorylation and activation by neurotrophins. *J Neurosci* 24:4324-32

Bachevalier J, Nemanic S, Alvarado MC. 2015. The influence of context on recognition memory in monkeys: effects of hippocampal, parahippocampal and perirhinal lesions. *Behav Brain Res* 285:89-98

Badhwar A, Lerch JP, Hamel E, Sled JG. 2013. Impaired structural correlates of memory in Alzheimer's disease mice. *Neuroimage Clin* 3:290-300

Bailey CH, Bartsch D, Kandel ER. 1996. Toward a molecular definition of long-term memory storage. *Proc Natl Acad Sci U S A* 93:13445-52

Bailey CH, Kandel ER. 1993. Structural changes accompanying memory storage. *Annu Rev Physiol* 55:397-426

Bailey CH, Kandel ER. 2008. Synaptic remodeling, synaptic growth and the storage of long-term memory in Aplysia. *Prog Brain Res* 169:179-98

Bailey CH, Kandel ER, Harris KM. 2015. Structural Components of Synaptic Plasticity and Memory Consolidation. *Cold Spring Harb Perspect Biol* 7

Barbosa FF, Pontes IM, Ribeiro S, Ribeiro AM, Silva RH. 2012. Differential roles of the dorsal hippocampal regions in the acquisition of spatial and temporal aspects of episodic-like memory. *Behav Brain Res* 232:269-77

Barker GR, Bird F, Alexander V, Warburton EC. 2007. Recognition memory for objects, place, and temporal order: a disconnection analysis of the role of the medial prefrontal cortex and perirhinal cortex. *J Neurosci* 27:2948-57

Barker GR, Warburton EC. 2011. When is the hippocampus involved in recognition memory? *J Neurosci* 31:10721-31

Barrett GL. 2000. The p75 neurotrophin receptor and neuronal apoptosis. *Prog Neurobiol* 61:205-29

Bean AJ, Elde R, Cao YH, Oellig C, Tamminga C, et al. 1991. Expression of acidic and basic fibroblast growth factors in the substantia nigra of rat, monkey, and human. *Proc Natl Acad Sci U S A* 88:10237-41

Bekinschtein P, Cammarota M, Igaz LM, Bevilaqua LR, Izquierdo I, Medina JH. 2007. Persistence of long-term memory storage requires a late protein synthesis- and BDNF- dependent phase in the hippocampus. *Neuron* 53:261-77

Bekinschtein P, Cammarota M, Izquierdo I, Medina JH. 2008a. BDNF and memory formation and storage. *Neuroscientist* 14:147-56

Bekinschtein P, Cammarota M, Katche C, Slipczuk L, Rossato JI, et al. 2008b. BDNF is essential to promote persistence of long-term memory storage. *Proc Natl Acad Sci U S A* 105:2711-6

Bekinschtein P, Cammarota M, Medina JH. 2014. BDNF and memory processing. *Neuropharmacology* 76 Pt C:677-83

Berman DM, Gilman AG. 1998. Mammalian RGS proteins: barbarians at the gate. *J Biol Chem* 273:1269-72

Berman DM, Wilkie TM, Gilman AG. 1996. GAIP and RGS4 are GTPase-activating proteins for the Gi subfamily of G protein alpha subunits. *Cell* 86:445-52

Bjellqvist B, Ek K, Righetti PG, Gianazza E, Gorg A, et al. 1982. Isoelectric focusing in immobilized pH gradients: principle, methodology and some applications. *J Biochem Biophys Methods* 6:317-39

Bloss EB, Janssen WG, Ohm DT, Yuk FJ, Wadsworth S, et al. 2011. Evidence for reduced experience-dependent dendritic spine plasticity in the aging prefrontal cortex. *J Neurosci* 31:7831-9

Blurton-Jones M, Kitazawa M, Martinez-Coria H, Castello NA, Muller FJ, et al. 2009. Neural stem cells improve cognition via BDNF in a transgenic model of Alzheimer disease. *Proc Natl Acad Sci U S A* 106:13594-9

Bogush A, Pedrini S, Pelta-Heller J, Chan T, Yang Q, et al. 2007. AKT and CDK5/p35 mediate brain-derived neurotrophic factor induction of DARPP-32 in medium size spiny neurons in vitro. *J Biol Chem* 282:7352-9

Bosch M, Castro J, Saneyoshi T, Matsuno H, Sur M, Hayashi Y. 2014. Structural and molecular remodeling of dendritic spine substructures during long-term potentiation. *Neuron* 82:444-59

Bradford MM. 1976. A rapid and sensitive method for the quantitation of microgram quantities of protein utilizing the principle of protein-dye binding. *Anal Biochem* 72:248-54

Bramham CR, Messaoudi E. 2005. BDNF function in adult synaptic plasticity: the synaptic consolidation hypothesis. *Prog Neurobiol* 76:99-125

Broadie K, Rushton E, Skoulakis EM, Davis RL. 1997. Leonardo, a Drosophila 14-3-3 protein involved in learning, regulates presynaptic function. *Neuron* 19:391-402

Brown MW, Aggleton JP. 2001. Recognition memory: what are the roles of the perirhinal cortex and hippocampus? *Nat Rev Neurosci* 2:51-61

Brown NE, Goswami D, Branch MR, Ramineni S, Ortlund EA, et al. 2015. Integration of G protein alpha (Galpha) signaling by the regulator of G protein signaling 14 (RGS14). *J Biol Chem* 290:9037-49

Burke SN, Barnes CA. 2006. Neural plasticity in the ageing brain. *Nat Rev Neurosci* 7:30-40

Bussey TJ, Duck J, Muir JL, Aggleton JP. 2000. Distinct patterns of behavioural impairments resulting from fornix transection or neurotoxic lesions of the perirhinal and postrhinal cortices in the rat. *Behav Brain Res* 111:187-202

Bussey TJ, Muir JL, Aggleton JP. 1999. Functionally dissociating aspects of event memory: the effects of combined perirhinal and postrhinal cortex lesions on object and place memory in the rat. *J Neurosci* 19:495-502

Caccamo A, Maldonado MA, Bokov AF, Majumder S, Oddo S. 2010. CBP gene transfer increases BDNF levels and ameliorates learning and memory deficits in a mouse model of Alzheimer's disease. *Proc Natl Acad Sci U S A* 107:22687-92

Candiano G, Bruschi M, Musante L, Santucci L, Ghiggeri GM, et al. 2004. Blue silver: a very sensitive colloidal Coomassie G-250 staining for proteome analysis. *Electrophoresis* 25:1327-33

Caroni P, Donato F, Muller D. 2012. Structural plasticity upon learning: regulation and functions. *Nat Rev Neurosci* 13:478-90

Castellucci VF, Blumenfeld H, Goelet P, Kandel ER. 1989. Inhibitor of protein synthesis blocks long-term behavioral sensitization in the isolated gill-withdrawal reflex of Aplysia. *J Neurobiol* 20:1-9

Cetin A, Komai S, Eliava M, Seeburg PH, Osten P. 2006. Stereotaxic gene delivery in the rodent brain. *Nat Protoc* 1:3166-73

Comeau WL, Hastings E, Kolb B. 2007. Pre- and postnatal FGF-2 both facilitate recovery and alter cortical morphology following early medial prefrontal cortical injury. *Behav Brain Res* 180:18-27

Conner JM, Franks KM, Titterness AK, Russell K, Merrill DA, et al. 2009. NGF is essential for hippocampal plasticity and learning. *J Neurosci* 29:10883-9

Connor B, Young D, Yan Q, Faull RL, Synek B, Dragunow M. 1997. Brain-derived neurotrophic factor is reduced in Alzheimer's disease. *Brain Res Mol Brain Res* 49:71-81

Cooley RK, Vanderwolf CH, eds. 2005. *Stereotaxic surgery in the rat: a photographic series*. London, Canada: A.J. Kirby Co.

Chao MV. 2003. Neurotrophins and their receptors: a convergence point for many signalling pathways. *Nat Rev Neurosci* 4:299-309

Chao MV, Bothwell M. 2002. Neurotrophins: to cleave or not to cleave. *Neuron* 33:9-12

Cheah PS, Ramshaw HS, Thomas PQ, Toyo-Oka K, Xu X, et al. 2012. Neurodevelopmental and neuropsychiatric behaviour defects arise from 14-3-3zeta deficiency. *Mol Psychiatry* 17:451-66

Chen KS, Masliah E, Mallory M, Gage FH. 1995. Synaptic loss in cognitively impaired aged rats is ameliorated by chronic human nerve growth factor infusion. *Neuroscience* 68:19-27

Chen KS, Nishimura MC, Armanini MP, Crowley C, Spencer SD, Phillips HS. 1997. Disruption of a single allele of the nerve growth factor gene results in atrophy of basal forebrain cholinergic neurons and memory deficits. *J Neurosci* 17:7288-96

Cheng Y, Black IB, DiCicco-Bloom E. 2002. Hippocampal granule neuron production and population size are regulated by levels of bFGF. *Eur J Neurosci* 15:3-12

Cho H, Kozasa T, Takekoshi K, De Gunzburg J, Kehrl JH. 2000. RGS14, a GTPase-activating protein for Gialpha, attenuates Gialpha- and G13alpha-mediated signaling pathways. *Mol Pharmacol* 58:569-76

Christensen R, Marcussen AB, Wortwein G, Knudsen GM, Aznar S. 2008. Abeta(1-42) injection causes memory impairment, lowered cortical and serum BDNF levels, and decreased hippocampal 5-HT(2A) levels. *Exp Neurol* 210:164-71

Churchill JD, Stanis JJ, Press C, Kushelev M, Greenough WT. 2003. Is procedural memory relatively spared from age effects? *Neurobiol Aging* 24:883-92

de Brabander JM, Kramers RJ, Uylings HB. 1998. Layer-specific dendritic regression of pyramidal cells with ageing in the human prefrontal cortex. *Eur J Neurosci* 10:1261-9

De Vries L, Farquhar MG. 2002. Screening for interacting partners for G alpha i3 and RGS-GAIP using the two-hybrid system. *Methods Enzymol* 344:657-73

De Vries L, Zheng B, Fischer T, Elenko E, Farquhar MG. 2000. The regulator of G protein signaling family. *Annu Rev Pharmacol Toxicol* 40:235-71

Dechant G, Barde YA. 2002. The neurotrophin receptor p75(NTR): novel functions and implications for diseases of the nervous system. *Nat Neurosci* 5:1131-6

Diana RA, Yonelinas AP, Ranganath C. 2007. Imaging recollection and familiarity in the medial temporal lobe: a three-component model. *Trends Cogn Sci* 11:379-86

Dickerson BC, Eichenbaum H. 2010. The episodic memory system: neurocircuitry and disorders. *Neuropsychopharmacology* 35:86-104

Dijkhuizen PA, Ghosh A. 2005. BDNF regulates primary dendrite formation in cortical neurons via the PI3-kinase and MAP kinase signaling pathways. *J Neurobiol* 62:278-88

Donaldson W. 1996. The role of decision processes in remembering and knowing. *Mem Cognit* 24:523-33

Drag LL, Bieliauskas LA. 2010. Contemporary review 2009: cognitive aging. *J Geriatr Psychiatry Neurol* 23:75-93

Duan H, Wearne SL, Rocher AB, Macedo A, Morrison JH, Hof PR. 2003. Age-related dendritic and spine changes in corticocortically projecting neurons in macaque monkeys. *Cereb Cortex* 13:950-61

Eckenstein F, Woodward WR, Nishi R. 1991. Differential localization and possible functions of aFGF and bFGF in the central and peripheral nervous systems. *Ann N Y Acad Sci* 638:348-60

Egan MF, Kojima M, Callicott JH, Goldberg TE, Kolachana BS, et al. 2003. The BDNF val66met polymorphism affects activity-dependent secretion of BDNF and human memory and hippocampal function. *Cell* 112:257-69

Eichenbaum H, Yonelinas AP, Ranganath C. 2007. The medial temporal lobe and recognition memory. *Annu Rev Neurosci* 30:123-52

Ennaceur A, Delacour J. 1988. A new one-trial test for neurobiological studies of memory in rats. 1: Behavioral data. *Behav Brain Res* 31:47-59

Escribano L, Simon AM, Perez-Mediavilla A, Salazar-Colocho P, Del Rio J, Frechilla D. 2009. Rosiglitazone reverses memory decline and hippocampal glucocorticoid receptor down-regulation in an Alzheimer's disease mouse model. *Biochem Biophys Res Commun* 379:406-10

Evans PR, Lee SE, Smith Y, Hepler JR. 2014. Postnatal developmental expression of regulator of G protein signaling 14 (RGS14) in the mouse brain. *J Comp Neurol* 522:186-203

Eyal G, Mansvelder HD, de Kock CP, Segev I. 2014. Dendrites impact the encoding capabilities of the axon. *J Neurosci* 34:8063-71

Formstecher E, Aresta S, Collura V, Hamburger A, Meil A, et al. 2005. Protein interaction mapping: a Drosophila case study. *Genome Res* 15:376-84

Fornari RV, Wichmann R, Atsak P, Atucha E, Barsegyan A, et al. 2012. Rodent stereotaxic surgery and animal welfare outcome improvements for behavioral neuroscience. *J Vis Exp*:e3528

Francis BM, Kim J, Barakat ME, Fraenkl S, Yucel YH, et al. 2012. Object recognition memory and BDNF expression are reduced in young TgCRND8 mice. *Neurobiol Aging* 33:555-63

Friedman D, de Chastelaine M, Nessler D, Malcolm B. 2010. Changes in familiarity and recollection across the lifespan: an ERP perspective. *Brain Res* 1310:124-41

Fu M, Zuo Y. 2011. Experience-dependent structural plasticity in the cortex. *Trends Neurosci* 34:177-87

Gamiz F, Gallo M. 2012. Spontaneous object recognition memory in aged rats: Complexity versus similarity. *Learn Mem* 19:444-8

Gilman AG. 1987. G proteins: transducers of receptor-generated signals. *Annu Rev Biochem* 56:615-49

Gomez-Pinilla F, Lee JW, Cotman CW. 1994. Distribution of basic fibroblast growth factor in the developing rat brain. *Neuroscience* 61:911-23

Gomez-Pinilla F, So V, Kesslak JP. 1998. Spatial learning and physical activity contribute to the induction of fibroblast growth factor: neural substrates for increased cognition associated with exercise. *Neuroscience* 85:53-61

Gonzalez AM, Berry M, Maher PA, Logan A, Baird A. 1995. A comprehensive analysis of the distribution of FGF-2 and FGFR1 in the rat brain. *Brain Res* 701:201-26

Gorg A, Drews O, Luck C, Weiland F, Weiss W. 2009. 2-DE with IPGs. *Electrophoresis* 30 Suppl 1:S122-32

Gorg A, Postel W, Gunther S. 1988. The current state of two-dimensional electrophoresis with immobilized pH gradients. *Electrophoresis* 9:531-46

Gorski JA, Zeiler SR, Tamowski S, Jones KR. 2003. Brain-derived neurotrophic factor is required for the maintenance of cortical dendrites. *J Neurosci* 23:6856-65

Grafstein-Dunn E, Young KH, Cockett MI, Khawaja XZ. 2001. Regional distribution of regulators of G-protein signaling (RGS) 1, 2, 13, 14, 16, and GAIP messenger ribonucleic acids by in situ hybridization in rat brain. *Brain Res Mol Brain Res* 88:113-23

Granholm AC. 2010. Why do we need to use animal models to study cognition and aging? *Neuropsychopharmacology* 35:1621-2

Grothe C, Janet T. 1995. Expression of FGF-2 and FGF receptor type 1 in the adult rat brainstem: effect of colchicine. *J Comp Neurol* 353:18-24

Gutierrez H, Miranda MI, Bermudez-Rattoni F. 1997. Learning impairment and cholinergic deafferentation after cortical nerve growth factor deprivation. *J Neurosci* 17:3796-803

Haist F, Shimamura AP, Squire LR. 1992. On the relationship between recall and recognition memory. *J Exp Psychol Learn Mem Cogn* 18:691-702

Hamm HE. 1998. The many faces of G protein signaling. *J Biol Chem* 273:669-72

He DY, Neasta J, Ron D. 2010. Epigenetic regulation of BDNF expression via the scaffolding protein RACK1. *J Biol Chem* 285:19043-50

Hepler JR. 1999. Emerging roles for RGS proteins in cell signalling. *Trends Pharmacol Sci* 20:376-82

Hepler JR, Gilman AG. 1992. G proteins. *Trends Biochem Sci* 17:383-7

Hock CH, Heese K, Olivieri G, Hulette CH, Rosenberg C, et al. 2000. Alterations in neurotrophins and neurotrophin receptors in Alzheimer's disease. *J Neural Transm Suppl* 59:171-4

Hofer SB, Mrsic-Flogel TD, Bonhoeffer T, Hubener M. 2009. Experience leaves a lasting structural trace in cortical circuits. *Nature* 457:313-7

Hollinger S, Hepler JR. 2002. Cellular regulation of RGS proteins: modulators and integrators of G protein signaling. *Pharmacol Rev* 54:527-59

Hollinger S, Ramineni S, Hepler JR. 2003. Phosphorylation of RGS14 by protein kinase A potentiates its activity toward G alpha i. *Biochemistry* 42:811-9

Hollinger S, Taylor JB, Goldman EH, Hepler JR. 2001. RGS14 is a bifunctional regulator of Galphai/o activity that exists in multiple populations in brain. *J Neurochem* 79:941-9

Hong EJ, McCord AE, Greenberg ME. 2008. A biological function for the neuronal activity-dependent component of Bdnf transcription in the development of cortical inhibition. *Neuron* 60:610-24

Horch HW. 2004. Local effects of BDNF on dendritic growth. *Rev Neurosci* 15:117-29

Horch HW, Katz LC. 2002. BDNF release from single cells elicits local dendritic growth in nearby neurons. *Nat Neurosci* 5:1177-84

Horch HW, Kruttgen A, Portbury SD, Katz LC. 1999. Destabilization of cortical dendrites and spines by BDNF. *Neuron* 23:353-64

Hunsaker MR, Fieldsted PM, Rosenberg JS, Kesner RP. 2008. Dissociating the roles of dorsal and ventral CA1 for the temporal processing of spatial locations, visual objects, and odors. *Behav Neurosci* 122:643-50

Ichim CV, Wells RA. 2011. Generation of high-titer viral preparations by concentration using successive rounds of ultracentrifugation. *J Transl Med* 9:137

Intlekofer KA, Berchtold NC, Malvaez M, Carlos AJ, McQuown SC, et al. 2013. Exercise and sodium butyrate transform a subthreshold learning event into long-term memory via a brain-derived neurotrophic factor-dependent mechanism. *Neuropsychopharmacology* 38:2027-34

Ishii M, Kurachi Y. 2003. Physiological actions of regulators of G-protein signaling (RGS) proteins. *Life Sci* 74:163-71

Iwasaki Y, Negishi T, Inoue M, Tashiro T, Tabira T, Kimura N. 2012. Sendai virus vector-mediated brain-derived neurotrophic factor expression ameliorates memory deficits and synaptic degeneration in a transgenic mouse model of Alzheimer's disease. *J Neurosci Res* 90:981-9

Jacobs B, Driscoll L, Schall M. 1997. Life-span dendritic and spine changes in areas 10 and 18 of human cortex: a quantitative Golgi study. *J Comp Neurol* 386:661-80

Ji Y, Pang PT, Feng L, Lu B. 2005. Cyclic AMP controls BDNF-induced TrkB phosphorylation and dendritic spine formation in mature hippocampal neurons. *Nat Neurosci* 8:164-72

Jin X, Hu H, Mathers PH, Agmon A. 2003. Brain-derived neurotrophic factor mediates activity-dependent dendritic growth in nonpyramidal neocortical interneurons in developing organotypic cultures. *J Neurosci* 23:5662-73

Kamenetz F, Tomita T, Hsieh H, Seabrook G, Borchelt D, et al. 2003. APP processing and synaptic function. *Neuron* 37:925-37

Kauppi K, Nilsson LG, Adolfsson R, Lundquist A, Eriksson E, Nyberg L. 2013. Decreased medial temporal lobe activation in BDNF (66)Met allele carriers during memory encoding. *Neuropsychologia* 51:2462-8

Kemp A, Manahan-Vaughan D. 2007. Hippocampal long-term depression: master or minion in declarative memory processes? *Trends Neurosci* 30:111-8

Khan ZU, Martin-Montanez E, Navarro-Lobato I, Muly EC. 2014. Memory deficits in aging and neurological diseases. *Prog Mol Biol Transl Sci* 122:1-29

Kiel C, Wohlgemuth S, Rousseau F, Schymkowitz J, Ferkinghoff-Borg J, et al. 2005. Recognizing and defining true Ras binding domains II: in silico prediction based on homology modelling and energy calculations. *J Mol Biol* 348:759-75

Kimple RJ, De Vries L, Tronchere H, Behe CI, Morris RA, et al. 2001. RGS12 and RGS14 GoLoco motifs are G alpha(i) interaction sites with guanine nucleotide dissociation inhibitor Activity. *J Biol Chem* 276:29275-81

Kimple RJ, Kimple ME, Betts L, Sondek J, Siderovski DP. 2002. Structural determinants for GoLoco-induced inhibition of nucleotide release by Galpha subunits. *Nature* 416:878-81

Knafo S, Venero C. 2015. *Cognitive enhancement*. New York: Academic press

Koelle MR. 1997. A new family of G-protein regulators - the RGS proteins. *Curr Opin Cell Biol* 9:143-7

Koen JD, Yonelinas AP. 2014. The effects of healthy aging, amnestic mild cognitive impairment, and Alzheimer's disease on recollection and familiarity: a meta-analytic review. *Neuropsychol Rev* 24:332-54

Kopec AM, Carew TJ. 2013. Growth factor signaling and memory formation: temporal and spatial integration of a molecular network. *Learn Mem* 20:531-9

Koponen E, Voikar V, Riekki R, Saarelainen T, Rauramaa T, et al. 2004. Transgenic mice overexpressing the full-length neurotrophin receptor trkB exhibit increased activation of the trkB-PLCgamma pathway, reduced anxiety, and facilitated learning. *Mol Cell Neurosci* 26:166-81

Korsching S, Auburger G, Heumann R, Scott J, Thoenen H. 1985. Levels of nerve growth factor and its mRNA in the central nervous system of the rat correlate with cholinergic innervation. *EMBO J* 4:1389-93

Kwon M, Fernandez JR, Zegarek GF, Lo SB, Firestein BL. 2011. BDNF-promoted increases in proximal dendrites occur via CREB-dependent transcriptional regulation of cypin. *J Neurosci* 31:9735-45

Laemmli UK. 1970. Cleavage of structural proteins during the assembly of the head of bacteriophage T4. *Nature* 227:680-5

Lamprecht R, LeDoux J. 2004. Structural plasticity and memory. *Nat Rev Neurosci* 5:45-54

Large TH, Bodary SC, Clegg DO, Weskamp G, Otten U, Reichardt LF. 1986. Nerve growth factor gene expression in the developing rat brain. *Science* 234:352-5

Larminie C, Murdock P, Walhin JP, Duckworth M, Blumer KJ, et al. 2004. Selective expression of regulators of G-protein signaling (RGS) in the human central nervous system. *Brain Res Mol Brain Res* 122:24-34

Lee I, Hunsaker MR, Kesner RP. 2005. The role of hippocampal subregions in detecting spatial novelty. *Behav Neurosci* 119:145-53

Lee JL, Everitt BJ, Thomas KL. 2004. Independent cellular processes for hippocampal memory consolidation and reconsolidation. *Science* 304:839-43

Lee SE, Simons SB, Heldt SA, Zhao M, Schroeder JP, et al. 2010. RGS14 is a natural suppressor of both synaptic plasticity in CA2 neurons and hippocampal-based learning and memory. *Proc Natl Acad Sci U S A* 107:16994-8

Levi-Montalcini R, Angeletti PU. 1968. Nerve growth factor. *Physiol Rev* 48:534-69

Li J, Ding X, Zhang R, Jiang W, Sun X, et al. 2015. Harpagoside ameliorates the amyloid-beta-induced cognitive impairment in rats via up-regulating BDNF expression and MAPK/PI3K pathways. *Neuroscience* 303:103-14

Lindwall G, Cole RD. 1984. Phosphorylation affects the ability of tau protein to promote microtubule assembly. *J Biol Chem* 259:5301-5

Linnarsson S, Bjorklund A, Ernfors P. 1997. Learning deficit in BDNF mutant mice. *Eur J Neurosci* 9:2581-7

Lopez-Aranda MF, Acevedo MJ, Carballo FJ, Gutierrez A, Khan ZU. 2006. Localization of the GoLoco motif carrier regulator of G-protein signalling 12 and 14 proteins in monkey and rat brain. *Eur J Neurosci* 23:2971-82

Lopez-Aranda MF, Lopez-Tellez JF, Navarro-Lobato I, Masmudi-Martin M, Gutierrez A, Khan ZU. 2009. Role of layer 6 of V2 visual cortex in object-recognition memory. *Science* 325:87-9

Lowry OH, Rosebrough NJ, Farr AL, Randall RJ. 1951. Protein measurement with the Folin phenol reagent. *J Biol Chem* 193:265-75

Lu B. 2003. BDNF and activity-dependent synaptic modulation. *Learn Mem* 10:86-98

Luo L, Hendriks T, Craik FI. 2007. Age differences in recollection: three patterns of enhanced encoding. *Psychol Aging* 22:269-80

Maisonpierre PC, Belluscio L, Friedman B, Alderson RF, Wiegand SJ, et al. 1990. NT-3, BDNF, and NGF in the developing rat nervous system: parallel as well as reciprocal patterns of expression. *Neuron* 5:501-9

Maren S. 2005. Synaptic mechanisms of associative memory in the amygdala. *Neuron* 47:783-6

Massey PV, Bashir ZI. 2007. Long-term depression: multiple forms and implications for brain function. *Trends Neurosci* 30:176-84

McAllister AK, Katz LC, Lo DC. 1999. Neurotrophins and synaptic plasticity. *Annu Rev Neurosci* 22:295-318

Meunier M, Bachevalier J, Mishkin M, Murray EA. 1993. Effects on visual recognition of combined and separate ablations of the entorhinal and perirhinal cortex in rhesus monkeys. *J Neurosci* 13:5418-32

Michalski B, Fahnestock M. 2003. Pro-brain-derived neurotrophic factor is decreased in parietal cortex in Alzheimer's disease. *Brain Res Mol Brain Res* 111:148-54

Miller FD, Kaplan DR. 2001. On Trk for retrograde signaling. *Neuron* 32:767-70

Miller JA, Oldham MC, Geschwind DH. 2008. A systems level analysis of transcriptional changes in Alzheimer's disease and normal aging. *J Neurosci* 28:1410-20

Minichiello L, Calella AM, Medina DL, Bonhoeffer T, Klein R, Korte M. 2002. Mechanism of TrkB-mediated hippocampal long-term potentiation. *Neuron* 36:121-37

Mittal V, Linder ME. 2004. The RGS14 GoLoco domain discriminates among Galphai isoforms. *J Biol Chem* 279:46772-8

Mittal V, Linder ME. 2006. Biochemical characterization of RGS14: RGS14 activity towards G-protein alpha subunits is independent of its binding to Rap2A. *Biochem J* 394:309-15

Mizui T, Ishikawa Y, Kumanogoh H, Lume M, Matsumoto T, et al. 2015. BDNF pro-peptide actions facilitate hippocampal LTD and are altered by the common BDNF polymorphism Val66Met. *Proc Natl Acad Sci U S A* 112:E3067-74

Mizuno M, Yamada K, Olariu A, Nawa H, Nabeshima T. 2000. Involvement of brain-derived neurotrophic factor in spatial memory formation and maintenance in a radial arm maze test in rats. *J Neurosci* 20:7116-21

Morici JF, Bekinschtein P, Weisstaub NV. 2015. Medial prefrontal cortex role in recognition memory in rodents. *Behav Brain Res* 292:241-51

Morrison JH, Hof PR. 1997. Life and death of neurons in the aging brain. *Science* 278:412-9

Mucke L, Masliah E, Yu GQ, Mallory M, Rockenstein EM, et al. 2000. High-level neuronal expression of abeta 1-42 in wild-type human amyloid protein precursor transgenic mice: synaptotoxicity without plaque formation. *J Neurosci* 20:4050-8

Mufson EJ, Counts SE, Perez SE, Ginsberg SD. 2008. Cholinergic system during the progression of Alzheimer's disease: therapeutic implications. *Expert Rev Neurother* 8:1703-18

Mumby DG, Pinel JP. 1994. Rhinal cortex lesions and object recognition in rats. *Behav Neurosci* 108:11-8

Nagahara AH, Mateling M, Kovacs I, Wang L, Eggert S, et al. 2013. Early BDNF treatment ameliorates cell loss in the entorhinal cortex of APP transgenic mice. *J Neurosci* 33:15596-602

Nagahara AH, Merrill DA, Coppola G, Tsukada S, Schroeder BE, et al. 2009. Neuroprotective effects of brain-derived neurotrophic factor in rodent and primate models of Alzheimer's disease. *Nat Med* 15:331-7

Narisawa-Saito M, Wakabayashi K, Tsuji S, Takahashi H, Nawa H. 1996. Regional specificity of alterations in NGF, BDNF and NT-3 levels in Alzheimer's disease. *Neuroreport* 7:2925-8

Neasta J, Kiely PA, He DY, Adams DR, O'Connor R, Ron D. 2012. Direct interaction between scaffolding proteins RACK1 and 14-3-3zeta regulates brain-derived neurotrophic factor (BDNF) transcription. *J Biol Chem* 287:322-36

Neubig RR, Siderovski DP. 2002. Regulators of G-protein signalling as new central nervous system drug targets. *Nat Rev Drug Discov* 1:187-97

Neves SR, Ram PT, Iyengar R. 2002. G protein pathways. *Science* 296:1636-9

Niewiadomska G, Mietelska-Porowska A, Mazurkiewicz M. 2011. The cholinergic system, nerve growth factor and the cytoskeleton. *Behav Brain Res* 221:515-26

Nilsson LG. 2003. Memory function in normal aging. *Acta Neurol Scand Suppl* 179:7-13

O'Farrell PH. 1975. High resolution two-dimensional electrophoresis of proteins. *J Biol Chem* 250:4007-21

Oldham WM, Hamm HE. 2008. Heterotrimeric G protein activation by G-protein-coupled receptors. *Nat Rev Mol Cell Biol* 9:60-71

Ornitz DM, Herr AB, Nilsson M, Westman J, Svahn CM, Waksman G. 1995. FGF binding and FGF receptor activation by synthetic heparan-derived di- and trisaccharides. *Science* 268:432-6

Page TL, Einstein M, Duan H, He Y, Flores T, et al. 2002. Morphological alterations in neurons forming corticocortical projections in the neocortex of aged Patas monkeys. *Neurosci Lett* 317:37-41

Panja D, Bramham CR. 2014. BDNF mechanisms in late LTP formation: A synthesis and breakdown. *Neuropharmacology* 76 Pt C:664-76

Park H, Poo MM. 2013. Neurotrophin regulation of neural circuit development and function. *Nat Rev Neurosci* 14:7-23

Paxinos G, Franklin KBJ. 2001. *The mouse brain in stereotaxic coordinates*. San Diego: Academic Press

Paxinos G, Watson C. 1998. *The Rat Brain In Stereotaxic Coordinates*. Orlando: Academic Press

Pear WS, Nolan GP, Scott ML, Baltimore D. 1993. Production of high-titer helper-free retroviruses by transient transfection. *Proc Natl Acad Sci U S A* 90:8392-6

Peng S, Garzon DJ, Marchese M, Klein W, Ginsberg SD, et al. 2009. Decreased brain-derived neurotrophic factor depends on amyloid aggregation state in transgenic mouse models of Alzheimer's disease. *J Neurosci* 29:9321-9

Peng S, Wuu J, Mufson EJ, Fahnestock M. 2005. Precursor form of brain-derived neurotrophic factor and mature brain-derived neurotrophic factor are decreased in the pre-clinical stages of Alzheimer's disease. *J Neurochem* 93:1412-21

Peters A, Sethares C, Moss MB. 1998. The effects of aging on layer 1 in area 46 of prefrontal cortex in the rhesus monkey. *Cereb Cortex* 8:671-84

Peters J, Daum I. 2008. Differential effects of normal aging on recollection of concrete and abstract words. *Neuropsychology* 22:255-61

Philip N, Acevedo SF, Skoulakis EM. 2001. Conditional rescue of olfactory learning and memory defects in mutants of the 14-3-3zeta gene leonardo. *J Neurosci* 21:8417-25

Poo MM. 2001. Neurotrophins as synaptic modulators. *Nat Rev Neurosci* 2:24-32

Purves D, Hadley RD. 1985. Changes in the dendritic branching of adult mammalian neurones revealed by repeated imaging in situ. *Nature* 315:404-6

Puzzo D, Privitera L, Leznik E, Fa M, Staniszewski A, et al. 2008. Picomolar amyloid-beta positively modulates synaptic plasticity and memory in hippocampus. *J Neurosci* 28:14537-45

Puzzo D, Privitera L, Palmeri A. 2012. Hormetic effect of amyloid-beta peptide in synaptic plasticity and memory. *Neurobiol Aging* 33:1484 e15-24

Qiao H, Foote M, Graham K, Wu Y, Zhou Y. 2014. 14-3-3 proteins are required for hippocampal long-term potentiation and associative learning and memory. *J Neurosci* 34:4801-8

Raballo R, Rhee J, Lyn-Cook R, Leckman JF, Schwartz ML, Vaccarino FM. 2000. Basic fibroblast growth factor (Fgf2) is necessary for cell proliferation and neurogenesis in the developing cerebral cortex. *J Neurosci* 20:5012-23

Rapp PR, Gallagher M. 1996. Preserved neuron number in the hippocampus of aged rats with spatial learning deficits. *Proc Natl Acad Sci U S A* 93:9926-30

Rasmussen T, Schliemann T, Sorensen JC, Zimmer J, West MJ. 1996. Memory impaired aged rats: no loss of principal hippocampal and subicular neurons. *Neurobiol Aging* 17:143-7

Reiser J. 2000. Production and concentration of pseudotyped HIV-1-based gene transfer vectors. *Gene Ther* 7:910-3

Reissner KJ, Shobe JL, Carew TJ. 2006. Molecular nodes in memory processing: insights from Aplysia. *Cell Mol Life Sci* 63:963-74

Restivo L, Vetere G, Bontempi B, Ammassari-Teule M. 2009. The formation of recent and remote memory is associated with time-dependent formation of dendritic spines in the hippocampus and anterior cingulate cortex. *J Neurosci* 29:8206-14

Rioult-Pedotti MS, Friedman D, Hess G, Donoghue JP. 1998. Strengthening of horizontal cortical connections following skill learning. *Nat Neurosci* 1:230-4

Rizzo V, Richman J, Puthanveettil SV. 2014. Dissecting mechanisms of brain aging by studying the intrinsic excitability of neurons. *Front Aging Neurosci* 6:337

Roberts TF, Tschida KA, Klein ME, Mooney R. 2010. Rapid spine stabilization and synaptic enhancement at the onset of behavioural learning. *Nature* 463:948-52

Romero-Granados R, Fontan-Lozano A, Delgado-Garcia JM, Carrion AM. 2010. From learning to forgetting: behavioral, circuitry, and molecular properties define the different functional states of the recognition memory trace. *Hippocampus* 20:584-95

Ross EM, Wilkie TM. 2000. GTPase-activating proteins for heterotrimeric G proteins: regulators of G protein signaling (RGS) and RGS-like proteins. *Annu Rev Biochem* 69:795-827

Sadik G, Tanaka T, Kato K, Yamamori H, Nessa BN, et al. 2009a. Phosphorylation of tau at Ser214 mediates its interaction with 14-3-3 protein: implications for the mechanism of tau aggregation. *J Neurochem* 108:33-43

Sadik G, Tanaka T, Kato K, Yanagi K, Kudo T, Takeda M. 2009b. Differential interaction and aggregation of 3-repeat and 4-repeat tau isoforms with 14-3-3zeta protein. *Biochem Biophys Res Commun* 383:37-41

Salehi A, Delcroix JD, Mobley WC. 2003. Traffic at the intersection of neurotrophic factor signaling and neurodegeneration. *Trends Neurosci* 26:73-80

Sangha S, Scheibenstock A, Lukowiak K. 2003. Reconsolidation of a long-term memory in Lymnaea requires new protein and RNA synthesis and the soma of right pedal dorsal 1. *J Neurosci* 23:8034-40

Schiapparelli L, Simon AM, Del Rio J, Frechilla D. 2006. Opposing effects of AMPA and 5-HT1A receptor blockade on passive avoidance and object recognition performance: correlation with AMPA receptor subunit expression in rat hippocampus. *Neuropharmacology* 50:897-907

Segal M. 2005. Dendritic spines and long-term plasticity. *Nat Rev Neurosci* 6:277-84

Selkoe DJ. 2002. Alzheimer's disease is a synaptic failure. *Science* 298:789-91

Shankar GM, Li S, Mehta TH, Garcia-Munoz A, Shepardson NE, et al. 2008. Amyloid-beta protein dimers isolated directly from Alzheimer's brains impair synaptic plasticity and memory. *Nat Med* 14:837-42

Shimada T, Fournier AE, Yamagata K. 2013. Neuroprotective function of 14-3-3 proteins in neurodegeneration. *Biomed Res Int* 2013:564534

Shin MK, Kim HG, Baek SH, Jung WR, Park DI, et al. 2014. Neuropep-1 ameliorates learning and memory deficits in an Alzheimer's disease mouse model, increases brain-derived neurotrophic factor expression in the brain, and causes reduction of amyloid beta plaques. *Neurobiol Aging* 35:990-1001

Shu FJ, Ramineni S, Amyot W, Hepler JR. 2007. Selective interactions between Gi alpha1 and Gi alpha3 and the GoLoco/GPR domain of RGS14 influence its dynamic subcellular localization. *Cell Signal* 19:163-76

Shu FJ, Ramineni S, Hepler JR. 2010. RGS14 is a multifunctional scaffold that integrates G protein and Ras/Raf MAPkinase signalling pathways. *Cell Signal* 22:366-76

Siderovski DP, Diverse-Pierluissi M, De Vries L. 1999. The GoLoco motif: a Galphai/o binding motif and potential guanine-nucleotide exchange factor. *Trends Biochem Sci* 24:340-1

Skoulakis EM, Davis RL. 1996. Olfactory learning deficits in mutants for leonardo, a Drosophila gene encoding a 14-3-3 protein. *Neuron* 17:931-44

Skoulakis EM, Davis RL. 1998. 14-3-3 proteins in neuronal development and function. *Mol Neurobiol* 16:269-84

Slipczuk L, Bekinschtein P, Katche C, Cammarota M, Izquierdo I, Medina JH. 2009. BDNF activates mTOR to regulate GluR1 expression required for memory formation. *PLoS One* 4:e6007

Snow BE, Antonio L, Suggs S, Gutstein HB, Siderovski DP. 1997. Molecular cloning and expression analysis of rat Rgs12 and Rgs14. *Biochem Biophys Res Commun* 233:770-7

Spires-Jones T, Knafo S. 2012. Spines, plasticity, and cognition in Alzheimer's model mice. *Neural Plast* 2012:319836

Squire LR, Stark CE, Clark RE. 2004. The medial temporal lobe. *Annu Rev Neurosci* 27:279-306

Squire LR, Wixted JT, Clark RE. 2007. Recognition memory and the medial temporal lobe: a new perspective. *Nat Rev Neurosci* 8:872-83

Szebenyi G, Dent EW, Callaway JL, Seys C, Lueth H, Kalil K. 2001. Fibroblast growth factor-2 promotes axon branching of cortical neurons by influencing morphology and behavior of the primary growth cone. *J Neurosci* 21:3932-41

Tanaka J, Horiike Y, Matsuzaki M, Miyazaki T, Ellis-Davies GC, Kasai H. 2008. Protein synthesis and neurotrophin-dependent structural plasticity of single dendritic spines. *Science* 319:1683-7

Teng Y, Zhang MQ, Wang W, Liu LT, Zhou LM, et al. 2014. Compound danshen tablet ameliorated abeta25-35-induced spatial memory impairment in mice via rescuing imbalance between cytokines and neurotrophins. *BMC Complement Altern Med* 14:23

Tesmer JJ, Berman DM, Gilman AG, Sprang SR. 1997. Structure of RGS4 bound to AlF4--activated G(i alpha1): stabilization of the transition state for GTP hydrolysis. *Cell* 89:251-61

Timmusk T, Persson H, Metsis M. 1994. Analysis of transcriptional initiation and translatability of brain-derived neurotrophic factor mRNAs in the rat brain. *Neurosci Lett* 177:27-31

Tongiorgi E. 2008. Activity-dependent expression of brain-derived neurotrophic factor in dendrites: facts and open questions. *Neurosci Res* 61:335-46

Tongiorgi E, Baj G. 2008. Functions and mechanisms of BDNF mRNA trafficking. *Novartis Found Symp* 289:136-47; discussion 47-51, 93-5

Traver S, Bidot C, Spassky N, Baltauss T, De Tand MF, et al. 2000. RGS14 is a novel Rap effector that preferentially regulates the GTPase activity of galphao. *Biochem J* 350 Pt 1:19-29

Traver S, Splingard A, Gaudriault G, De Gunzburg J. 2004. The RGS (regulator of G-protein signalling) and GoLoco domains of RGS14 co-operate to regulate Gi-mediated signalling. *Biochem J* 379:627-32

Tromp D, Bernard F, Dufour A, Lithfous S, Pebayle T, Despres O. 2015. Episodic memory in normal aging and Alzheimer Disease: Insights from imaging and behavioral studies. *Ageing Res Rev*

Tyler WJ, Alonso M, Bramham CR, Pozzo-Miller LD. 2002. From acquisition to consolidation: on the role of brain-derived neurotrophic factor signaling in hippocampal-dependent learning. *Learn Mem* 9:224-37

Umahara T, Uchihara T, Iwamoto T. 2012. Structure-oriented review of 14-3-3 protein isoforms in geriatric neuroscience. *Geriatr Gerontol Int* 12:586-99

Van der Zee CE, Lourenssen S, Stanisz J, Diamond J. 1995. NGF deprivation of adult rat brain results in cholinergic hypofunction and selective impairments in spatial learning. *Eur J Neurosci* 7:160-8

Vellano CP, Brown NE, Blumer JB, Hepler JR. 2013. Assembly and function of the regulator of G protein signaling 14 (RGS14).H-Ras signaling complex in live cells are regulated by Galphai1 and Galphai-linked G protein-coupled receptors. *J Biol Chem* 288:3620-31

Wang TH, de Chastelaine M, Minton B, Rugg MD. 2012. Effects of age on the neural correlates of familiarity as indexed by ERPs. *J Cogn Neurosci* 24:1055-68

Webster MJ, Weickert CS, Herman MM, Kleinman JE. 2002. BDNF mRNA expression during postnatal development, maturation and aging of the human prefrontal cortex. *Brain Res Dev Brain Res* 139:139-50

Westerberg C, Mayes A, Florczak SM, Chen Y, Creery J, et al. 2013. Distinct medial temporal contributions to different forms of recognition in amnestic mild cognitive impairment and Alzheimer's disease. *Neuropsychologia* 51:2450-61

Westerberg CE, Paller KA, Weintraub S, Mesulam MM, Holdstock JS, et al. 2006. When memory does not fail: familiarity-based recognition in mild cognitive impairment and Alzheimer's disease. *Neuropsychology* 20:193-205

Whitlock JR, Heynen AJ, Shuler MG, Bear MF. 2006. Learning induces long-term potentiation in the hippocampus. *Science* 313:1093-7

Wickelgren I. 1996. For the cortex, neuron loss may be less than thought. *Science* 273:48-50

Wilson IA, Gallagher M, Eichenbaum H, Tanila H. 2006. Neurocognitive aging: prior memories hinder new hippocampal encoding. *Trends Neurosci* 29:662-70

Willard FS, Kimple RJ, Siderovski DP. 2004. Return of the GDI: the GoLoco motif in cell division. *Annu Rev Biochem* 73:925-51

Willard FS, Willard MD, Kimple AJ, Soundararajan M, Oestreich EA, et al. 2009. Regulator of G-protein signaling 14 (RGS14) is a selective H-Ras effector. *PLoS One* 4:e4884

Wirth MJ, Brun A, Grabert J, Patz S, Wahle P. 2003. Accelerated dendritic development of rat cortical pyramidal cells and interneurons after biolistic transfection with BDNF and NT4/5. *Development* 130:5827-38

Wohlgemuth S, Kiel C, Kramer A, Serrano L, Wittinghofer F, Herrmann C. 2005. Recognizing and defining true Ras binding domains I: biochemical analysis. *J Mol Biol* 348:741-58

Wolk DA, Dunfee KL, Dickerson BC, Aizenstein HJ, DeKosky ST. 2011. A medial temporal lobe division of labor: insights from memory in aging and early Alzheimer disease. *Hippocampus* 21:461-6

Wong TP, Campbell PM, Ribeiro-da-Silva A, Cuello AC. 1998. Synaptic numbers across cortical laminae and cognitive performance of the rat during ageing. *Neuroscience* 84:403-12

Wong TP, Marchese G, Casu MA, Ribeiro-da-Silva A, Cuello AC, De Koninck Y. 2000. Loss of presynaptic and postsynaptic structures is accompanied by compensatory increase in action potential-dependent synaptic input to layer V neocortical pyramidal neurons in aged rats. *J Neurosci* 20:8596-606

Woo NH, Teng HK, Siao CJ, Chiaruttini C, Pang PT, et al. 2005. Activation of p75NTR by proBDNF facilitates hippocampal long-term depression. *Nat Neurosci* 8:1069-77

Woodard GE, Jardin I, Berna-Erro A, Salido GM, Rosado JA. 2015. Regulators of G-protein-signaling proteins: negative modulators of G-protein-coupled receptor signaling. *Int Rev Cell Mol Biol* 317:97-183

Woolf NJ, Milov AM, Schweitzer ES, Roghani A. 2001. Elevation of nerve growth factor and antisense knockdown of TrkA receptor during contextual memory consolidation. *J Neurosci* 21:1047-55

Xia SZ, Feng CH, Guo AK. 1998. Multiple-phase model of memory consolidation confirmed by behavioral and pharmacological analyses of operant conditioning in Drosophila. *Pharmacol Biochem Behav* 60:809-16

Xu T, Yu X, Perlik AJ, Tobin WF, Zweig JA, et al. 2009. Rapid formation and selective stabilization of synapses for enduring motor memories. *Nature* 462:915-9

Yaka R, He DY, Phamluong K, Ron D. 2003. Pituitary adenylate cyclase-activating polypeptide (PACAP(1-38)) enhances N-methyl-D-aspartate receptor function and brain-derived neurotrophic factor expression via RACK1. *J Biol Chem* 278:9630-8

Yang G, Pan F, Gan WB. 2009. Stably maintained dendritic spines are associated with lifelong memories. *Nature* 462:920-4

Ye J, Coulouris G, Zaretskaya I, Cutcutache I, Rozen S, Madden TL. 2012. Primer-BLAST: a tool to design target-specific primers for polymerase chain reaction. *BMC Bioinformatics* 13:134

Ying SW, Futter M, Rosenblum K, Webber MJ, Hunt SP, et al. 2002. Brain-derived neurotrophic factor induces long-term potentiation in intact adult hippocampus: requirement for ERK activation coupled to CREB and upregulation of Arc synthesis. *J Neurosci* 22:1532-40

Yonelinas AP. 2001. Components of episodic memory: the contribution of recollection and familiarity. *Philos Trans R Soc Lond B Biol Sci* 356:1363-74

Yonelinas AP, Aly M, Wang WC, Koen JD. 2010. Recollection and familiarity: examining controversial assumptions and new directions. *Hippocampus* 20:1178-94

Yonelinas AP, Kroll NE, Quamme JR, Lazzara MM, Sauve MJ, et al. 2002. Effects of extensive temporal lobe damage or mild hypoxia on recollection and familiarity. *Nat Neurosci* 5:1236-41

Yonelinas AP, Levy BJ. 2002. Dissociating familiarity from recollection in human recognition memory: different rates of forgetting over short retention intervals. *Psychon Bull Rev* 9:575-82

Zhao M, Li D, Shimazu K, Zhou YX, Lu B, Deng CX. 2007. Fibroblast growth factor receptor-1 is required for long-term potentiation, memory consolidation, and neurogenesis. *Biol Psychiatry* 62:381-90

Zhao P, Nunn C, Ramineni S, Hepler JR, Chidiac P. 2013. The Ras-binding domain region of RGS14 regulates its functional interactions with heterotrimeric G proteins. *J Cell Biochem* 114:1414-23

Zuccato C, Cattaneo E. 2009. Brain-derived neurotrophic factor in neurodegenerative diseases. *Nat Rev Neurol* 5:311-22

IX. APPENDICES

1 APPENDIX 1. MOLECULAR BIOLOGY

1.A. ELECTROPHORESIS IN AGAROSE GEL

1.A.1) Tris-borate-EDTA buffer (TBE) 5X, (1L)

REAGENT	AMOUNT	CONCENTRATION
Tris (Sigma-Aldrich,T1503)	54 g	0.445 M
Boric Acid (Sigma-Aldrich, b6768)	27.5 g	0.445 M
EDTA (Sigma-Aldrich,E5134)	3.72 g	0.01 M
Milli-Q water	Up to 1 L	--

Note: TBE 1X was prepared mixing 200 ml of TBE 5X with 800 ml of Milli-Q water.

1.A.2) 1 % Agarose gel

REAGENT	Small gel (8 wells)	Big gel (15 wells)
Agarose (E0301, EuRx)	0.4 g	1 g
TBE 1X buffer (appendix 1.A.1)	40 ml	100 ml
[1]**Ethidium bromide (EtBr) 0.1 mg/ ml**	68 µl	170 µl

[1]The 0.1 mg/ml EtBr solution was prepared using 10 mg/m EtBr stock solution (Invitrogen, 15585-011).

1. The agarose was dissolved in TBE buffer by heating the solution in microwave.
2. The solution was cooled ≈ 50 ºC and the EtBr was added.
3. The mixed solution was poured into the adequate cuvette and comb was placed.
4. The agarose was allowed to polymerize for 35 min (small gel) or 45 min (big gel).

1.B. GENE AMPLIFICATION IN BACTERIA

1.B.1) Bacterial growth media: 100 µg/ml ampicillin LB and LB-Agar

1. 20 g of LB Broth Base (Invitrogen, 12780-052) and 5 g of sodium chloride (Sigma-Aldrich, S3014) were dissolved in 1 L of Milli-Q water.
2. The medium was distributed into two 1 L glass bottles (500 ml each one).
3. 7.5 g of LB-Agar (Invitrogen, 22700-025) were added to one of the bottles and LB-Agar medium was made. The medium without LB-Agar was called LB liquid medium.
4. Both were sterilized by moist heat at 121 ºC/15 min in an autoclave (sterilclav-75, Raypa).
5. The medium was chilled to 50 ºC and 500 µl of 100 mg/ml ampicillin solution (Sigma-Aldrich, A9393) was added to each bottle of medium under the laminar flow cabinet.

Note: The ampicillin antibiotic was supported in powder and it was dissolved in Nuclease-Free water (Gibco, 10977) up to a concentration of 100 mg/ml. The antibiotic solution was filtered in a 0.45 µm (Sarsteds, 83.1826) and 1 ml aliquots were done and stored at -20 ºC up to 6 months.

6. The 100 µg/ml ampicillin LB medium was stored at 4 ºC, whereas the 100 µg/ml ampicillin LB-Agar was dispensed in 90 mm Petri plates (20-25 ml per plate). Once the agar had solidified, plates were stored at 4 ºC.

1.B.2) Freezing bacterial stocks

To generate a long-term storage of bacteria containing the recombinant DNA of interest:
1. 2.5 ml of 99 % glycerol (Sigma, G6279) were added to 7.5 ml of the bacterial culture at the laminar flow cabinet.
2. The suspension was well mixed, and 1.8 ml aliquots were done in cryogenic vials (Nunc, 363401) and stored at -80 ºC.

1.C. DNA PURIFICATION BY MINICOLUMN SYSTEMS

1.C.1) DNA purification from agarose gel

The DNA purification from agarose gel was performed using the *Wizard® SV Gel and PCR Clean-Up System kit* (Promega, A9281) following the manufacture's protocol:

1. Extraction of DNA from agarose gel. DNA band was carefully excised from the agarose gel under UV light using a sterile scalpel and then transferred to a previously weighted 1.5 ml microcentrifuge tube. The gel slice weight was recorded. At this step the manufacturer recommends irradiate the gel for the absolute minimum time possible to reduce nicking.

The gel was dissolved by adding 1 µl of Membrane Binding Buffer (Promega, A930B) per 1 mg of gel slice and incubated at 60 ºC. Vortex and spin were done every 10 min.

2. Binding. The dissolved gel mixture was transferred to the Wizard SV Minicolumn assembly (Promega, A129A) and left for 5 min at room temperature. Column was centrifuged at 16000 x g for 1 min (Mikro-22 microcentrifuge from Hettich Zentrifugen) and the flowthrough was discarded.

3. Washing. Column-bound DNA was washed with 700 µl of Wash Buffer containing 95 % (v/v) ethanol by centrifugation at 16000 x g for 1 min. This step was repeated with 500 µl of the same buffer. Residual wash buffer from column was removed by centrifugation and further dried at 37 ºC for 90 min to remove any residual ethanol.

4. Elution. DNA was eluted by adding 50 µl of Nuclease-Free Water (Promega, P119a) to the center of column membrane. Following, column was incubated at room temperature for 5 min and then centrifuged at 16,000 × g for 5 min. Eluted DNA was stored at -20 ºC.

5. Determination of DNA concentration. DNA purity and concentration were determined by measuring absorbance at 260 and 280 nm in Nanodrop1000, v3.7 (Thermo Scientific). Samples were stored at 4 ºC.

1.C.2) Miniprep

To extract and purify DNA from bacteria culture was used the *StrataPrep plasmid miniprep kit* (Agilent technologies, 400761) following the manufacturer's protocol with some modifications:

1. Lysing bacteria and DNA extraction. Aliquots of 1 ml of bacterial culture were pellet by centrifugation at 13,000 x g for 1 min in a Mikro-22 centrifuge (Hettich Zentrigugen). To destroy bacterial membranes and release DNA, pellets were resuspended in 100 µl of solution 1 (Stratagene, 400763-13), vortexing vigorously and pipetting up and down to disperse cells completely. Then 100 µl of solution 2 (Stratagene, 400763-14) were added and mixed by inverting several times. Following 125 µl of solution 3 (Stratagene, 400763-15) were added and mixed again by inversion. Finally, the cellular debris were settled down by centrifugation at 13,000 x g for 5 min, and the supernatants containing the DNA were carefully collected.

2. Binding. Supernatants were transferred to a microspin cup, incubated for 1 min at room temperature and then centrifuged at 13,000 x g for 1 min. The flowthrough was recovered and passed through the column again. An additional re-centrifugation was done.

3. Elimination of endonucleases. To avoid DNA degradation, endonucleases were removed by adding 650 µl of nuclease-removal buffer and centrifuging at 13,000 x g for 1 min.

4. Washing. The DNA bound was washed by adding 700 µl of wash buffer (Stratagene, 400763-16) diluted in absolute ethanol and then was centrifuged as above. Re-centrifugation for 30 s was done to eliminate any residual ethanol-wash buffer. The column was transferred to a new clear 1.5 ml tube and left overnight at room temperature to evaporate any residual ethanol.

5. Elution. Finally, to elute DNA, 50 µl of Nucleases Free Water (Gibco, 10977) were added directly onto the fiber matrix at the bottom of the microspin cup. The sample was incubated for 5 min at room temperature and then centrifuged at 13,000 x g for 1 min. DNA obtained was stored at 4 ºC.

1.C.3) Maxiprep

An amount of 300 ml of liquid bacterial culture (see section III.1.2.1.2.3.3) were used to purify $RGS14_{414}$ recombinant DNA using the *Wizard ® Plus Maxiprep DNA Purification System kit* (Promega, A7270) following the manufacturer's protocol:

1. **Lysing bacteria and DNA extraction.** Aliquots of 35 ml of bacterial culture were centrifuged at 5,000 x g for 10 min at the Rotine 420 centrifuge (Hettich Zentrifugen). To destroy bacterial membranes and release DNA, each pellet was resuspended in 10 ml of solution P1 (Qiagen, 1014841), pipetting up and down and vortexing to disperse cells completely. Then 10 ml of lysis solution P2 (Quiagen, 1014935) was added and mixed by inversion several times. The mixture was incubated for 5 min at room temperature before adding 10 ml of neutralization solution P3 (Quiagen, 1014952). The solution was mixed again by gently inversion until the solution lost the blue color. Then it was incubated on ice for 15 min. Cellular debris was pellet by centrifugation at 20,000 x g for 30 min at 4 ºC at Sorvall RC5C centrifuge, using the rotor SS34. The supernatant containing the DNA was collected and filtered by using a Whatman filter.

2. Column equilibration and DNA binding. During the DNA filtration, the affinity column (Quiagen, 1011721) was equilibrated by applying 10 ml of equilibration buffer, QBF (Quiagen, 1018489) and allowing the column to empty by gravity flow. Then, filtered DNA solution was passed through the equilibrated column by gravity.

3. Washing. The DNA bound to the column was washed twice applying 30 ml of wash buffer, QC (Quiagen, 1015367) by gravity.

4. Elution. The DNA was eluted from the column with 15 ml of elution buffer, QF (Elution buffer, Quiagen, 1014856) and collected in a 50 ml centrifuge tube (Nalgene, 3115-0050).

5. Concentration of DNA. 10.5 ml of isopropanol (Sigma Aldrich, I9030) were added and the sample was mixed, incubated for 5 min at room temperature and then centrifuged at 20,000 x g for 30 min at 4 ºC at Sorval RC5C centrifuge with the rotor SS34. The supernatant was discarded and the pellet was resuspended in 5 ml of 70 % (v/v) ethanol by pipetting up and down. Another centrifugation at 15,000 x g for 10 min at Rotina 420 centrifuge (Hettich Zentrifugen) was done and the supernatant was discarded. The tube was incubated for 65 min at 37 ºC to eliminate any residual ethanol. The pellet was resuspended in 1 ml Nuclease Free Water (Gibco, 10977) and the DNA solution was stored at 4 ºC.

6. Determination of DNA concentration. The purified DNA concentration was estimated spectrophotometrically at 260 nm in Nanodrop1000, v3.7 (Thermo Scientific).

1.D. TOTAL RNA EXTRACTION

The total RNA from V2 area was isolated using the *RNeasy Tissue Mini kit* (Quiagen, 74124) according to the manufacturer's protocol:

1. Lysis and homogenated: The RNAlater stabilized tissue was removed from the RNA later with a forceps, and frozen into liquid nitrogen. Immediately the sample was grinded thoroughly with a mortar and pestle. The tissue powder was collected in 1 ml of *QIAzol Lysis Reagent* and incubated for 5 min at room temperature. 200 µl of chloroform were added and gently mixed for 15 s. The mixture was incubated for 3 min at room temperature.

2. Separation of liquid phases: A centrifugation at 12,000 x g for 15 min at 4 ºC in a centrifuge (Beckman CS-15R, rotor F2402H) was carried out, and the aqueous phase was collected in a new 1.5 ml tube. The aqueous phase was mixed with the same volume of 70 % (v/v) ethanol by vigorous vortex.

3. RNA binding: The sample was transferred to an *RNeasy* column and incubated for 2 min at room temperature. A centrifugation at ≥8,000 x g for 15 s at room temperature (15-25 ºC) was done, and the throughflow was discarded.

4. Washing: The RNA bound to the membrane was washed by adding 700 µl de *Buffer RW1* to the column and repeating the centrifugation in step 3. Then 500 µl of Buffer RPE was added and centrifuged again. Finally others 500 µl were passed through the column by a centrifugation for 2 min. To eliminate any residual buffer, the column was centrifuged once more at maximum speed for 1 min.

5. Elution: The *RNeasy* column was placed onto a new clear 1.5 ml tube and 30 µl of Nuclease-Free water (Gibco, 10977) directly on the membrane**.** An incubation of 2 min at room temperature was done before collecting the RNA by centrifugation at ≥8,000 x g for 1 min at room temperature.

6. RNA samples were stored at -80 ºC.

2 APPENDIX 2. CELL CULTURE

2.A. GROWTH MEDIA

2.A.1) Growth medium for 293T cell line (500 ml)

293 T BASE GROWTH MEDIUM COMPONENTS	AMOUNT
Dulbecco's Modified Eagle's Medium (DMEM) with high glucose (4.5 g/L) (Gibco, 52100-021)	6.69 g
Sodium bicarbonate (Sigma Aldrich, S5761)	1.85 g
Non-Essential amino acids 100X (Gibco, 11140-050)	5 ml
L-glutamine 200 mM (Gibco, 25030-032)	5 ml
Sodium pyruvate 100 mM (Gibco, 11360-070)	5 ml
Milli-Q water	485 ml

1. DMEM and sodium bicarbonate were dissolved in Milli-Q water.
2. Non-essential aminoacid, L-glutamine and sodium pyruvate solutions were added at the laminar flow cabinet.
3. The base culture medium for 293T cell line, was sterilized by vacuum filtration using a 0.22 µm pore filter membrane (Sartolab, 180C2-E), and then stored at 4 ºC.
4. Finally complete 293T medium was prepared by adding the following components:

293 T COMPLETE GROWTH MEDIUM COMPONENTS	AMOUNT
293T Base medium (see above)	450 ml
Fetal Bovine Serum (Tet System Approved FBS) (Clontech, 631105)	50 ml
Penicillin and Streptomycin (Gibco, 15140-122)	5 ml

2.A.2) Growth medium for HT1080 cell line (500 ml)

HT1080 BASE GROWTH MEDIUM COMPONENTS	AMOUNT
Eagle's Minimum Essential Medium (MEM) (Gibco, 41500-018)	4.81 g
Sodium bicarbonate (Sigma Aldrich, S5761)	0.75 g
Sodium pyruvate 100 mM (Gibco, 11360-070)	5 ml
Milli-Q water	495 ml

1. MEM and sodium bicarbonate were dissolved in Milli-Q water.
2. Sodium pyruvate solution was added at the laminar flow cabinet.
3. The base culture medium for HT1080 cell line, was sterilized by vacuum filtration using 0.22 µm pore filter membrane (Sartolab, 180C2-E), and then stored at 4 ºC.
4. Finally complete HT1080 medium was prepared as follows:

HT1080 COMPLETE GROWTH MEDIUM COMPONENTS	AMOUNT
HT1080 Base medium (see above)	450 ml
Fetal Bovine Serum (Gibco, 10500-064)	50 ml
Penicillin and Streptomycin (Gibco, 15140-122)	5 ml

2.B. GELATIN-COATED CULTURE FLASKS

1. 0.3 (w/v) gelatin solution was prepared dissolving 1.5 g of gelatin (Sigma Aldrich, G-9391) in 500 ml of Milli-Q water. The solution was sterilized by moist heat at 121ºC/20 min in an autoclave (sterilclav-75, Raypa) and then stored at 4 ºC.
2. 5 ml of 0.3 (w/v) gelatin solution were added to each flask covering the entire surface area and then, the flasks were placed in a 37 ºC incubator for 20 min. The excess of solution was removed and flasks were dried at room temperature overnight before seeding.

2.C. THAWING FROZEN CELLS

Cryopreserved eukaryotic cells were thawed as follows:

1. The cryovial was thawed rapidly in a 37 °C water bath and then was dry off the outside of the cryovial and wiped with 70 % (v/v) ethanol solution.
2. The content was transferred to a 15 ml conical centrifuge tube containing 10 ml of pre-warmed complete medium and mixed gently at the laminar flow cabinet.
3. Cells were settled down by centrifugation at 150 x g for 5 min, the supernatant was carefully aspirated and cells were resuspended in 2 ml of complete medium. This step is necessary to eliminate any residual cryopreservative DMSO (Sigma Aldrich, D8418).
4. The cellular suspension was added to a T-75 flask containing 10 ml of pre-warmed complete medium and gently rocked to distribute the cells evenly over the growth surface.
5. The cell culture was place in a 37 °C humidity incubator (5 % CO_2) for 24 h.
6. Once the culture had been started and the cells were growing normally, aliquots of cellular suspension were prepared to frozen in order to have a renewable source of cells.

2.D. FREEZING A CELL STOCK

As it was indicated in appendix 2.C. a stock of cells was frozen following the next protocol:
1. A cryopreservative DMSO (Sigma Aldrich, D8418) was added to the adequate complete medium at a final concentration of 10 % (v/v) (freezing medium).
2. A 90 %-confluence subculture was performed as it is detailed in appendix 2.E.
3. Once the cellular density and viability were estimated, the total number of cells was determined and then cells were deposited by centrifugation at 150 x g for 5 min discarding the supernatant carefully.
4. The pellet was resuspended in freezing medium at the recommended viable cell density of 3×10^6 cells/ml.
5. Aliquots of the cell suspension were dispensed into cryovials, then frozen and stored in liquid nitrogen.

2.E. CELL SUBCULTURES

The follow protocol was performed:

1. The flask was washed with 5 ml (T75 flask) or 10 ml (T175 flask) of pre-warmed PBS pH 7.4 (Gibco, 10010) for 1 min after removing the medium.
2. The PBS was aspirated and cells were detached by adding 3 ml (T75 flask) or 5 ml (T175 flask) of trypsin-EDTA (Gibco, 25200-072) to each flask for 5 min at 37 ºC.
3. When majority of the cells were detached, an equal volume of pre-warmed complete media into the flask were added to neutralize the trypsin-EDTA and the suspension of cells was collected in a 50 ml conical centrifuge tube.
4. Cell suspension was centrifuged at 1,500 rpm for 5 min at the Labofuge 400 (Heraeus) and the supernatant was carefully discarded. The cell pellet was resuspended in 10 ml pre-warmed complete medium by pipetting up and down gently.
5. New culture flasks were seeded at cell density recommended by cell line's manuals after estimating the number of viable cells/ml using a Neubauer chamber (Bright Line, Rbichert).

3 APPENDIX 3. ORM TESTS

3.A. OBJECTS USED DURING ORM TEST IN RATS

SET No	OBJECTS
1	
2	
3	
4	
5	

3.B. OBJECTS USED DURING ORM TEST IN MICE

SET No	OBJECTS
1	
2	

4 APPENDIX 4. HISTOLOGY

4.A. BUFFERS AND SOLUTIONS

4.A.1) 0.4 M Phosphate Buffer, pH 7.4 (PB buffer) (1L)

REAGENT	AMOUNT
Sodium phosphate dibasic dihydrate ($HNa_2O_4P\ 2H_2O$) (Fluka, 71645)	53.4 g
Sodium dihydrogen phosphate ($NaH_2PO_4.H_2O$) (Panreac, 131965)	13.8 g
Milli-Q water	Up to 1L

The pH was adjusted to 7.4 and the buffer was stored at room temperature.

4.A.2) 0.1 M Phosphate Buffered Saline pH 7.4 (PBS buffer) (1L)

REAGENT	AMOUNT
Sodium chloride (NaCl) (Panreac, 131659)	9 g
0.4 M PB buffer pH 7.4 (appendix 4.A.1)	250 ml
Milli-Q water	Up to 1L

The pH was adjusted up to 7.4 and the buffer was stored at room temperature.

4.A.3) Fixative solution: 10 mM Periodate, 75 mM lysine, 4 % paraformaldehyde (PLP) in 0.1 M PB, pH 7.4 (1L)

REAGENT	AMOUNT
Paraformaldehyde $(CH_2O)_n$ (Merck, 1.04005)	40 g
L-lysine monohydrochloride ($C_6H_{14}N_2O_2HCl$) (Sigma-Aldrich, 62929)	13.7 g
Sodium (meta) periodate ($INaO_4$) (Sigma Aldrich, 30323)	2.14 g
0.4 M PB buffer pH 7.4 (appendix 4.A.1)	250 ml
Milli-Q water	Up to 1L

The PLP fixative solution was prepared just before the animals perfusions as follows:

1. Paraformaldehyde was dissolved in 500 ml of Milli-Q water at 60 ºC. Some drops of 8 N NaOH solution were added to facilitate the dissolution.
2. The solution was filtered using filter paper, and Milli-Q water was added up to 750 ml.
3. Apart, the lysine and the sodium (meta) periodate were dissolved in 200 ml of 0.4 M PB buffer pH 7.4, and then PB was added up to 250 ml.
4. Finally, both solutions were mixed.

4.A.4) 30 % (w/v) sucrose, 0.02 % (w/v) sodium azide in 0.1M PBS buffer (100 ml)

REAGENT	AMOUNT
Sucrose (Panreac, 131621)	30 g
10 % (w/v) Sodium azide (Na_3N) (Sigma-Aldrich, S2002)	200 µl
0.1 M PBS buffer pH 7.4 (appendix 4.A.2)	Up to 100 ml

The solution was stored at 4ºC.

4.A.5) 1,4-Diazabicyclo [2.2.2] octane (DABCO) fluorescence mounting medium

1. The 1:1 PBS-glycerol mix was prepare with glycerol (141339, Panreac) and 0.1 M PBS buffer pH 7.4 (appendix 4.A.2).
2. DABCO (Sigma-Aldrich, D-2522) was added to 3 % (w/v).
3. The solution was stored at 4 ºC.

4.B. PREPARATION OF GELATIN-COATED SLIDES

A solution of gelatin was prepared as it is shown in the table below:

REAGENT	AMOUNT
Gelatin (Panreac, 142060)	3 g
Chromium (III) potassium sulphate (Panreac, 131284)	0.3 g
Milli-Q water	600 ml

1. The gelatin was dissolved in 60 ºC pre-warmed Milli-Q water and then the chromium (III) potassium sulphate was added.
2. The slides were treated with the gelatin solution as follows:
   a. They were degreased in a mixture of absolute ethanol: ether (1:1) for at least 24 h.
   b. The degreasing solution was removed and the slides were dried manually and then 2 min at room temperature.
   c. The slides were immersed in the gelatin solution for 1 min. Then the action was repeated five times for a few seconds.
   d. The slices were dried for 48 h at 37 ºC (they can be used up to two month after treatment).

4.C. FIXATION BY TRANSCARDIAL PERFUSION AND BRAIN EXTRACTION

1. Anesthesia and surgery. Animals were deeply anesthetized by an intraperitoneally injection of 120 mg/Kg of sodium pentobarbital (Eutanax 200 mg/ml, Fatro) before proceeding with the transcardial perfusion. In order to access the heart, it was made a 5-6 cm lateral incision through the integument and abdominal wall just beneath the rib cage. Then the diaphragm was carefully incised along the entire length of the rib cage to expose the pleural cavity. Cutting through the lateral part of the rib cage on both sides, heart was exposed.

2. Washing. A 21 gauge perfusion needle connected to a peristaltic pump (Cole Parmer) was introduced into left ventricle, and then an incision was made to the animal's right atrium. Thus, whole blood was removed by injecting 120 ml of 0.1 M PBS buffer (appendix 4.A.2) at a steady flow rate of 8 ml/min.

3. Fixation. Once blood vessels were washed, 350 ml of PLP fixative solution (appendix 4.A.3) were passed through the circulatory system in order to obtain the best possible preservation of the brain.

4. Brain dissection. Head was guillotined and brain was carefully extracted cutting the integument, the skull and muscles.

5. Post-fixation. The brain was kept in the fixative solution for 24 h at 4 ºC.

4.D. CRYOPROTECTION AND FREEZING

1. **Washing.** Post-fixed brain was washed with 0.1 M PBS buffer for 10 min by exchanging the media 3 times and swirling each time to remove any residual PLP.

2. **Cryoprotection.** Brain was immersed in 30 % (w/v) sucrose, 0.02 % (w/v) sodium azide in 0.1 M PBS buffer (see appendix 4.A. 4) for 7 days at 4 ºC.

3. Finally brain was frozen using dry ice and stored at -80 ºC.

4.E. BRAIN SECTIONING

30-µm-thick brain tissue sections were cut using a cryostat (Leica CM-1325) and were immersed in 0.02 % (w/v) sodium azide in 0.1 M PBS buffer. Sections containing the RGS14/vehicle-injection area were selected and stored at 4 ºC.

4.F. FLUORESCENT IMMUNOHISTOCHEMISTRY FOR RGS14 PROTEIN

Overexpression of RGS14 protein in tissue sections was detected by fluorescent immunohistochemistry (IHC) as it is detailed below:

1. Washing. Before proceeding with the IHC, selected sections were washed 3 times for 10 min at room temperature in 0.1M PBS buffer (appendix 4.A.2) with gentle agitation.

2. Inactivation of endogenous avidin-biotin was carried out using the avidin/biotin blocking kit (Vector Laboratories, SP-2001). Sections were incubated in each solution for 30 min at room temperature with gentle agitation.

3. Incubation in primary antibody. The commercial RGS14-polyclonal antibody (Novus biological, NBP1-31174; dilution 1:500) produced in rabbit and diluted in 0.3 % (v/v) triton X-100 (Sigma-Aldrich, 9002-93-1), 0.1 % (w/v) sodium azide in PBS buffer was applied and incubated overnight at 4 ºC with gentle agitation. Then sections were rinsed with PBS to remove the excess of primary antibody.

4. Incubation in secondary antibody. The Alexa fluor® 488-conjugated secondary antibody goat anti-rabbit IgG (Life technologies, A11008; dilution 1:1000) diluted in 0.3 % (v/v) triton X-100, 0.1 % (w/v) sodium azide, 0.1 M PBS buffer was incubate for 2.5 h at room temperature in darkness. Then sections were rinsed with PBS.

5. Mounting brain sections. Finally, slices were mounted on gelatin-coated slides (appendix 4.B) and kept overnight at room temperature to dry. Then, 1-2 drops of DABCO (see appendix 4.A.5) were applied on sections and covered with the coverslip.

6. Samples were observed under a Leica confocal microscope (Leica DM IRE2).

5 APPENDIX 5. PROTEOMICS

5.A. WESTERN-BLOT

5.A.1) Homogenization buffer: 0.01 M Tris-HCl buffer, pH 7.4 (50 ml)

This buffer was prepared by dissolving 0.06 g of Tris (Sigma-Aldrich, T1503) in Milli-Q water up to 50 ml. To adjust the pH at 7.4, some drops of HCl solution (T-Bakes, 6081) were added.

5.A.2) Lowry Method for protein determination

The protein concentration of samples were estimated by the colorimetric Lowry method (Lowry et al 1951) according to the protocol detailed below:

1. A BSA standard curve (from 0 to 267 µg/ml) was prepared using a 500 µg/ml BSA stock solution. Three replicates were used for each concentration.

Note: The 500 µg/ml BSA stock solution was prepared by dissolving 5 mg of BSA (Sigma-Aldrich, A3059) in 10 ml of Milli-Q water. The solution was aliquoted in small volume of 500 µl and stored at -80 ºC.

Tube	Volume of 500µg/ml BSA (µl)	Volume of Milli-Q water (µl)	[BSA] (µg/ml)
T1	0	75	0
T2	5	75	33
T3	10	65	67
T4	20	55	133
T5	30	45	200
T6	40	35	267

2. Two replicates of 1/5 and 1/10 dilutions of each sample were prepared, and 75 µl of them were placed in a 1.5 ml tube. In addition, 1/5 and 1/10 dilutions of Tris-HCl 0.01M pH 7.4 in Milli-Q water were prepared as blanks.
3. 75 µl of NaOH 1.2 N were added to each tube (BSA tubes, sample and blanks) and mixed by vortex.
Note: 50 ml of NaOH 1.2 N solution was previously prepared. For that purpose, 2.4 g of NaOH (Panreac, 1316877787.1211) were dissolved in 50 ml of Milli-Q water and the solution was stored at 4 ºC.
4. According to the number of tubes, the adequate volume of Alkaline Cooper Reagent (ACR) was prepared at the moment of use, mixing in a proportion of 100:1:1 the 2 % (w/v) Na_2CO_3, 2 % (w/v) Na_2 tartrate and 1 % (w/v) $CuSO_4$ respectively. Then 750 µl of ACR were added to each tube and mixed by vortex.
Note. The solutions used in this step were prepared the previous day as it is detailed below:
-50 ml of 2 % (w/v) Na_2CO_3 solution: 1 g of sodium carbonate anhydrous (Panreac, 131648.1210) was dissolved in 50 ml of Milli-Q water and solution was stored at 4 ºC.
-50 ml of 1 % (w/v) copper sulphate: 0.5 g of Cooper (II) sulphate anhydrous (Panreac, 122726.1209) were dissolved in 50 ml of Milli-Q and the solution was stored at 4 ºC.
-50 ml of 2 % (v/v) Na_2 tartrate solution: 1 g of sodium tartrate anhydrous (Panreac, 121720.1210) was dissolved in 50ml of Milli-Q water and the solution was stored at 4 ºC.

5. The mixture was incubated for 15 min at room temperature. The reaction result in a blue color as a consequence of the complex formed between the nitrogen of peptide bonds and copper under alkaline conditions (Biuret reaction).
6. The 2 N Folin-Ciocolteus´s phenol reagent (Sigma-Aldrich, F9252) was diluted 1:1with Milli-Q water immediately before use in dark conditions. 75µl of Folin-Ciocolteus´s phenol 2 N reagent were added to each sample and mixed by vortex.
7. The mixture was incubated for 45 min at room temperature and the blue color obtained from Biuret reaction was intensified as a consequence of the phosphomolybdotungstate reduction to heteropolymolybdenum blue.
8. Absorbance was read spectrophotometrically (S30, Boeco) at 750 nm.

5.A.3) Loading buffer 1X (8 ml) (Laemmli 1970)

REAGENT	AMOUNT	CONCENTRATION
2-β-mercaptoethanol (Sigma Aldrich, M3148)	0.4 ml	5 % (v/v)
Glycerol (Sigma Aldrich, G6279)	0.8 ml	20 % (v/v)
[1]**10 % (w/v) SDS** (Sigma Aldrich, L3771)	1.6 ml	2 % (w/v)
[2]**Tris-HCl 0.5 M pH 6.8** (Sigma Aldrich, T1503)	1 ml	62.5 mM
0.05 % (w/v) Bromophenol blue (Sigma Aldrich, B8026)	Some drops	--
Milli-Q water	4.2 ml	

[1] *5 g of SDS were dissolved in 50 ml of Milli-Q water.*
[2] *30.29 g of Tris was dissolved in Milli-Q water up to 500 ml and the pH was adjusted up to 6.8.*

5.A.4) Tris-Glycine-SDS (TGS) buffer 5X (1 L) (Laemmli 1970)

REAGENT	AMOUNT	CONCENTRATION
Tris (Sigma Aldrich, T1503)	15 g	0.125 M
Glycine (Sigma Aldrich, G7126)	72 g	0.96 M
SDS (Sigma Aldrich, L3771)	5 g	0.5 % (w/v)
Milli-Q water	Up to 1L	

5.A.5) Phosphate Buffered Saline (PBS buffer) 10X (1 L)

REAGENT	AMOUNT
Sodium chloride (NaCl) (Panreac, 121659.1214)	72.2 g
Potassium dihydrogen phosphate (KH_2PO_4) (Merck, 1.04873.0250)	4.3 g
Dibasic sodium phosphate (Na_2HPO_4 $2H_2O$) (Fluka, 71645)	19 g
Milli-Q water	Up to 1L

5.A.6) 0.1 % Tween PBS buffer 1X (TPBS) (1 L)

REAGENT	AMOUNT
PBS buffer 10X (appendix 5.A.5)	100 ml
Milli-Q water	900 ml
Tween® 20 (Sigma Aldrich, P7949)	1 ml

5.B. TWO DIMENSIONAL ELECTROPHORESIS

5.B.1) Sample solubilization buffer (20 ml)

REAGENT	AMOUNT	CONCENTRATION
Urea (Bio-Rad, 161-0731)	8.41 g	7 M
Thiourea (Sigma Aldrich, T8656)	3.04 gl	2 M
3-[(3-cholamidopropyl)dimmethylammonio] propanesulfonate (CHAPS) (Bio-Rad, 161-0465)	0.8 g	4 %
1,4 Ditrhioerythritol (DTE) (Fluka, 43794)	0.2 g	1 %
40 % Carrier 3/10 Ampholytes (Bio-Rad, 163-1112)	(see point 6 below)	0.4 %
Milli-Q water	Up to 20 ml	

1. The urea was dissolved in Milli-Q water with gently heating (< 37 ºC) in order to reduce the risk of protein carbamylation.
2. Once the solution turned to room temperature thiourea was added.
3. 0.2 g of ion exchange AG501-X8 resin (Bio-Rad, 143-7425) were added, stirred for 10 min and filtered (resin is used in order to remove urea polymers).
4. Then, CHAPS and DTE were added and the solution was adjusted to a final volume of 20 ml with Milli-Q water.
5. Small aliquots (2 ml) were done and frozen at -80 ºC until use.
   Note: Sample buffer should be prepared fresh.
6. Carrier ampholytes 3/10 were added to the homogenate just before isoelectric focusing (1.25 µl of 40 % solution carrier ampholytes in 125 µl of total sample volume).

5.B.2) Equilibration buffer (1L)

REAGENT	AMOUNT	CONCENTRATION
Urea (Bio-Rad, 161-0731)	360 g	6 M
1.5 M Tris-HCl pH 8.8 (Bio-Rad, 161-0798)	30 ml	0.05 M
Glycerol (Sigma Aldrich, G6279)	300 ml	30 %
20 % Sodium dodecyl sulfate (SDS) solution (BioRad, 161-0418)	100 ml	2 %
Milli-Q water	Up to 1 L	

1. Urea was dissolved in Milli-Q water as is described above.
2. Once the solution turned to room temperature, 2 g of ion exchange AG501-X8 resin (Bio-Rad, 143-7425) were added and stirred for 15 min; then solution was filtered.
3. Next, Tris-HCl solution, glycerol and SDS were added and stirred.
4. Finally, Milli-Q water was added up to 1 L and aliquots (50 ml) were done and freeze at -80 ºC until use.

Note: Equilibration buffer should be prepared fresh.

5.B.3) Bradford method for protein determination

The protein concentration of samples was performed by Bradford method using the *Protein Assay Kit II* (Bio-Rad, 500-0002) as follows:

1. A BSA standard curve was prepared using a 2 mg/ml BSA stock solution. Duplicates were used for each concentration.

TUBE	BSA SOLUTION VOLUME (µl)	MILLI-Q WATER (µl)	[BSA] (µg/ml)
1	75 (2 mg/ml stock)	25	1,500
2	70 (2 mg/ml stock)	70	1,000
3	35 (Tube 1)	35	750
4	70 (Tube 2)	70	500
5	70 (Tube 4)	70	250
6	70 (Tube 5)	70	125
7 (Blank)	0	70	0

2. Then, duplicates of 1/25 and 1/50 dilutions of samples were prepared in Milli-Q water.
3. 20 µl of each BSA standard, unknown samples and blanks were mixed with 1 ml of 1X dye reagent into separate clean cuvettes and incubated for 5-10 min at room temperature.

Note: Dye reagent should be warmed to room temperature and be well mixed before use.

4. Finally, absorbance was measured spectrophotometrically (S30, Boeco) at 595 nm.

5.B.4) 12 % Resolving 1.5 mm Mini Gels for Tris-Glycine SDS-Polyacrylamide Gel Electrophoresis

REAGENT	VOLUME
Milli-Q water	3.4 ml
30 % Acrylamide/Bisacrylamide Solution 37.5:1 (BioRad, 161-0158)	4.0 ml
1.5 M Tris-HCl buffer pH 8.8 (BioRad, 161-0798)	2.5 ml
20 % Sodium dodecyl sulfate (SDS) solution (BioRad, 161-0418)	0.1 ml
10 % (w/v) ammonium persulfate (APS)[1] (AppliChem, A1142,0250)	0.05 ml
TEMED (AppliChem, A1148,0100)	0.005 ml
TOTAL VOLUME	10 ml

[1] *The 10 % (w/v) solution was prepared as follows: 1 g of ammonium persulfate was dissolved in 10 ml of H_2O and stored at 4°C. Ammonium persulfate decays slowly in solution, so the stock solution should be replaced every 2-3 weeks. Ammonium persulfate is used as a catalyst for the copolymerization of acrylamide and bisacrylamide gels. The polymerization reaction is driven by free radicals generated by an oxide-reduction reaction in which a diamine (TEMED) is used as the adjunct catalyst*

1. All reagents except APS and TEMED were combined. Then, APS and TEMED were added and the gel monomer solution was poured into the support (Mini-Protean Tetra Handcast System, Bio-Rad) using a Pasteur pipette. A 1.5 mm-thickness spacer plates were used.
2. Then, in order to avoid drying, gel surface was carefully covered with Milli-Q water on top.
3. Finally, gel was left to polymerize for two hours at room temperature.

5.C. BLUE-SILVER STAIN

5.C.1) Brilliant Blue G-Colloidal dye solution (600 ml)

REAGENT	AMOUNT	CONCENTRATION
Methanol (Panreac, 131091.1612)	120 ml	20 % (v/v)
85 % (w/v) Orthophosphoric acid solution (AppliChem, A0637,1000)	70.5 ml	10 % (w/v)
Ammonium sulphate (AppliChem, A3598,1000)	60 g	10 % (w/v)
Colloidal Brilliant Blue Coomassie G-250 (Bio-Rad, 161-0406)	0.72 g	0.12 % (w/v)
Milli-Q water	Up to 600 ml	

5.C.2) Destain solution

REAGENT	AMOUNT	CONCENTRATION
NH_4HCO_3 (Sigma Aldrich, A6141)	0.1976 g	50 mM
Acetonitrile (Fluka, 34967)	15 ml	30 % (v/v)
Milli-Q water	Up to 50 ml	

Note. Glass containers are recommended to use.

5.D. MALDI-TOFF SAMPLE PREPARATION

5.D.1) Tryptic solution

REAGENT	AMOUNT	CONCENTRATION
Trypsin (Sigma Aldrich, T6567)	20 µg	10 ng/µl
10 mM NH_4HCO_3 (Sigma Aldrich, A6141) pH 8.5 [1]	2 ml	

[1] *10 mM NH_4HCO_3 was prepared, dissolving 79.06 mg of ammonium bicarbonate in 100 ml of Milli-Q water and adjusting the pH up 8.5.*

The tryptic solution was aliquoted and stored at -20 ºC (thaw/freeze the solution more than twice is not recommended).

5.D.2) Peptide extraction solution from spots

REAGENT	AMOUNT	CONCENTRATION
Triofluoracetic acid (Fluka, 40967)	0.05 ml	0.1 % (v/v)
Acetonitrile (ACN) (Fluka, 34967)	25 ml	50 % (v/v)
Milli-Q water	Up to 50 ml	

La ciencia siempre vale la pena porque sus descubrimientos, tarde o temprano, siempre se aplican.

Severo Ochoa.

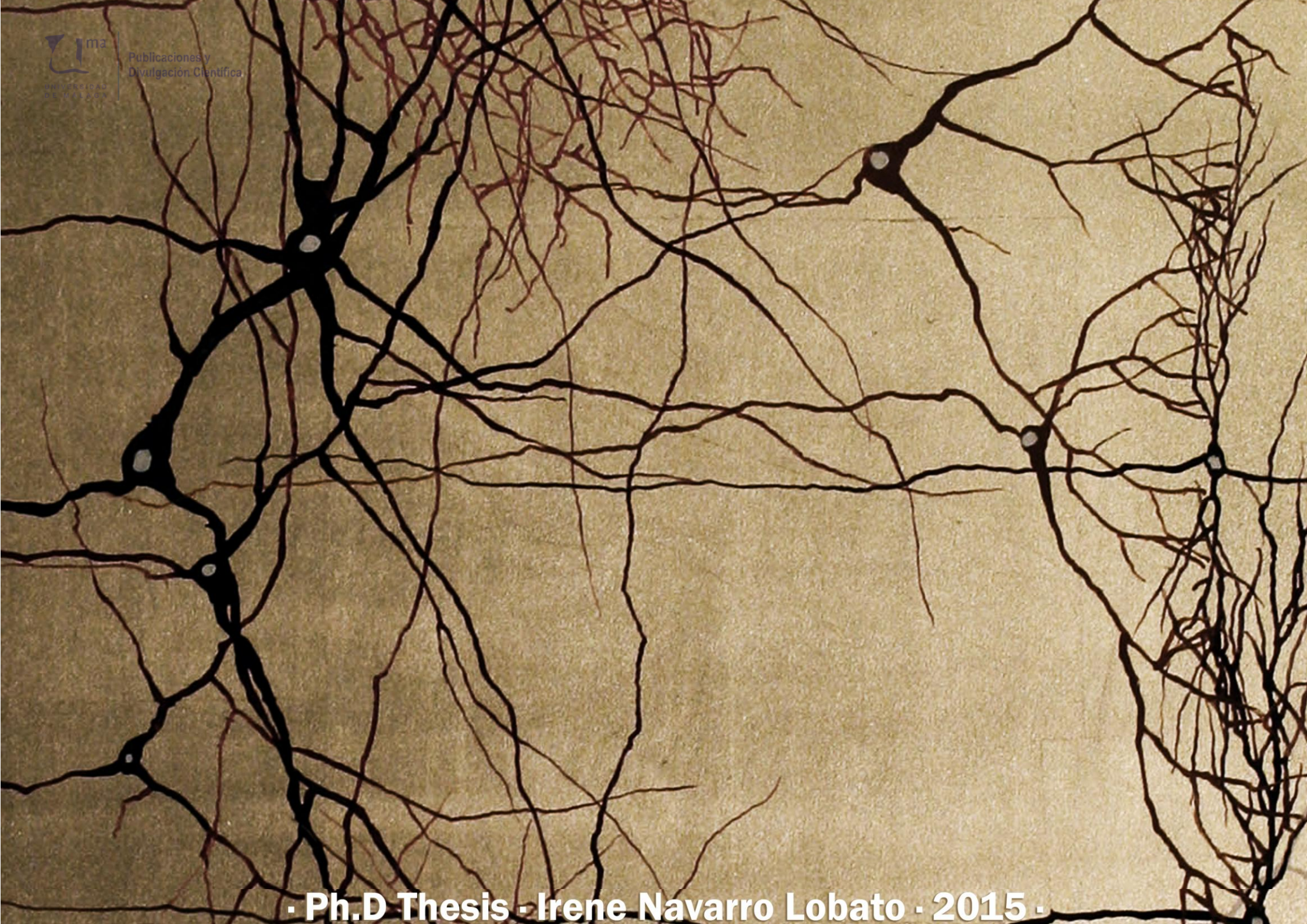

· Ph.D Thesis · Irene Navarro Lobato · 2015 ·